



DISSERTATION

# Safeguarding the ephemeral – photogrammetry for graffiti documentation

Eine Dissertation zur Erlangung des akademischen Grades  
**Doktor der technischen Wissenschaften (Dr.techn.)**

unter der Betreuung von  
**Univ.-Prof. Dipl.-Ing. Dr.techn. Norbert Pfeifer**

Durchgeführt an der  
TU Wien  
Fakultät für Mathematik und Geoinformation  
Forschungsgruppe Photogrammetrie

von

**BENJAMIN WILD**  
Matrikelnummer 01504060

Wien, am 16. März 2025

.....  
Unterschrift





DISSERTATION

# Safeguarding the ephemeral – photogrammetry for graffiti documentation

A thesis submitted in fulfillment of the academic degree of  
**Doktor der technischen Wissenschaften (Dr.techn.)**

under the supervision of  
**Univ.-Prof. Dipl.-Ing. Dr.techn. Norbert Pfeifer**

research conducted at  
TU Wien  
Faculty of Mathematics and Geoinformation  
Research group Photogrammetry

by

**BENJAMIN WILD**  
Matriculation number: 01504060

Vienna, April 15, 2025

.....  
Signature

**Supervisor:**

Prof. Dr. Norbert Pfeifer  
Technische Universität Wien  
Department of Geodesy and Geoinformation  
Wiedner Hauptstraße 8/E120, 1040 Vienna, Austria  
E-Mail: Norbert.Pfeifer@geo.tuwien.ac.at

.....

**Referee:**

Jun.-Prof. Dr.-Ing. Anette Eltner  
TU Dresden  
Institute of Photogrammetry and Remote Sensing  
Helmholtzstraße 10, D-01069 Dresden  
anette.eltner@tu-dresden.de

.....

**Referee:**

Name: Prof. Dr. Marco Scaioni  
Politecnico di Milano  
Dept. of Architecture, Built environment and Construction engineering (DABC)  
Via Ponzio 31, 20133 Milano  
marco.scaioni@polimi.it

.....

# Erklärung zur Verfassung der Arbeit

## Author's Statement

Ich erkläre hiermit, dass ich diese Dissertation eigenständig verfasst habe und dass alle verwendeten Quellen und Referenzen korrekt zitiert wurden. Alle Tabellen, Karten, Abbildungen oder sonstigen Inhalte, die aus externen Quellen stammen - sei es aus veröffentlichten Manuskripten, dem Internet oder anderen Quellen - sind im Text deutlich angegeben und die entsprechenden Quellen ordnungsgemäß zitiert. Während der Überarbeitung dieser Arbeit habe ich ChatGPT (GPT-4o und GPT-4o Mini) und DeepL verwendet, um die Lesbarkeit und Sprache des Manuskripts zu verbessern. Nach der Verwendung dieser Werkzeuge habe ich den Inhalt sorgfältig überprüft und in meinem Sinne überarbeitet, um Genauigkeit und Originalität zu gewährleisten. Ich übernehme die volle Verantwortung für den endgültigen Inhalt dieser Dissertation.

I hereby declare that I independently drafted this thesis and that all sources and references used have been correctly cited. Any tables, maps, figures, or other content included from external sources—whether from published manuscripts, the internet, or other references—have been clearly indicated in the text, with all respective sources properly cited. During the revision of this work, I used ChatGPT (GPT-4o and GPT-4o Mini) and DeepL to improve the readability and language of the text. After using these tools, I carefully reviewed and edited the content as needed to ensure correctness and originality. I take full responsibility for the final content of this thesis.

Benjamin Wild  
Huttengasse 23/28  
1160 Wien  
Österreich

.....  
*Unterschrift/Signature*

# Acknowledgments

First and foremost, I would like to express my deepest gratitude to Norbert. Thank you for giving me the opportunity to work on a topic that truly ignited my motivation and curiosity. Under your guidance, I have learned so much and grown both academically and personally. I deeply admire your constructive pragmatism and am truly grateful to be part of the research group you lead. Your support and insights have been invaluable—not only providing inspiration when needed but, more importantly, granting me the freedom to find inspiration on my own.

I would like to express my heartfelt thanks to Geert, the mastermind behind the INDIGO project. It was a privilege to work with you, and I have learned so much from our collaboration. Your professionalism is truly inspiring, and your expertise is overwhelming. It has been—and continues to be—a pleasure to work with you. I want to extend my gratitude to all INDIGO colleagues who contributed to making this project such a success.

Thanks to all the peers who took the time to review my works and helped me improve both the publications and this dissertation. Your invaluable feedback and expertise are the true cornerstones of science.

A heartfelt thank you to the entire photo group—working with all of you has been and continues to be a true *highlight* for me. Special thanks Anna, Taşkın, Florian, Laure-Anna, Lucas, and the other Photo PhD colleagues with whom I had the privilege of exchanging ideas and experiences. A big thanks to Camillo, Markus, Johannes, Gottfried, Martin, and Willi who were always ready to discuss, review and support. I am truly grateful to each and every one of you for making my time here so informally informative and enjoyable.

I also want to extend my appreciation to all my colleagues at the GEO Department, with a special mention to my former CLIMERS colleagues, for the countless lunches and coffees, the many hallway chats, the cold beverages after work, and the occasional table tennis matches. So many of you have become true friends, and for that, I am incredibly grateful. A special thank you to Emanuel for being such an iconic office mate. Thanks to Bernhard, Oto and all my other colleagues from the corridor for either accepting—or at least silently enduring—my whistling. Thanks to Willi, Elmar, Hans, and everyone from GEO-IT for your patience, friendliness, and for solving so many problems and offering helpful hints. Thanks to Ali, Max, Anna, Felix, Petra and Nina for always having a solution. Thanks also to all the students I had the privilege to work with through courses and theses.

A big thanks to Johannes and the whole *Turkey team*. You are a true inspiration. I feel privileged to have been part of this project.

I want to express my deepest gratitude to my family, who made all of this possible in the first place and never stopped encouraging and supporting me: my parents, Doris and Markus, my sisters, Krissi and Moni, my grandmother, Elli, and Hermann, and all the others from the *Wild-Crew*. I know I can always count on you.

Lastly, but certainly not least, I want to express my gratitude to you, Rahel. Thank you for always being there for me and supporting me, no matter the circumstances. You are my adventurous safe space, and I am more than grateful to have you by my side.

Benjamin Wild

# Abstract

Graffiti are full of polarising contrasts. Constantly visible in urban living spaces, they are also very transient. Hated by many, tolerated by some, loved by others. Graffiti, applied in public, often stir up the public. Despite its prominent role in public discourse and public space, there are comparatively few academic initiatives that deal with the literally multi-layered phenomenon of graffiti. This is surprising when you consider the wealth of content that graffiti represents. There are now more and more academics who view (modern) graffiti as cultural heritage that touches on linguistic, anthropological, criminological, ethnographic, historical and many other areas. Regardless of the position in the discourse, there has been a lack of solid data for well-founded analyses on the subject of graffiti. Although there are some documentation projects, these often show gaps in documentation or a lack of scientific objectivity. This dissertation uses photogrammetry to develop a methodological framework in order to set a basis for a comprehensive and reliable data basis.

This dissertation examines Viennese Donaukanal (eng. *Danube Channel*), one of the world's largest contiguous graffiti-scapes with a length of approximately 13 km. A central challenge of graffiti documentation is the identification of new works, which is difficult and time-consuming due to the large areas and rapid changes. To improve this process, an automated, image-based method for recognizing changes was developed. The method uses an incremental bundle block adjustment approach and synthetic cameras to generate synthetic co-registered graffiti images. These are fed into a hybrid change detection pipeline that combines pixel- and feature-based methods. The approach was validated on a publicly available reference dataset with 6902 image pairs, which was created as part of this work. With an accuracy of 87% and a recall of 77%, the results show that the proposed change detection workflow can effectively indicate newly added graffiti while ignoring other, irrelevant changes such as shadows.

In addition to the identification of new graffiti, the spatial and temporal decontextualization is one of the greatest challenges in graffiti documentation, as graffiti is usually tightly bound to space and time. Photographs alone are not sufficient to preserve this context. This study therefore investigates the use of photogrammetric techniques to better capture the spatial and temporal aspect. Orthophotos proved to be particularly suitable as they allow precise georeferencing and are free from topographic, perspective and lens distortions. A workflow was developed and implemented in the AUTOGRAf (AUTomated Orthorectification of GRAffiti photos) software to efficiently convert large quantities of images into orthophotos. AUTOGRAf uses an incremental bundle block adjustment approach to orient new photos, generate up-to-date 3D models of the scenes and finally orthorectify and georeference the images. In an experiment with 826 photos depicting a total of 100 graffiti, AUTOGRAf was able to process 95% of the graffiti without major errors and thus provide the data basis for a 3D web platform to display graffiti in its native, albeit virtual, context.

In addition to the studies along the Donaukanal, this dissertation is dedicated to a case study on the documentation of migrants' graffiti in clandestine migration stations on the Turkish west coast, a key region on the dangerous route from Turkey to Greece. The basis for this study was a 12-day research trip during which, among others, two abandoned buildings featuring extensive graffiti related to clandestine migration were examined. The graffiti found there are silent witnesses to these formative experiences. Given their ephemeral nature and the difficult conditions on site - limited access, poor lighting and stress - the documentation presented particular difficulties. The graffiti, mostly made with chalk, stones or lipstick, and the rapidly decaying buildings make systematic recording all the more urgent. By preserving these fragile traces in the form of orthophotos and textured 3D models, this study contributes to a deeper understanding of contemporary migration and its hidden narratives. It also serves as a collection of primary evidence of events that not only shape individual destinies but also influence public discourse and the political agenda.

The studies show the diversity of the subject of graffiti and the various possibilities that photogrammetry offers to (digitally) preserve this ephemeral cultural and inherently participatory phenomenon. By presenting and making available these ideas, results and implementations, this work aims to provide valuable assistance to both graffiti enthusiasts and professionals in their efforts to document this unique form of human expression.

# Kurzfassung

Graffiti sind voller polarisierender Gegensätze. Ständig sichtbar in urbanen Lebensräumen sind sie auch sehr vergänglich. Von vielen gehasst, von einigen geduldet, von manchen geliebt. Trotz der herausragenden Rolle im öffentlichen Diskurs und im öffentlichen Raum gibt es vergleichsweise wenige wissenschaftliche Initiativen, die sich mit dem, im wahrsten Sinne, vielschichtigen Phänomen Graffiti beschäftigen. Dies ist überraschend, wenn man den Reichtum an Inhalten bedenkt, den Graffiti darstellen. Inzwischen gibt es immer mehr Wissenschaftler und Wissenschaftlerinnen, die (moderne) Graffiti als kulturelles Erbe betrachten, das linguistische, anthropologische, kriminologische, ethnografische, historische und viele andere Bereiche berührt. Unabhängig von der Position in diesem Diskurs fehlt es bisher an soliden Daten für fundierte Analysen zum Thema Graffiti. Zwar gibt es einzelne Dokumentationsprojekte, diese weisen jedoch häufig Lücken oder mangelnde Objektivität auf. In dieser Dissertation wird mit Hilfe der Photogrammetrie ein methodischer Rahmen entwickelt, um die Basis für eine umfassende Datengrundlage für eine tiefere Auseinandersetzung mit Graffiti zu schaffen.

Diese Dissertation untersucht den Wiener Donaukanal, mit ca. 13km Länge eine der weltweit größten zusammenhängenden Graffitilandschaften. Eine zentrale Herausforderung der Graffiti-Dokumentation ist die Identifizierung neuer Werke, die aufgrund der großen Fläche und schnellen Veränderungen besonders zeitaufwändig ist. Um diesen Prozess zu verbessern, wurde eine automatisierte, bildbasierte Methode zur Erkennung von relevanten Veränderungen entwickelt. Das Verfahren nutzt einen inkrementellen Bündelblock und synthetische Kameras zur Erzeugung synthetischer ko-registrierter Graffitibilderpaare. Diese fließen in eine hybride Änderungserkennungspipeline ein, die pixel- und merkmalsbasierte Methoden kombiniert. Der Ansatz wurde an einem öffentlich verfügbaren Referenzdatensatz mit 6902 Bildpaaren validiert, der im Rahmen dieser Arbeit erstellt wurde. Mit einer Genauigkeit (accuracy) von 87% und einer Sensitivität (recall) von 77% zeigen die Ergebnisse, dass der vorgeschlagene Arbeitsablauf zur Erkennung von Veränderungen neu hinzugefügte Graffiti in einer Graffitilandschaft detektieren kann und somit eine umfassendere Graffitidokumentation unterstützt.

Neben der Identifikation neuer Graffiti ist die räumliche und zeitliche Dekontextualisierung eine der größten Herausforderungen in der Graffiti-Dokumentation, da Graffiti meist an Ort und Zeit gebunden sind. Fotografien allein reichen nicht aus, um diesen Kontext zu bewahren. Diese Studie untersucht daher den Einsatz photogrammetrischer Techniken zur besseren Erfassung des räumlichen und zeitlichen Bezugs. Orthophotos erweisen sich als besonders geeignet, da sie eine präzise Georeferenzierung ermöglichen und frei von topografischen und perspektivischen Verzerrungen sind und die Linsenverzeichnung korrigiert wird. Zur effizienten Umwandlung großer Bildmengen in Orthophotos wurde ein Workflow entwickelt und in der Software AUTOGRAf (AUTomated Orthorectification of GRAffiti photos) implementiert. AUTOGRAf nutzt einen inkrementellen Bündelblock-Ansatz, um neue Fotos zu orientieren, daraus aktuelle 3D-Modelle der Szenen zu generieren und schließlich die Bilder zu orthorektifizieren. In einem Experiment mit 826 Fotos, die insgesamt 100 neue Graffiti abbilden, zeigte sich, dass AUTOGRAf für 95% der Graffiti zufriedenstellend Orthophotos generiert und damit auch die Datenbasis für eine 3D-Webplattform liefern kann, um Graffiti in ihrem ursprünglichen, wenn auch virtuellen, Kontext darzustellen.

Zusätzlich zu den Studien entlang des Donaukanals widmet sich diese Dissertation einer Fallstudie zur Dokumentation von Graffiti von Migranten und Migrantinnen in heimlichen Migrationsstationen an der türkischen Westküste, einer Schlüsselregion auf der gefährlichen Route von der Türkei nach Griechenland. Grundlage für diese Studie war eine 12-tägige Forschungsreise, in der zwei verlassene, von Migranten und Migrantinnen genutzte Gebäude untersucht wurden. Die dort gefundenen Graffiti sind stille Zeugen dieser prägenden Erfahrungen. Angesichts ihres vergänglichen Charakters sowie der schwierigen Bedingungen vor Ort - begrenzter Zugang, schlechte Beleuchtung und Stress - stellte die Dokumentation besondere Schwierigkeiten dar. Die meist mit Kreide, Steinen oder Lippenstift angebrachten Graffiti und die schnell verfallenden Gebäude machen eine systematische Erfassung umso dringlicher. Durch die Bewahrung dieser fragilen Spuren in Form von Orthophotos und texturierten 3D-Modellen trägt diese Studie zu einem tieferen



Verständnis zeitgenössischer Migration und ihrer verborgenen Erzählungen bei. Sie dient zugleich als Sammlung von Primärbelegen für Ereignisse, die nicht nur individuelle Schicksale prägen, sondern auch den öffentlichen Diskurs und die politische Agenda beeinflussen.

Die vorgestellten Studien zeigen die Vielfältigkeit des Themas Graffiti und die diversen Möglichkeiten, die die Photogrammetrie bietet um dieses flüchtige Kulturerbe (digital) zu bewahren. Durch die Vorstellung und freien Verfügungstellung dieser Ansätze und Implementierungen soll diese Arbeit sowohl Graffiti-Enthusiasten und Enthusiastinnen als auch Wissenschaftler und Wissenschaftlerinnen Unterstützung und Inspiration für die Dokumentation dieser einzigartigen Form des menschlichen Ausdrucks bieten.

# List of Abbreviations

AGP	The Ancient Graffiti Project
AR	Augmented Reality
AUTOGRAF	AUTomated Orthorectification of GRAffiti Photos
BRISK	Binary Robust Invariant Scalable Keypoints
CCA	Canonical Correlation Analysis
CIE	Commission Internationale de l'Éclairage (International Commission on Illumination)
CIEDE2000	International Commission on Illumination's 2000 Color Difference Formula
CIELAB	International Commission on Illumination's L*a*b* colour space
CIDOC CRM	CIDOC Conceptual Reference Model
CNP	Control Network Point
EPOSA	Echtzeit-Positionierung-Austria (eng. Real-Time Positioning Austria)
EXIF	Exchangeable Image File Format
FLANN	Fast Library for Approximate Nearest Neighbours
FOV	Field of View
GCP	Graffiti-scape Control Point
GP	Graffiti-scape Point
GSD	Ground Sampling Distance
IMU	Inertial Measurement Unit
INDIGO	Inventory and Disseminate Graffiti along the Donaukanal
INGRID	Informationssystem Graffiti in Deutschland
ISO	International Organization for Standardization
MAD	Multivariate Alteration Detection
IR-MAD	Iteratively-Reweighed Multivariate Alteration Detection
LIDAR	Light Detection and Ranging
MGI	Militärgeographischen Institutes (eng. Military Geographic Institute Austria)
ÖBB	Österreichische Bundesbahnen (eng. Austrian Federal Railways)
RANSAC	Random Sample Consensus
RTK-GNSS	Real-Time Kinematic Global Navigation Satellite System
SfM	Structure from Motion
SIFT	Scale Invariant Feature Transform
SURF	Speeded-Up Robust Features
UNHCR	United Nations High Commissioner for Refugees
VR	Virtual Reality

# Preface

Graffiti are an omnipresent feature of our public spaces. In urban areas, at least in non-authoritarian systems, it is nearly impossible to walk through urban streets without encountering them. As such, graffiti represent an inherently democratic phenomenon. While only a small portion of graffiti convey explicit political messages, their very existence often serves as a subtle act of resistance, a quiet assertion of freedom. Graffiti-less cities are thus suspect, even alarming, to me.

For many, graffiti evoke strong and often polarizing reactions. Admittedly, many or even most graffiti do not conform to conventional notions of beauty. Yet, in this dissertation, terms like *smearing* or *scribblings* are consciously avoided to describe graffiti, just as much as *artists* or *artworks*. Such labels miss, in my opinion, the essence of graffiti. The real value of graffiti never lies in conventional aesthetics but in their raw, unfiltered expression of humanity. At their core, graffiti embody one of the most primal human impulses: the need to declare *I am here*. This simple yet profound statement speaks to a collective desire for presence and permanence. A world where such messages are completely erased would be inhuman. It would be a world stripped of freedom, stripped of culture.

Graffiti are omnipresent, yet among the most transient forms of expression. While some works may endure for years, every graffito is inherently impermanent, defined by its constant vulnerability to vanishing. This ephemerality has led some to argue that documenting graffiti, i.e. digitally safeguarding it, undermines its core essence. Nevertheless, without documentation, graffiti risks vanishing without a trace, as it never existed for future generations. Viennese graffiti creator Manuel Skirl expressed this idea during a discussion on graffiti documentation [1]:

*Maybe it starts mattering after some time. For some reason, you can't see now.*

Although this statement may be too vague to serve as sufficient scientific justification for this dissertation, it underscores my personal motivation for this topic. It is fascinating to me how much attention prehistoric graffiti receive. The very use of the term *cave painting* to describe these ancient graffiti highlights the strikingly unequal treatment of two fundamentally identical phenomena. We, as society, do not yet see much value in what is created along the walls of our inner cities today. It is my belief that we can only really start seeing this value once they are long gone. Thus, this thesis.

*Benjamin Wild*

# Contents

<b>Acknowledgments</b>	<b>vi</b>
<b>Abstract</b>	<b>vii</b>
<b>Kurzfassung</b>	<b>viii</b>
<b>Abbreviations</b>	<b>x</b>
<b>Preface</b>	<b>xi</b>
<b>Contents</b>	<b>xii</b>
<b>1 Introduction</b>	<b>1</b>
1.1 Towards a definition of graffiti . . . . .	1
1.2 State-of-the-art graffiti documentation and research . . . . .	4
1.2.1 The Ancient Graffiti Project . . . . .	5
1.2.2 INGRID . . . . .	6
1.2.3 Non-academic graffiti documentation . . . . .	7
1.2.4 The role of social media in graffiti documentation . . . . .	12
1.3 Graffiti - a matter of space and time . . . . .	13
1.4 Research Questions . . . . .	14
1.5 Related Publications . . . . .	16
1.6 Structure of this thesis . . . . .	18
<b>2 Donaukanal and project INDIGO</b>	<b>20</b>
2.1 Donaukanal - a graffiti-scape . . . . .	20
2.2 Objectives and Achievements of Project INDIGO . . . . .	21
2.2.1 INDIGO's photogrammetric backbone . . . . .	22
2.2.2 Ethical considerations surrounding INDIGO's objectives . . . . .	27
<b>3 An automated framework for graffiti change detection</b>	<b>29</b>
3.1 State-of-the-art in graffiti change detection . . . . .	29
3.2 Challenges in Image-Based Graffiti Change Detection . . . . .	31
3.3 Change detection data and methods . . . . .	33
3.4 Image acquisition at test site . . . . .	34
3.5 Image co-registration . . . . .	38
3.6 Generating reference change maps . . . . .	42
3.7 Hybrid change detection framework . . . . .	44
3.7.1 Pixel-based change maps . . . . .	44
3.7.2 Introducing image feature descriptors as change indicators . . . . .	47
3.7.3 Change map merging and threshold optimisation . . . . .	50
3.8 Results and discussion . . . . .	51
3.8.1 Pixel-based results . . . . .	51
3.8.2 Descriptor-based results . . . . .	54
3.8.3 Threshold optimisation and change map merging . . . . .	54
3.8.4 Hybrid change detection assessment . . . . .	55

<b>4</b>	<b>An automated framework for generating rectified and georeferenced graffiti images</b>	<b>61</b>
4.1	Image distortions . . . . .	62
4.2	Planar rectification . . . . .	63
4.2.1	Quality assessment of the planar rectification approach . . . . .	64
4.2.2	Considerations regarding the large scale applicability of planar rectification . . . . .	65
4.3	AUTOGRAF - AUTomated Orthorectification of GRAffiti Photos . . . . .	66
4.3.1	The orthophoto principle . . . . .	66
4.3.2	Acquiring and managing graffiti photos . . . . .	69
4.3.3	Initial SfM and quality checks . . . . .	69
4.3.4	Incremental SfM approach . . . . .	70
4.3.5	Creation of the 3D Model and determination of a custom projection plane . . . . .	71
4.3.6	Orthophoto creation and graffiti segmentation . . . . .	73
4.3.7	Orthorectification experiment . . . . .	74
4.4	Results from the orthorectification experiment . . . . .	76
4.4.1	Initial local and incremental SfM . . . . .	76
4.4.2	Derivation of the 3D surface model and the projection planes . . . . .	77
4.4.3	Quantity and quality of the derived orthophotos . . . . .	77
4.4.4	Feasibility of the workflow . . . . .	79
4.5	The potential of incorporating highly-accurate direct georeferencing . . . . .	81
4.6	Potential dissemination of the results . . . . .	83
<b>5</b>	<b>Documenting graffiti related to clandestine migration along the Turkish west coast</b>	<b>85</b>
5.1	A brief overview on recent clandestine migration in the Eastern Mediterranean region . . . . .	85
5.2	Status-quo in documentation of clandestine <i>migration stations</i> . . . . .	87
5.3	Research project <i>Flüchtige Spuren</i> . . . . .	89
5.4	The importance and challenges of documenting migrant graffiti . . . . .	90
5.5	Ethical considerations . . . . .	93
5.6	Photogrammetric data acquisition . . . . .	94
5.7	Photogrammetric processing . . . . .	95
5.8	Deriving other value-added products . . . . .	96
5.9	Conclusions and outlook . . . . .	99
<b>6</b>	<b>Summary, Outlook and Conclusions</b>	<b>100</b>
6.1	Summary Chapter 3 and 4 . . . . .	100
6.2	Summary Chapter 5 . . . . .	103
6.3	Outlook and Conclusions . . . . .	103
	<b>Bibliography</b>	<b>106</b>

# List of Figures

1.1	Ancient graffito from Lascaux Cave in France and a contemporary graffito from Donaukanal . .	2
1.2	Hand-written mark on a train of the Austrian Federal Railways . . . . .	3
1.3	Graffiti advertisement for a soft drink brand . . . . .	4
1.4	Screenshot of INGRID's database interface . . . . .	7
1.5	Exemplary graffiti records from three online archives displaying graffiti from Vienna, Tamnougalt, and Chicago . . . . .	9
1.6	Screenshots from the Streetartifacts platform . . . . .	9
1.7	Screenshots from the Graffiti Archaeology platform . . . . .	10
1.8	Screenshot of a graffiti creator's Instagram feed . . . . .	12
1.9	Example of a dynamic graffiti scene at Donaukanal . . . . .	13
1.10	Manipulated graffiti of two Viennese football clubs . . . . .	13
2.1	Example images of the graffiti-covered surfaces at the Donaukanal and their locations . . . . .	20
2.2	Main goals of project INDIGO . . . . .	22
2.3	Overview of the prime research zone including the GCP clusters . . . . .	24
2.4	Three typical GPs out of the thirty that constitute cluster L7 on the left Donaukanal bank . . . .	26
2.5	Tie points established between images taken from opposite sides of Donaukanal . . . . .	26
2.6	Cleaned 3D tie point cloud and the locations of the photographs close to Marienbrücke . . . . .	27
3.1	Example for challenges in image-based change detection . . . . .	32
3.2	Challenges in image-based change detection of graffiti . . . . .	33
3.3	Workflowchart of the main steps in the hybrid change detection approach . . . . .	34
3.4	INDIGO's Donaukanal area with test zone inset and legal graffiti surfaces . . . . .	37
3.5	The three GoPro cameras mounted in a frame . . . . .	38
3.6	The base mesh of the change detection zone showing camera orientations across three epochs with textured views and their respective texture atlases . . . . .	40
3.7	Textured 3D surface mesh with black wireframe synthetic cameras and exemplary rendered images from the synthetic cameras . . . . .	41
3.8	Illustration of change map creation for graffiti-affected images, epochs, and computed maps . .	43
3.9	RGB normalisation results show input images under varying illumination and their normalised versions . . . . .	46
3.10	Examples of the feature detection, description and matching process . . . . .	48
3.11	Comparison of original and smoothed image snippets with varying parameter settings . . . . .	52
3.12	Example results from the pixel-based processing chain . . . . .	53
3.13	Example results from the descriptor-based processing chain . . . . .	54
3.14	The tested tie points ( $T_{TP}$ ) and CIEDE2000 ( $T_{\Delta E_{00}}$ ) thresholds with their corresponding assessment values. . . . .	55
3.15	Exemplary results from the Iteratively-Reweighed Multivariate Alteration Detection (IR-MAD) .	56
3.16	Four exemplary results from the different tested and developed change detection methods . . .	58
4.1	Example photograph showing different distortion types . . . . .	62
4.2	Example of a planarly rectified image depicting graffiti at the testing zone . . . . .	64
4.3	Exemplary errors in a planarly rectified graffito image . . . . .	65
4.4	Overview of the orthophoto generation process with the three required data sources . . . . .	67
4.5	Automated orthorectification workflow diagram . . . . .	68
4.6	Logo of AUTOGRAF . . . . .	69
4.7	Tie points established between new and old photos . . . . .	71

4.8	An example of a RANSAC-classified tie point cloud . . . . .	72
4.9	Example collection of nine images for one graffito . . . . .	73
4.10	Histogram of $RMSE_{img}$ for the 823 images of the orthophoto experiment . . . . .	76
4.11	Overview images of the three graffiti for which the incremental SfM approach failed . . . . .	77
4.12	Overview map showing the orthophoto of the Donaukanal area and the outlines of all orthorectified graffiti projected in top view . . . . .	80
4.13	The RTK-enabled GNSS-IMU logging device. . . . .	82
4.14	Map showing the accuracies of the direct georeferencing solution . . . . .	82
4.15	Screenshot of the developed interactive webmap in 2D view featuring various filtering options and density clustering . . . . .	84
4.16	Screenshot of the developed interactive webmap in 3D view featuring various filtering options . . . . .	84
5.1	Evolution of sea and land arrivals in Greece between 2014 and 2024 including the number of missing and dead people . . . . .	86
5.2	Sea and land arrivals in Greece: Breakdown by island for the period from January to December 8, 2015 . . . . .	87
5.3	Collection of photos acquired during visits at different clandestine migration stations along the Turkish west coast . . . . .	89
5.4	Textured 3D meshes of Building 1 and 2 and floorplans for each building . . . . .	90
5.5	Unfinished graffito created with a red lipstick which was found in close vicinity . . . . .	91
5.6	The island of Lesbos (Greece) as seen from the Turkish mainland . . . . .	93
5.7	The two camera setups used for the image acquisition of the two abandoned buildings . . . . .	94
5.9	Example of tie points established between an outdoor and one indoor photo of Building 1 . . . . .	95
5.8	Two example photographs of the buildings' interiors to highlight the scaling and lightning issues . . . . .	95
5.10	Polymesh with and without texture on one room in Building 1 . . . . .	96
5.11	Diagonal cross section of the textured 3D mesh of Building 1 . . . . .	96
5.12	Examples of graffiti orthophotos created in building 1 . . . . .	97
5.13	Original and processed image of one graffito from Building 2 . . . . .	98

## List of Tables

1.1	Example for different contexts of an example graffito . . . . .	3
1.2	Overview of online graffiti archives . . . . .	8
2.1	Full photographic coverage acquisition parameters . . . . .	23
2.2	Summary of GCP data quality . . . . .	25
2.3	Accuracy metrics for the full photographic coverage . . . . .	25
3.1	Protocol of the the 29 GoPro photo collections for the change detection . . . . .	36
3.2	Results from the pixel-based change detection with different parameters used for the edge-aware smoothing . . . . .	52
3.3	Results from the pixel-based change detection . . . . .	53
3.4	Optimised thresholds, runtime, and median metrics for three approaches on 6902 image pairs. . . . .	57
3.5	Exemplary results from the hybrid change detection approach . . . . .	59
4.1	Classification scheme for the quality assessment of the generated graffiti orthophotos. . . . .	75
4.2	Classification result of the orthophoto experiment. Adopted from [53] . . . . .	79
4.3	PC Specifications used in the experiment . . . . .	80

4.4 Processing times for the orthorectification experiments . . . . .	81
5.1 Pushback incidents as documented by the Turkish Coast Guard Command . . . . .	87
5.2 Details of the surveyed buildings . . . . .	90
5.3 Summary of photo acquisition and processing results for the two surveyed buildings . . . . .	94





# 1 Introduction

© Traumrune / Wikimedia Commons / CC BY-SA 3.0

## 1.1 Towards a definition of graffiti

To gain a clearer understanding of what defines graffiti, it is useful to delve into the history and evolution of the term *graffito* (the singular form of *graffiti*). *Graffito* along with *sgraffito* (which includes the prefix *s*), was used in an art-technical context as early as 1550. This usage dates back to the first edition of Giorgio Vasari's *Vite* [2]. Vasari describes a wall decoration technique he calls *sgraffito*, executed in three steps [3]:

- ▶ A layer of dark-colored plaster is applied to the wall and left to dry.
- ▶ A second layer of plaster in a contrasting color is spread over the first.
- ▶ Decorative patterns are scratched into the top layer with a metal tool, revealing the differently colored base layer beneath.

This description focuses on a specific method of creating graffiti that differs from our contemporary understanding of it. However, Vasari's exploration extends beyond technical details. He notes that graffiti stand apart from other decorative techniques due to their swift creation process and durability, designating them for exclusive use on exterior building surfaces, particularly facades of houses and palaces [2]. This aligns more closely with our modern concept of what constitutes graffiti [4].

While the term graffiti is relatively new in the context of human history, graffiti-like activities are likely as old as humanity, as evidenced by the various paintings found wherever prehistoric human settlements occurred, such as in the caves of Lascaux (Figure 1.1). Despite the close connection between *ancient* and *contemporary* graffiti, the former are typically not referred to as graffiti but rather as *rock art* or, if done inside, *cave paintings*. This distinction appears arbitrary.

Interestingly, if we apply the widely cited definition of graffiti by Ross (2016, p.1):

*graffiti typically refers to words, figures, and images that have been drawn, marked, scratched, etched, sprayed, painted, and/or written on surfaces where the owner of the property (whether public or private) has NOT given permission to the perpetrator* [5]

we might conclude that the right horse in Figure 1.1 is not a graffiti, as it was created with the permission of the property owner, the city of Vienna. This is evidenced by the pigeon symbol, which denotes a *Wienerwand*<sup>1</sup>, a surface provided by the city of Vienna for legal graffiti, an oxymoron, at

1.1	Towards a definition of graffiti . . . . .	1
1.2	State-of-the-art graffiti documentation and research . . . . .	4
1.2.1	The Ancient Graffiti Project . . . . .	5
1.2.2	INGRID . . . . .	6
1.2.3	Non-academic graffiti documentation . . . . .	7
1.2.4	The role of social media in graffiti documentation . .	12
1.3	Graffiti - a matter of space and time . . . . .	13
1.4	Research Questions . . .	14
1.5	Related Publications . . .	16
1.6	Structure of this thesis . .	18

[4]: Schlegel et al. (2022), 'Making a Mark—Towards a Graffiti Thesaurus'

[5]: Ross (2016), *Routledge Handbook of Graffiti and Street Art*

1: The pigeon was not chosen at random, as it is, like graffiti, a controversial part of the city, symbolising the population's ambivalent relationship to graffiti



**Figure 1.1:** Ancient graffito from Lascaux Cave in France (left; <https://commons.wikimedia.org/w/index.php?curid=68724647>) and a contemporary graffiti from Donaukanal (right; photographed in 2021 and downloaded from <https://spraycity.at>)

least according to Ross' definition given above. For left horse, we cannot definitively determine the legality, we can only hypothesise whether the people who might have lived in the cave encouraged or neglected them. This example demonstrates the difficulty in defining graffiti. It is also to be noted, that the word *typically* in Ross' definition indicates a certain fuzziness of defining graffiti and that a rigid dictionary-approach might not be suited to capture this diverse phenomenon.

Instead, let us delve deeper into how graffiti can be defined from different perspectives. Asking ten individuals to define graffiti will likely yield ten distinct responses, with common elements such as *spray*, *illegal*, *street*, *protest*, and *art*. Each person holds a personal conception of what constitutes graffiti making the activity of defining graffiti an enlightening experience when exploring cities. Any mark encountered can be analysed and categorised as either a graffito or non-graffito. Conducting this activity in a group reveals the diversity of perspectives on graffiti. Some may classify a sticker featuring the local soccer club as graffiti, while others may not. Similarly, opinions may differ on whether a moustache drawn on a billboard's politician face qualifies as graffiti. A large painting advertising a local soft drink brand on a building facade may be considered graffiti by some and not by others.

Consider Figure 1.2, which depicts a handwritten mark *Maskenpflicht* (English: *mandatory mask-wearing*) on the door to the economy class carriage of an Austrian Federal Railways (Österreichische Bundesbahnen; ÖBB) train. The mark was created by a human using a white permanent marker within the train and was documented on May 16, 2024, between the Austrian cities of Klagenfurt and Villach. However, key details about this graffito remain unknown:

- ▶ Who created it? (Attribution)
- ▶ When was it created? (Chronology)
- ▶ Why was it created? (Motivation)

The answers to these questions could determine whether this *Maskenpflicht* mark qualifies as graffito or not. Consider the following scenarios:



**Figure 1.2:** Door to the economy class carriage on an Austrian Federal Railways (Österreichische Bundesbahnen; ÖBB) train with a hand-written mark “Maskenpflicht” (eng. Mandatory mask wearing).

**Table 1.1:** Different potential scenarios illustrating the attribution, chronology, and motivation for the (potential) graffito depicted in Figure 1.2.

Scenario	Attribution	Chronology	Motivation
1	Employee of ÖBB	April 2020	Reminding travelers of the mask mandate at that time.
2	Traveler	April 2020	Reminding co-travelers of the mask mandate at that time.
3	Traveler	May 2024	Reminiscence of COVID-times when masks were mandatory.

In scenarios 2 and 3, the acts are unauthorised, potentially leading to consequences for the creator, while in scenario 1, the creator is authorised and possibly obligated and paid to mark the door. Blanché (2015) [6] centres the discussion on authorisation, noting *self-authorisation* as a defining characteristic of graffiti. This perspective is supported by [7], [8], and [9], who emphasise that graffiti are typically *unofficial*, *unsolicited*, and *uncommissioned*.

Another significant aspect in analysing graffiti is practicality [4]. In scenarios 1 and 2, the mark serves a practical purpose by enforcing mask mandates. In scenario 3, however, the practicality is less clear, functioning more as a nostalgic reference to COVID times. This example highlights the crucial role of context when defining graffiti, underscoring its significance as a key factor, if not the most critical, in graffiti documentation. In fact, decontextualisation is one of the key issues, in graffiti documentation which also guides the aims of this thesis and Chapter 1.3 will shed more light on this challenge.

Lastly, consider Figure 1.3, an advertisement for a soft-drink located along Vienna’s Donaukanal, a prominent graffiti area and research area for this thesis. This likely commissioned creation blends seamlessly with its graffitied environment. However, this creation has a practical intention that is to promote a specific product. Such practicality challenges the straightforward classification of graffiti. Furthermore, its potential authorisation by the city of Vienna, as the wall’s owner, could argue against its categorisation as graffiti.

Providing an overview on potential approaches for defining *graffiti* at

[6]: Blanché (2015), ‘Street Art and related terms’

[7]: Krause et al. (2006), *Street Art, Die Stadt als Spielplatz*

[8]: Siegl (2009), ‘Kulturphänomen Graffiti. Das Wiener Modell der Graffiti-Forschung’

[9]: Bengtsen (2014), *Street Art World*

[4]: Schlegel et al. (2022), ‘Making a Mark—Towards a Graffiti Thesaurus’



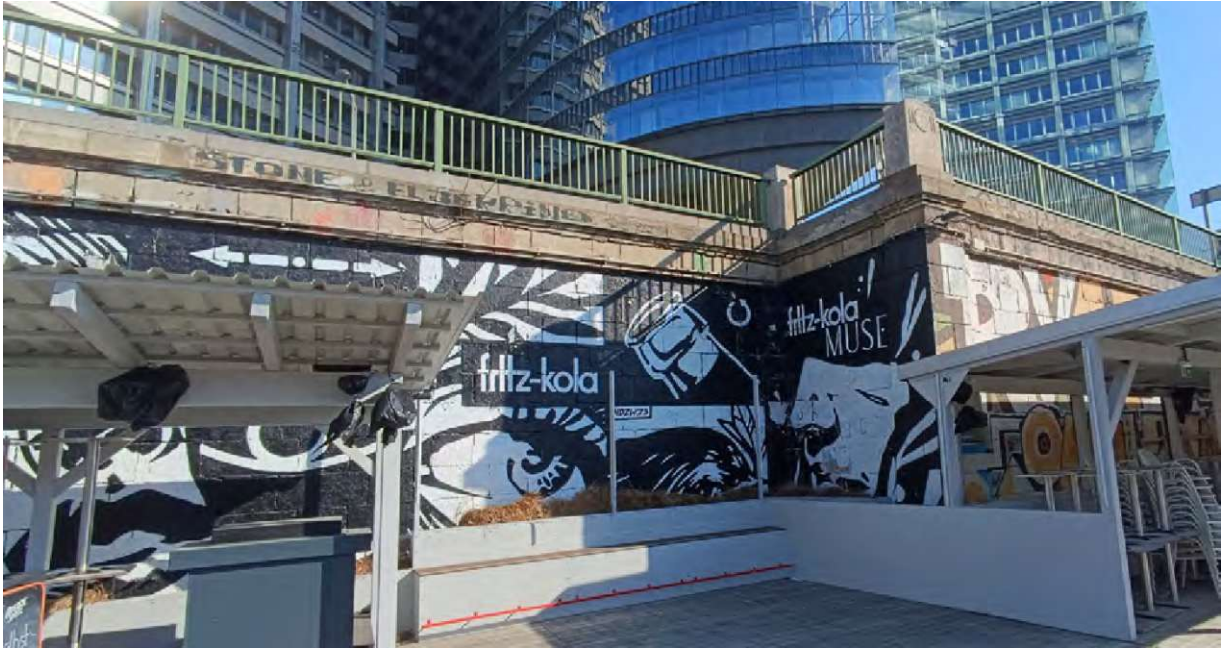


Figure 1.3: Graffiti advertisement for a soft drink brand

the outset seems crucial for this work. However, each single definition is definitively prone to falsification due to varied interpretations and contexts. It remains questionable, whether a definition for such a diverse phenomenon can be practical at all. As shown above, a single mark could lead to different conclusions depending on the specific context which is generally not evident to the mere observer of the mark. It seems that self-authorisation and practicality play key roles in determining whether something is classified as graffiti [4]. Nevertheless, the approach taken in this dissertation leans towards an intuitive understanding, reflecting the spontaneous nature often associated with graffiti creations. Strictly speaking, it would be more accurate to avoid using the term *graffiti* altogether and instead use the more general term *mark* [10]. However, this term seems too vague and distances itself significantly from the terminology commonly used. Therefore, the terms *graffito* (for a single mark) and *graffiti*<sup>2</sup> (for multiple marks or describing the concept) will still be used throughout this thesis, while acknowledging the ambiguity associated with them.

[4]: Schlegel et al. (2022), 'Making a Mark—Towards a Graffiti Thesaurus'

[10]: Verhoeven et al. (2022), 'Project IN-DIGO: document, disseminate & analyse a graffiti-scape'

2: Today, the term *graffiti* is also sometimes used for one and the analogous plural *graffitis* is used to denote several.

## 1.2 State-of-the-art graffiti documentation and research

Graffiti reveals polarising traits: despised and admired, encouraged and criminalised, subversive and charming. Despite their ephemeral nature, graffiti remain ubiquitous in urban landscapes, spanning from ancient times to modernity. The polarisation associated with contemporary graffiti might contribute to the attention graffiti increasingly receive by the public which is evidenced by numerous magazines, coffee table books and newspaper showcasing graffiti and their creators (e.g., [11–13]).

Although graffiti has transitioned from a questionable and clandestine

[11]: Saenz Gordon (2021), *Mural MAST-ER: From painting in the streets to the Graffiti Museum in Miami*, how muralist MAST managed to translate a teenage hobby into a career

[12]: Lohberger (2019), 'Graffiti - ist das Kunst?'

[13]: Peteranderl (2020), 'Corona-Graffitis weltweit: Wie Street-Art-Künstler ihre Nachbarn aufklären'

activity to a widely recognised cultural phenomenon featured in mainstream media, the scientific attention it receives remains small compared to its urban omnipresence and contextual richness. Although academic legitimacy has grown over the past decades the number of academic avenues focusing on contemporary graffiti is still limited [14]. This ambiguity is evident in the uncertain stance on whether graffiti should be regarded as cultural heritage. There is a growing number of scholars who argue that contemporary as well as ancient graffiti should be considered cultural heritage [15–17] but at the same time contemporary graffiti is often classified in a scientific context as nothing more than *damage* [18], *vandalism* [19], or *a threat* [20]. Maybe both can be true depending on the context, but regardless of the discussion on whether or not (contemporary) graffiti shall be considered cultural heritage, proper documentation is essential for a scientific analysis and understanding of this dynamic, unique and democratic phenomenon [21–23]. Ironically, there is significant research interest in graffiti removal techniques, as evidenced by the many scientific publications in this field [24–37]. Interestingly, many of these studies are published in journals focusing on cultural heritage, and one publication even explicitly focuses on the removal of graffiti from cultural heritage sites [20]. Based on this, one could conclude that removing graffiti is of higher importance than safeguarding them. At the very least, it seems that the topic of graffiti documentation is as polarising as the research object itself. Nevertheless, the following chapters shed light on the current state-of-the-art in graffiti documentation focusing on databases accessible to a wider scientific community. While the chapters aim to give a comprehensive overview on graffiti documentation from different perspective, a very recent project in this context, project INDIGO, will not be discussed in this state-of-the-art chapter but as this project constitutes parts of the organisational and scientific framework of this dissertation there is a separate Chapter (2.2) devoted to this graffiti-research project. Thus, project INDIGO and this dissertation are very much interconnected.

### 1.2.1 The Ancient Graffiti Project

It is important to note that generally a distinction is made between contemporary and ancient graffiti. Graffiti created millenia ago, by people who are now considered historical (but mostly unknown) figures, are likely to be preserved, documented, and analysed in detail, while contemporary graffiti are only in very rare instances treated in a similar way. This shift in perception highlights how graffiti from the past are valued for their historical and cultural insights, whereas contemporary graffiti are frequently solely viewed through the lenses of legality and vandalism. There are numerous publications focusing on documentation of ancient graffiti (e.g., [38–41]) and much less on their contemporary counterparts. Thus it seems fair to say, that documentation of ancient graffiti faces much less controversy compared to other types of inscriptions.

A notable project in this regard is *The Ancient Graffiti Project (AGP)*<sup>3</sup> [42], which serves as a key resource for studying early Roman graffiti from Pompeii and Herculaneum. The AGP offers a digital search engine that facilitates detailed queries of its extensive graffiti database. The project has catalogued over 2,000 graffiti and continues to update and

[14]: Ross et al. (2017), ‘In search of academic legitimacy: The current state of scholarship on graffiti and street art’

[15]: Forster et al. (2012), ‘Evaluating the cultural significance of historic graffiti’

[16]: Verhoeven et al. (2023), ‘Finding listeners for walls that speak’

[17]: Ronchi (2009), *eCulture: cultural content in the digital age*

[18]: Deacon (2010), ‘Heritage Resource Management in South Africa’

[19]: Tombari et al. (2008), ‘Graffiti detection using a time-of-flight camera’

[20]: Gomes et al. (2017), ‘Conservation strategies against graffiti vandalism on Cultural Heritage stones: Protective coatings and cleaning methods’

[21]: Holler (2014), ‘GraffitiDok — A Graffiti Documentation Application’

[22]: Iglesia (2015), ‘Towards the scholarly documentation of street art’

[23]: Novak (2015), ‘Photography and Classification of Information’

[38]: Valente et al. (2020), ‘Methods for Ancient Wall Graffiti Documentation: Overview and Applications’

[39]: DiBiasie Sammons (2018), ‘Application of Reflectance Transformation Imaging (RTI) to the study of ancient graffiti from Herculaneum, Italy’

[40]: Benefiel et al. (2023), ‘Documenting Ancient Graffiti: Text, Image, Support and Access’

[41]: Abate et al. (2019), ‘HIDDEN GRAFFITI IDENTIFICATION ON MARBLE SURFACES THROUGH PHOTOGRAMMETRY AND REMOTE SENSING TECHNIQUES’

3: The AGP can be accessed using this link: <http://ancientgraffiti.org/Graffiti/> (last accessed: 23/07/2024)

[42]: Benefiel et al. (2019), ‘Wall Inscriptions in the Ancient City: The Ancient Graffiti Project’

expand its database. Designed to be accessible to both professionals and hobbyists, the database allows users to locate graffiti based on their geographical position by interacting with an ancient city map of Pompeii and Herculaneum. To mitigate the risk of graffiti being removed by tourist, the AGP does not share exact locations of the graffiti but only indicates the ancient houses in which which graffiti can be found. Additionally, the search functionality can be refined using various filters, making the database a valuable resource for systematic scientific analysis of Roman graffiti and providing insights into Roman society during these times. As such, this tool cannot only be considered a valuable resource for scientists but also for tourists visiting the sites, an activity conducted as part of the research for this thesis.

### 1.2.2 INGRID

Moving away from ancient to contemporary graffiti, INGRID is a very notable project concerning graffiti documentation. INGRID is an acronym for *Informationssystem Graffiti in Deutschland* (eng.: *Graffiti information system in Germany*). INGRID is a research project initiated in 2016, aiming at creating a detailed and systematic database for graffiti. This project represents an collaboration between the Karlsruhe Institute of Technology and the University of Paderborn, involving art historians and linguists to cover both the visual and textual aspects of graffiti. INGRID contains over 130,000 photographs of graffiti, mostly sourced from police departments in Mannheim, Cologne, and Munich, as well as from private collections and public archives [43]. The project has also actively involved local graffiti creators in the creation of the ontology and annotation processes. Key objectives include documenting and analysing the temporal development of graffiti with a focus on their visual aesthetics (colours, styles, sizes, etc.), their linguistic features (grammaticality and orthography), their geography and social functions [43, 44].

The first phase of the project (2016-2019) concentrated on building the ontology and systematically documenting graffiti, resulting in the annotation of over 40,000 graffiti images from Mannheim and Munich. The second phase (2020-2023) expanded the database with more than 50,000 additional photos from various sources, including police departments and private collections. This phase also aimed to create a comprehensive knowledge graph of annotated graffiti images to support advanced search capabilities, statistical analysis, and machine learning applications [45].

INGRID provides a platform for researchers to study the cultural and linguistic aspects of graffiti in Germany, offering freely accessible graffiti (meta)data via a web interface (Figure 1.4, [43]). This database is a well-curated datasource for those researching graffiti. However, as INGRID sources most of the graffiti documents from police departments, their documentation is likely biased and spatially scattered. Prosecution as main motivation for the initial documentation of graffiti likely leads to an over-representation of certain motives, styles or creators in their database. While it is an invaluable source for graffiti research, the ideal scenario for graffiti documentation would be the comprehensive inventorying of every graffiti(-like) creation for a well-defined geographical area.

[43]: Niemann (2022), 'INGRID—Archiving Graffiti in Germany'

[44]: Papenbrock et al. (2018), 'Graffiti digital. Das Informationssystem Graffiti in Deutschland (INGRID)'

[45]: Sherif et al. (2023), 'IngridKG: A FAIR Knowledge Graph of Graffiti'



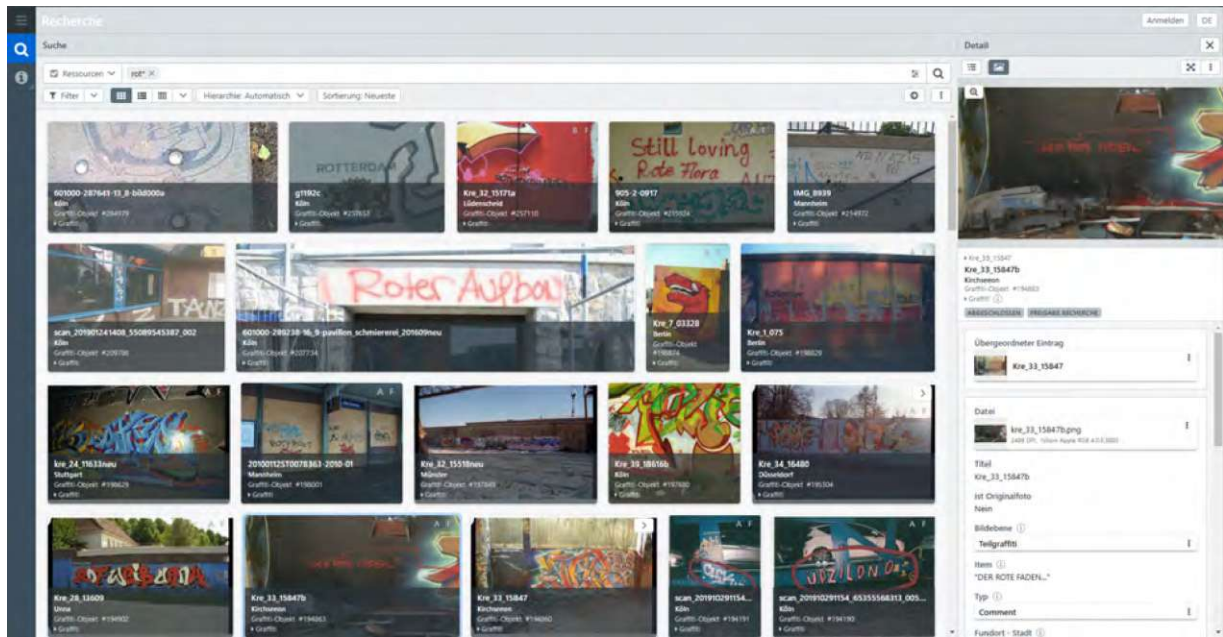


**Figure 1.4:** Screenshot of INGRID's database interface showing the results for the search term *rot* (eng. red) (accessible at: <https://media.uni-paderborn.de/search>, last accessed April 15, 2025).

### 1.2.3 Non-academic graffiti documentation

The distinction between academic and non-academic graffiti documentation and archival initiatives can be debated, as the criteria for what constitutes academic can be unclear. However, this distinction seems necessary in context of this dissertation, and is primarily based on the degree of institutionalisation and scientific outreach, such as through academic publications. The graffiti documentation initiatives classified as non-academic here do not explicitly target a scientific but a general graffiti-savvy audience. In fact, the largest existing graffiti archives lack an academic focus, instead they are mostly relying on individuals or small collectives who are passionate about graffiti.

Table 1.2 provides a non-exhaustive list of initiatives that freely disseminate graffiti records via the internet. The listed initiatives vary significantly in terms of geographical focus, scope, and methods of inventory and dissemination. While some projects collect graffiti from around the world, others focus exclusively on single cities, such as Mannheim (GER) or Atlanta (USA). The archives *Spraycity* and *Vagabundler* are notable for their extensive collections and wide geographical coverage, likely making them the most comprehensive managed graffiti archives available today.

*Art Crimes* stands out for several reasons. Firstly, it was a pioneering online graffiti archive made publicly available as early as 1994 [46]. It started as a static HTML web page at a time when the curator was unsure "(...) if the Web was going to be a big thing that the public ever accessed (...)" (Webb, 2024, p15). It defines itself as voluntary and collaborative, meaning that graffiti creators are encouraged to send photographs of their creations to *Art Crimes*. As such, it exemplifies the driving force behind non-academic graffiti inventories: enthusiasm for graffiti. Consequently, the quality of the photographs distributed on *Art Crimes* is varying. As they are often

[46]: Webb (2024), 'Building Art Crimes'

**Table 1.2:** Overview of online graffiti archives. The order of appearance is random. The corresponding websites were all last accessed on 24/07/2024. The number of graffiti records was either taken from the respective websites or by estimating the number from browsing through the corresponding archives or maps.

Name of Initiative	Focus Area	Number of Graffiti Records	URL
Mural Map - Open Urban Art Museum Mannheim	Mannheim (GER)	~40	<a href="https://www.stadt-wand-kunst.de">https://www.stadt-wand-kunst.de</a>
Art Crimes	Worldwide	~1,000	<a href="https://www.graffiti.org">https://www.graffiti.org</a>
Atlanta Street Art Map	Atlanta (USA)	~1,300	<a href="https://streetartmap.org">https://streetartmap.org</a>
George Floyd & Anti-Racist Street Art Map	Worldwide	~3,000	<a href="https://georgefloydstreetart.omeka.net">https://georgefloydstreetart.omeka.net</a>
Graffiti Archaeology	San Francisco (USA), New York (USA), Los Angeles (USA)	~100	<a href="http://grafarc.org/">http://grafarc.org/</a>
Streetartifacts	Portland and New York City (USA); Karachi (PK)	~200	<a href="https://streetartifacts.xyz/">https://streetartifacts.xyz/</a>
Street Art Belgrade	Belgrade (SRB)	~1,000	<a href="https://streetartbelgrade.com/">https://streetartbelgrade.com/</a>
Spraycity	Worldwide	~130,000	<a href="https://spraycity.at">https://spraycity.at</a>
Bombing Science	Worldwide	~1,000	<a href="https://www.bombingscience.com">https://www.bombingscience.com</a>
Street Art Cities	Worldwide	~10,000	<a href="https://streetartcities.com">https://streetartcities.com</a>
Vagabundler	Worldwide	~150,000	<a href="https://vagabundler.com">https://vagabundler.com</a>

old, they are of low resolution, many are cropped, blurry or severely under- or overexposed. Nevertheless they are, for most of the displayed graffiti, the only existing and accessible resource.

Generally, the mentioned initiatives centre the documentation around photographs. The ways the photographs are taken are almost as diverse as the graffiti they depict (Figure 1.5). Sometimes, a single graffito fills the entire camera frame, leaving no surrounding environment visible. In other instances, a graffito occupies only a small portion of the image, with the rest showing either other graffiti or the surrounding environment. Many images also show obvious post-processing. For example the example depicted in Figure 1.5C, which features several photographs stitched together to allow a complete and thus largely contextualised view of the graffitied wall.

While photographs are the backbone of most academic and non-academic graffiti archives, there is a notable exception: *Streetartifacts*. Instead of (2D) photographs, this platform features 3D models of approximately 200 graffiti in Portland (USA), New York (USA) and Karachi (PK) [47]. These models are presented interactively, allowing viewers to rotate the model, zoom in and out, and adjust the brightness of the texture (Figure 1.6). According to a discussion on the software developer platform *GitHub*<sup>4</sup>, initiated by the creator of *Streetartifacts*, the graffiti are scanned using an iPhone 12 Pro equipped with a LIDAR measurement unit, and the 2D

[47]: Baumann (2024), 'The Nuances of Mapping Street Art-Developing a Web Map for Interactive Graffiti Exploration (Master Thesis)'

4: <https://github.com/google/model-viewer/discussions/2337>, last accessed: 25/07/2024





**Figure 1.5:** Exemplary graffiti records from three online graffiti archives: (A) *Spraycity*: An overview photograph from 2024 of a section of Donaukanal, Vienna, Austria (accessible at: <https://spraycity.at/gallery/picture.php?/133158/category/1615>, last accessed 24/07/2024). (B) *Vagabundler*: An overview photograph (photographed by *Nomads on Wheels*) from 2024 showcasing various graffiti in the small Berber village Tamnougalt, Morocco (accessible at: <https://vagabundler.com/morocco/>, last accessed 24/07/2024). (C) *Art Crimes*: An image of graffiti in Chicago, USA, apparently stitched together from several photographs (accessible at: <https://www.graffiti.org/chicago/toystory.jpg>, last accessed 24/07/2024).

coordinates displayed on the map are measured with the same device. Additionally, *Streetartifacts* allows for the integration of the scanned graffiti walls in Augmented Reality (AR), which can be achieved by scanning a QR code with an AR-enabled device.



**Figure 1.6:** Screenshots from the *Streetartifacts* platform. A) depicts the map view which shows the location of the graffiti as point on a 2D map. B) depicts a textured 3D model of a graffiti. The 3D model can be accessed via the following link: <https://streetartifacts.xyz/?id=73>, last accessed: 25/07/2024.

The idea of placing graffiti in an AR is not entirely unique as it has also been implemented by an organisation called *Street Art Belgrade* in the form of a virtual exhibition [48]. This exhibition showcases photographs placed on artificially generated walls as well as fully 3D scanned graffiti-covered walls. It is curated, meaning the objects were manually placed at distinct location within the virtual space. This virtual exhibition allows users to virtually walk through the exhibition using compatible virtual reality headsets. Alternatively the exhibition can be accessed using any standard web browser. Descriptions about the graffiti are not as usually presented in the form of text but are available in the form of audio descriptions.

Both *Street Art Belgrade* and *Streetartifacts* add an additional geometric

[48]: Radošević (2022), 'Art in the Streets in the Virtual World'

dimension to the standard 2D surrogates typically published. In this context, *Graffiti Archaeology* is also noteworthy, as it extends the documentation dimension not geometrically but temporally. While most analysed archives capture temporality in a rudimentary manner, often represented as individual points in time indicating the date of documentation or graffiti creation, which is frequently difficult to reconstruct due to the typically clandestine nature of graffiti creation, *Graffiti Archaeology* offers a more nuanced approach.



**Figure 1.7:** Screenshots from the *Graffiti Archaeology* platform. Panels A), B), and C) show the wall *cavern-west B* at different times: A) on 02/11/2002, B) on 16/09/2007, and C) on 23/09/2007. The orange rectangles highlight the photo boundaries of the rectified and partially stitched images. Panel D) depicts the time slider situated at the bottom of the page, which allows users to navigate temporally through the scenes. The content can be accessed via the following link: <http://grafarc.org/flash/view.htm>, last accessed: 25/07/2024.



*Graffiti Archaeology* captures the process of constant change and makes it visually apparent. It features an interactive, time-lapse collage of photographs taken of 28 distinct walls in different cities in the United States over a span of several months to years. The photographs are undistorted and superimposed, allowing users to move through layers and experience the strong fluctuations of graffiti, with old graffiti being submerged beneath new ones (Figure 1.7). This dynamic visualisation enables viewers to observe the evolution of the displayed wall over time and explore the interactions between different graffitists as they create new graffiti.

This temporal component is solved by systematically revisiting and photographing graffiti that newly appeared along the selected walls. Each layer is composed of one or more photos, stitched together to create a panoramic image of the wall. To ensure a cohesive and accurate representation, all photos are aligned to correct for changes in perspective, and colour correction is applied if needed. According to the creator all this is achieved using *Adobe Photoshop*, along with a plug-in designed to fix issues like barrel lens distortion<sup>5</sup>. By carefully aligning and adjusting the photographs, a continuous view of the graffiti's evolution over time is created, allowing viewers to experience the dynamic nature of the graffiti in a detailed and engaging manner [50].

Most archives enhance basic digital images with metadata, which can be presented as a collection of individual words (usually referred to as *tags* or *keywords*). *Spraycity*, for example, enriches every photo of a graffito with certain standardised tags. These tags allow for a targeted filtering of certain graffiti according to their colours, styles, locations and documentation dates, substantially improving the usability of the database. Most archives also include some sort of geographical information alongside the mere images. In most instances a graffito's location is reduced to a 2D coordinate pair which is also often displayed on a map. Some archives additionally incorporate street addresses, name of the neighbourhoods or districts. *Spraycity*, for example, also adds information on the type of environment the graffito is situated in (e.g., *bridge pillar*, or *train*). It is evident that a central aspect of every archive is the location where graffiti were created. This is in line with what transpired during a discussion session [51] on graffiti documentation where Viennese graffiti creators *Janer One* and *Manual Skirl* stated the following:

**JANER ONE:** "[...] if you are a good photographer, you are mindful of the context and some pieces only are the way they look because of the wall. Oftentimes the spot determines how the piece flows."

**MANUEL SKIRL:** "If you have a beautiful scenery. I can only, again, talk for myself, but I'm sure that the other guys are doing that as well. You go to some abandoned building and you see some really nice rusty spots where you can already imagine what you are doing and even holding my phone there to see how big I'm going to paint. To have the perfect end result. And because the end result isn't paint on the wall, right? It's the photo on my phone. Because that's everything that's left for me."

Besides the relevance of a graffito's location, these remarks exemplarily emphasise that graffiti documentation is not only significant to the academic community but also to the graffiti creators themselves, who

5: Barrel lens distortion, often associated with wide-angle lenses, causes the image to appear curved and bowed outward at the edges, as if the photo has been wrapped around a curved surface [49]

[50]: Curtis et al. (2004), 'Graffiti archaeology'

[51]: Wild et al. (2022), 'Imagine Being a Racist': goINDIGO 2022's «Ethics & Legality in Graffiti (Research)» Discussion Round'

often see the digital representation as the final outcome of their work. Therefore, substantial thought is put into photographing graffiti, indicating that documenting the spatial context solely through 2D images and coordinates do not fully capture the essence of graffiti. This thesis, therefore, places strong emphasis on exploring new methods of documenting graffiti through photographs, while situating them within their accurate spatial and, consequently, temporal context.

### 1.2.4 The role of social media in graffiti documentation

Lastly, Meta's *Instagram*, along with other social media platforms such as *X* (formerly known as *Twitter*), *Pinterest*, and *Facebook*, significantly surpasses all other resources in terms of the sheer volume of graffiti records. Many graffiti creators today actively use *Instagram* to upload photographs and provide brief descriptions of their works, making it a central hub for graffiti content. An exemplary *Instagram* feed of a creator who is also active along Donaukanal can be seen in Figure 1.8. Some creators even state that they consider the, rather unusual, image aspect ratio of 1:1 when creating the graffiti to allow for an optimised dissemination via *Instagram* [51].

Graffiti has become an increasingly popular subject for social media posts, resulting in a vast number of graffiti images being shared online daily. This spontaneous and widespread sharing of graffiti imagery represents both a challenge and an opportunity for academic research. On one hand, the potential of *Instagram* as a comprehensive graffiti database is immense, offering a rich repository of visual records. On the other hand, its utility is significantly constrained by the almost complete lack of accompanying metadata. Typically, the only metadata available are the upload timestamp and the username of the uploader, which are often insufficient for detailed academic analysis.

The use of hashtags—keywords or phrases preceded by the “#” symbol that are used to categorise content, enhance searchability, and facilitate topic-based conversations—can somewhat mitigate this limitation by improving the discoverability of specific graffiti posts. Another challenge in social-media-driven graffiti analysis, particularly from a scientific perspective, is the inherent bias associated with social media posts. If one examines the social media accounts of some active graffiti creators, one gets the impression that these social media accounts are often carefully curated collections rather than a random or complete representation of their output leaving it largely impracticable to create a scientifically sound graffiti database based on social media posts. This was also mentioned by graffiti creators who are active along Donaukanal during a discussion session on this topic in 2022 [51].

Despite its limitations, *Instagram* has proven valuable in aiding the identification of graffiti changes in the early stages of the research project related to this dissertation (see Chapter 3.1).

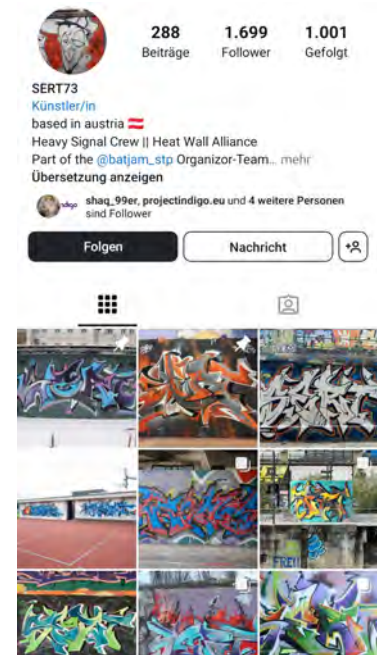


Figure 1.8: Screenshot of a graffiti creator's *Instagram* feed.

[51]: Wild et al. (2022), “Imagine Being a Racist”: goINDIGO 2022's «Ethics & Legality in Graffiti (Research)» Discussion Round

### 1.3 Graffiti - a matter of space and time

The preceding chapters have demonstrated that photographs serve as the cornerstone of graffiti documentation. However, photographs are inherently static, capturing the state of an object at a specific moment in time<sup>6</sup>. Graffiti on the other hand are inherently dynamic. Graffiti walls are like a living canvas continuously shaped by various factors. Each graffiti has its unique temporality — some works are quickly covered or destroyed, while others can persist for centuries. This temporal complexity, where new creations often emerge from modifying or incorporating elements of older works, adds layers of meaning and context (see Figures 1.9 and 1.10). While the date of a photograph captures a single moment, it does not encapsulate the graffiti's entire history. Therefore, documenting graffiti requires acknowledging the separation between the creation of the graffiti and the moment it is photographed, along with understanding the temporalities of production, visibility, and documentation [52].

*Graffiti Archaeology* is likely the only graffiti documentation project that explicitly addresses the challenge of time. It achieves this by overlaying consecutively created graffiti, thus creating a spatio-temporal connection between the layers of graffiti. This approach serves as an excellent example of how temporality in graffiti documentation can be resolved through geometrical analysis. This method assumes that graffiti are additive, with visible graffiti always being newer than the partially visible or invisible graffiti beneath. This spatio-temporal stratification concepts allows us to recover temporal information solely based on geometrical information.

Verhoeven et al. (2024) [52] suggest using polygons as basis for spatio-temporal reasoning in graffiti documentation. By knowing the *where* we can approximate the *when*. This spatio-temporal link is vital in graffiti due to its dynamic and interactive character. Especially but not exclusively for graffiti conveying political views, there is significant interaction (in)visible. In many cases graffiti artists communicate through their graffiti, but this dialogue is per-definition mostly destructive as reactions typically involve partially or entirely covering (or destroying) the underlying creations. A rare exception, where both the action as well as reaction can be seen is depicted in Figure 1.10.



6: While exposure times can extend for several seconds or longer, complicating the idea of a singular moment, the notion *moment* still seems appropriate in this context.

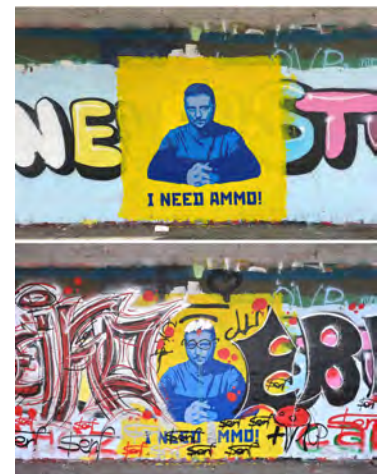


**Figure 1.9:** Example of a dynamic graffiti scene at one of Donaukanal's legal *Wienerwände* showing a political statement in the context of the war in Ukraine. Only days later this message has been largely covered and altered.

**Figure 1.10:** A graffiti dedicated to the Viennese football club Austria Wien (abbreviation: FAK). The original message above (highlighted in red) read "TOD UND HASS DEM FAK" (English: "Death and hate to the FAK"), but was later altered to "KOKS UND HASCH DEM FAK" (English: "Coke and hash to the FAK"). The image was downloaded from [spraycity.at](https://spraycity.at).



The short-lived nature of graffiti, often seen as one of its key features, creates challenges for those who study it. Because graffiti tends to disappear quickly, it can be difficult to get a complete and unbiased view of a graffiti-scape. Once a graffiti is covered by another layer, recovering it in their original setting is practically impossible, making it hard to analyse how graffiti evolve in space and time.

Although graffiti go through similar processes as artifacts found in archaeological sites or natural landscapes, the way we study them is different [10]. Unlike archaeological sites, where layers of history can be uncovered through careful physical digging, graffiti-scapes cannot be explored in this way. When graffiti is covered or removed, it often becomes a forgotten part of history. This loss can hide not only the cultural value but also the social and political messages they once might have conveyed. Instead of physical archaeological excavation, graffiti documentation requires action before stratification evolves. Thus, this dissertation deals with digital, photogrammetric approach to safeguard graffiti before they disappear.

[10]: Verhoeven et al. (2022), 'Project IN-DIGO: document, disseminate & analyse a graffiti-scape'

## 1.4 Research Questions

Despite the considerable activity in graffiti documentation, the current state-of-the-art reveals a lack of scientific rigour in certain areas, leaving them with limited usability for scholars who study graffiti.

### The overarching aim of this thesis is thus:

*Introducing scientific rigour in the documentation of graffiti through photogrammetry.*

One major issue with existing archives is their incompleteness, which is unsurprising given the high volatility of graffiti-scapes. Graffiti creation and destruction often occur simultaneously, and the spontaneous nature of graffiti means that many, especially smaller pieces, are created opportunistically *when nobody is looking*. Therefore, a key objective of this thesis is to explore the automation of new graffiti identification. This process of graffiti change detection represents the initial step in the documentation workflow.

### Chapter three will address graffiti change detection and will primarily focus on the following research questions:

1. What is the current state-of-the-art in graffiti change detection and comparable change detection tasks?
2. What are the primary challenges in detecting graffiti-related changes in images?
3. How can images of an extensive graffiti-scape be efficiently acquired? How feasible is the use of mobile camera systems (e.g., mounted on bikes) for comprehensive and repeatable graffiti documentation, and what are the key challenges in their implementation?
4. How can the the acquired imagery be co-registered to derive pixel-perfectly aligned images of two different epochs with minimal manual

*intervention.*

5. *What pre-processing strategies can be employed to enhance pixel-based change detection?*
6. *How can image descriptors be utilised to indicate changes in graffiti?*
7. *How effectively, accurately, and robustly can new graffiti be distinguished from unchanged scenes using an automated framework?*

Chapter four will address the procedures and strategies employed after the identification of graffiti. This chapter will specifically explore methods to mitigate the issue of decontextualisation in graffiti documentation by ensuring the preservation of the spatial and environmental context through photogrammetric techniques.

#### **The following research questions will be tackled in Chapter 4**

8. *Are orthophotos a suitable documentation of graffiti and what other strategies exist?*
9. *What is necessary to derive orthophotos and how can this process be automated?*
10. *What challenges and limitations arise when applying Structure-from-Motion (SfM) techniques to the orthorectification and georeferencing of graffiti imagery, and how can these be mitigated?*
11. *Can the proposed framework effectively process the large volumes of graffiti photos expected in rapidly changing urban graffiti-scapes, while maintaining high accuracy and efficiency?*
12. *What are the advantages and drawbacks of direct georeferencing techniques (e.g., using RTK GNSS and IMU) compared to the current incremental SfM approach in graffiti documentation?*
13. *How can occlusions and environmental constraints be managed during the image acquisition and processing phases to ensure the quality of orthophotos derived from graffiti scenes?*
14. *How can orthophotos be displayed in 2D and 3D maps. Which metadata is required and which generalisations need to be made.*
15. *Which quality and efficiency can be reached when applying the methodology to an extensive dataset?*

Chapter five will focus less on the technical aspects of large-scale graffiti documentation and instead present a case study involving graffiti of exceptional cultural and historical significance. The case study was conducted along sections of the Turkish West coast, a region known for frequent clandestine crossings of refugees across the Mediterranean to the European Union border on the island of Lesbos, Greece. Along the Turkish West Coast from where the island of Lesbos is well visible, several hidden, short-term migrant stations were documented, with a particular focus on graffiti created by migrants while they waited for the clandestine crossing towards the grounds of the European Union.

#### **The associated research topic tackled by this case study can be framed as follows:**

16. *This study explores how graffiti can be documented in a setting with limited time and a stressful environment, characterised by distressing*

*impressions and the constant concern about meeting local authorities and human traffickers. Given these circumstances, is the photogrammetric graffiti documentation limited or does the photographic approach provide advantages?*

## 1.5 Related Publications

This work is largely based on the following publications:

### Papers published in peer-reviewed journals:

1. Wild, B., Verhoeven, G. J., Wieser, M., Ressler, C., Schlegel, J., Wogrin, S., Otepka-Schremmer, J., & Pfeifer, N. (2022). AUTOGRAF—AUTomated Orthorectification of GRAffiti Photos. *Heritage*, 5(4), 2987–3009. <https://doi.org/10.3390/heritage5040155> [53]
2. Wild, B., Verhoeven, G., Muszyński, R. & Pfeifer, N. (2024). Detecting change in graffiti using a hybrid framework. *The Photogrammetric Record*, 00, 1–28. <https://doi.org/10.1111/phor.12496> [54]

### Papers published in peer-reviewed conference proceedings:

3. Wild, B., Verhoeven, G. J., & Pfeifer, N. (2023). Tracking the urban chameleon - towards a hybrid change detection of graffiti. In *Volume X-M-1-2023, 2023 | 29th CIPA Symposium "Documenting, Understanding, Preserving Cultural Heritage. Humanities and Digital Technologies for Shaping the Future"* (pp. 285–292). ISPRS, Copernicus Publications. <https://doi.org/10.5194/isprs-annals-X-M-1-2023-285-2023> [55]
4. Wild, B., Jungfleisch, J., & Pfeifer, N. (2025). Documenting migrant graffiti in the borderscapes of the Eastern Mediterranean. ISPRS Archives – Proceedings of the CIPA 2025 Conference. Seoul, South Korea. (Extended abstract, submitted for review). [56]
5. Wieser, M., Verhoeven, G., Wild, B., and Pfeifer, N.: Exterior Orientation in a Box: Cost-Effective RTK/IMU-Based Photo Geotagging, *Int. Arch. Photogramm. Remote Sens. Spatial Inf. Sci.*, XLVIII-2/W8-2024, 463–470, <https://doi.org/10.5194/isprs-archives-XLVIII-2-W8-2024-463-2024>, 2024 [57]
6. Verhoeven, G., Wild, B., Schlegel, J., Wieser, M., Pfeifer, N., Wogrin, S., Eysn, L., Carloni, M., Koschiček-Krombholz, B., Molada-Tebar, A., Otepka-Schremmer, J., Ressler, C., Trognitz, M., & Watzinger, A. (2022). PROJECT INDIGO – DOCUMENT, DISSEMINATE & ANALYSE A GRAFFITI-SCAPE. In *The International Archives of the Photogrammetry, Remote Sensing and Spatial Information Sciences* (pp. 513–520). <https://doi.org/10.5194/isprs-archives-xlvi-2-w1-2022-513-2022> [10]

### Other related publications:

7. Wild, B., Verhoeven, G. J., Wogrin, S., Wieser, M., Ressler, C., Otepka-Schremmer, J., & Pfeifer, N. (2023). Urban Creativity Meets Engi-



- neering. Automated Graffiti Mapping along Vienna's Donaukanal. In G. J. Verhoeven, J. Schlegel, B. Wild, S. Wogrin, & M. Carloni (Eds.), *Document, archive, disseminate graffiti-scapes: Proceedings of the goINDIGO 2022 International Graffiti Symposium* (pp. 131–145). Urban Creativity / AP2. <https://doi.org/10.48619/indigo.v0i0.705> [58]
8. Verhoeven, G. J., Carloni, M., Schlegel, J., Wild, B., & Wogrin, S. (2023). Finding listeners for walls that speak. In G. J. Verhoeven, J. Schlegel, B. Wild, S. Wogrin, & M. Carloni (Eds.), *Document, archive, disseminate graffiti-scapes: Proceedings of the goINDIGO 2022 International Graffiti Symposium* (pp. 6–15). Urban Creativity / AP2. <https://doi.org/10.48619/indigo.v0i0.699> [16]
  9. Verhoeven, G. J., Wogrin, S., Schlegel, J., Wieser, M., & Wild, B. (2023). Facing a chameleon - how project INDIGO discovers and records new graffiti. In G. J. Verhoeven, J. Schlegel, B. Wild, S. Wogrin, & M. Carloni (Eds.), *Document, archive, disseminate graffiti-scapes: Proceedings of the goINDIGO 2022 International Graffiti Symposium* (pp. 63–85). Urban Creativity / AP2. <https://doi.org/10.48619/indigo.v0i0.703> [59]
  10. Wild, B., Verhoeven, G., Pfeifer, N., Bonadio, E., HERO, D., F., ONE, J., SKIRL, M., Carloni, M., Ricci, C., Koblit, C., Niemann, S., Radošević, L., Schlegel, J., Watzinger, A., & Wogrin, S. (2023). 'Imagine Being a Racist': goINDIGO 2022's «Ethics & Legality in Graffiti (Research)» Discussion Round. *Document | Archive | Disseminate Graffiti-Scapes*, 45–62. <https://doi.org/10.48619/indigo.v0i0.702> [51]
  11. Wild, B., Verhoeven, G. J., Wieser, M., Ressler, C., Otepka-Schremmer, J., & Pfeifer, N. (2023). Graffiti-Dokumentation: Projekt INDIGO. In 22. *Internationale Geodätische Woche Obergurgl 2023* (pp. 322–325). Herbert Wichmann Verlag. [60]
  12. Merrill, S., Verhoeven, G., Wild, B., ONE, J., SKIRL, M., Carloni, M., de la Iglesia, M., Merino, F., Radošević, L., Ricci, C., Schlegel, J., & Wogrin, S. (2023). 'Different Folks, Different Strokes': goINDIGO 2022's «Creators vs Academics» Discussion Round. *Document | Archive | Disseminate Graffiti-Scapes*, 25–44. <https://doi.org/10.48619/indigo.v0i0.701> [1]
  13. Verhoeven, G. J., Schlegel, J., & Wild, B. (2024). Each Graffito Deserves Its Polygon—It Is About Time. *Disseminate, analyse, understand graffiti-scapes: Proceedings of the goINDIGO 2023 International Graffiti Symposium*, 163–185. <https://doi.org/10.48619/indigo.v0i0.981> [52]

## Bachelor and Master Theses supervised in the framework of this dissertation

14. Baumann, O. (2023). Mapping Street Art: Developing Cartographic Visualisation of Graffiti (Master's thesis). Master Programme Geodesy and Geoinformation (066 421), TU Wien. Supervised by Norbert Pfeifer and Benjamin Wild [47]
15. Rachbauer, M. (2022). Analyse verschiedener Methoden zur Graffiti Segmentierung (Bachelor's thesis). Bachelor Programme Geodesy and Geoinformation (033 221), TU Wien. Supervised by Norbert Pfeifer and Benjamin Wild [61]

For all publications in which I am the first author [53–55, 58, 60], except

[53]: Wild et al. (2022), 'AUTO-  
GRAF—AUTomated Orthorectification  
of GRAFFiti Photos'

[54]: Wild et al. (2024), 'Detecting change  
in graffiti using a hybrid framework'

[55]: Wild et al. (2023), 'TRACKING THE  
URBAN CHAMELEON - TOWARDS  
A HYBRID CHANGE DETECTION OF  
GRAFFITI'

[58]: Wild et al. (2023), 'Urban Creativity  
Meets Engineering. Automated Graffiti  
Mapping along Vienna's Donaukanal'

[60]: Wild et al. (2023), 'Graffiti-  
Dokumentation: Projekt INDIGO'

for [51], I was the main contributor and responsible for conceptualising, designing and implementing the study, as well as drafting the corresponding publication. [51] constitutes a special case as it is the result of a discussion session during the goINDIGO 2022 symposium with transcribed verbal contributions from multiple participants, including graffiti scholars and graffiti creators. In this case, first authorship primarily reflects responsibility in preparing the symposium, and the individual session as well as transcribing this discussion in which I also actively participated.

Verhoeven et al. (2022) [10] serves as a foundational work for this thesis, as Chapters 3 and 4 partly build upon the data collected, processed and presented in this study. My co-authorship in this publication mainly reflects my involvement in planning, executing, and processing total station measurements along the Donaukanal for georeferencing the geometric backbone (Chapter 2.2.1), investigating the applicability of planar rectification for graffiti photos (Chapter 4.2), and reviewing and revising the contribution text. Planning, executing and processing total station measurements to obtain control points and revising the written draft also led to co-authorship in [57]. The concept, design and execution was conducted by the respective first-authors.

For the remaining listed publications [1, 16, 52, 59], my level of involvement varied but was generally less substantial. However, I consistently contributed by reviewing and refining the written drafts and providing support to the co-authors as needed.

Regarding the Bachelor's and Master's theses [47, 61], I supported students in defining their research topics, providing relevant data, aiding in methodological approaches, and guiding them through the analysis and interpretation of results. Additionally, I offered feedback on their written work, and facilitated discussions among the main supervisor, Prof. Norbert Pfeifer, to ensure the academic quality and relevance of their studies. In addition to the two aforementioned theses, I co-supervised another Master thesis [62] and three Bachelor theses [63–65], all of which focused on applying photogrammetric techniques to forest-related topics.

This dissertation is formally submitted as a monography, unlike a cumulative dissertation, where previously published articles are typically included without any modifications, preserving their original layout and text. Although this work does not republish and reprint complete articles in that format, it bears some similarities to a cumulative dissertation due to the substantial number of publications produced during this PhD, with portions of this dissertation having been previously published in various forms across above-mentioned related publications. Notably, Chapters 3 and 4 are mostly directly based on peer-reviewed articles but have been extended, reformatted and partly reformulated to better integrate with the overall flow of this monography.

## 1.6 Structure of this thesis

This thesis is structured to address the challenges of graffiti documentation through automation and photogrammetric techniques. The remain-

[51]: Wild et al. (2022), 'Imagine Being a Racist': goINDIGO 2022's «Ethics & Legality in Graffiti (Research)» Discussion Round'

[10]: Verhoeven et al. (2022), 'Project INDIGO: document, disseminate & analyse a graffiti-scape'

[57]: Wieser et al. (2024), 'Exterior Orientation in a Box: Cost-Effective RTK/IMU-Based Photo Geotagging'

[47]: Baumann (2024), 'The Nuances of Mapping Street Art-Developing a Web Map for Interactive Graffiti Exploration (Master Thesis)'

[61]: Rachbauer (2022), *Analyse verschiedener Methoden zur Graffiti-Segmentierung (Bachelor Thesis)*

[62]: Neumayr (2024), *Assessing forest parameters through the evaluation of smartphone-based measurement techniques (Master Thesis)*

[63]: Starzer (2024), *Smartphone-basierte Bestimmung des Brusthöhendurchmessers von Bäumen (Bachelor Thesis)*

[64]: Leitner (2024), *Segmentierung und Klassifizierung von Bäumen auf Basis von Smartphone-Aufnahmen (Bachelor Thesis)*

[65]: Lamprecht (2024), *3D-Modellierung von Stadtbäumen mit RayCloudTools (Bachelor Thesis)*

ing content is divided into the following chapters:

**Chapter two** introduces the Donaukanal in Vienna, a 17.3 km canal that has become one of the largest graffiti hotspots globally and is thus an ideal study site in the framework of this thesis. Furthermore this chapter introduces the graffiti-centred research project INDIGO which provided the scientific and organisational framework for this dissertation. Lastly, INDIGO's so-called photogrammetric backbone is introduced in chapter two, setting the stage for the subsequent photogrammetric developments of this work.

**Chapter three** focuses on the initial step in graffiti documentation—detecting changes in graffiti over time. It explores current methods and challenges in image-based change detection, evaluates the use of mobile camera systems for efficient image capture, and discusses strategies for co-registering images for precise alignment. It also covers pre-processing techniques and the application of image descriptors to identify changes, aiming to develop a robust automated detection framework.

**Chapter four** details the techniques for processing images after graffiti identification to preserve their spatio-temporal context. It evaluates the effectiveness of planar rectification and orthophoto generation for documenting graffiti. Furthermore, this chapter introduces a novel tool enabling the automation of the orthorectification. The chapter lastly addresses challenges in processing and visualising large datasets and discusses the feasibility of utilising direct georeferencing techniques for speeding up the computation times and increasing robustness of the introduced approach.

**Chapter five** presents a case study that illustrate the challenges of graffiti in more complex scenarios. The case study was conducted during a research project along the Turkish west coast, highlights rapid documentation under time constraints and challenging conditions.

**Chapter six** summarises the developed methodologies and highlights the most important results. Furthermore conclusions are drawn and an outlook on possible further developments in the field of photogrammetric methods for graffiti documentation are given.





## 2 Donaukanal and project INDIGO

### 2.1 Donaukanal - a graffiti-scape

The Donaukanal (eng.: *Danube Canal*) is a branch of the Danube River that runs closest to Vienna's city centre. Spanning in total 17.3 km (measured along the center of the waterway), it diverges from the main river at *Nussdorf* and reconnects near the *Albern Harbor*. The canal serves as a natural boundary, separating the districts of *Leopoldstadt* (2nd district) and *Brigittenau* (20th district) from the Inner City and other districts on the right bank. Historically, the Donaukanal featured summer baths and wooden bathing ships. Over time, it has increasingly transformed into an important recreational area, home to numerous cultural and gastronomic venues. Today, it hosts regular music festivals and events, solidifying its status as a cultural hub in Vienna. Alongside its cultural significance, the Donaukanal has emerged as a prominent graffiti hotspot.

2.1 Donaukanal - a graffiti-scape . . . . .	20
2.2 Objectives and Achievements of Project INDIGO . . . . .	21
2.2.1 INDIGO's photogrammetric backbone . . . . .	22
2.2.2 Ethical considerations surrounding INDIGO's objectives . . . . .	27

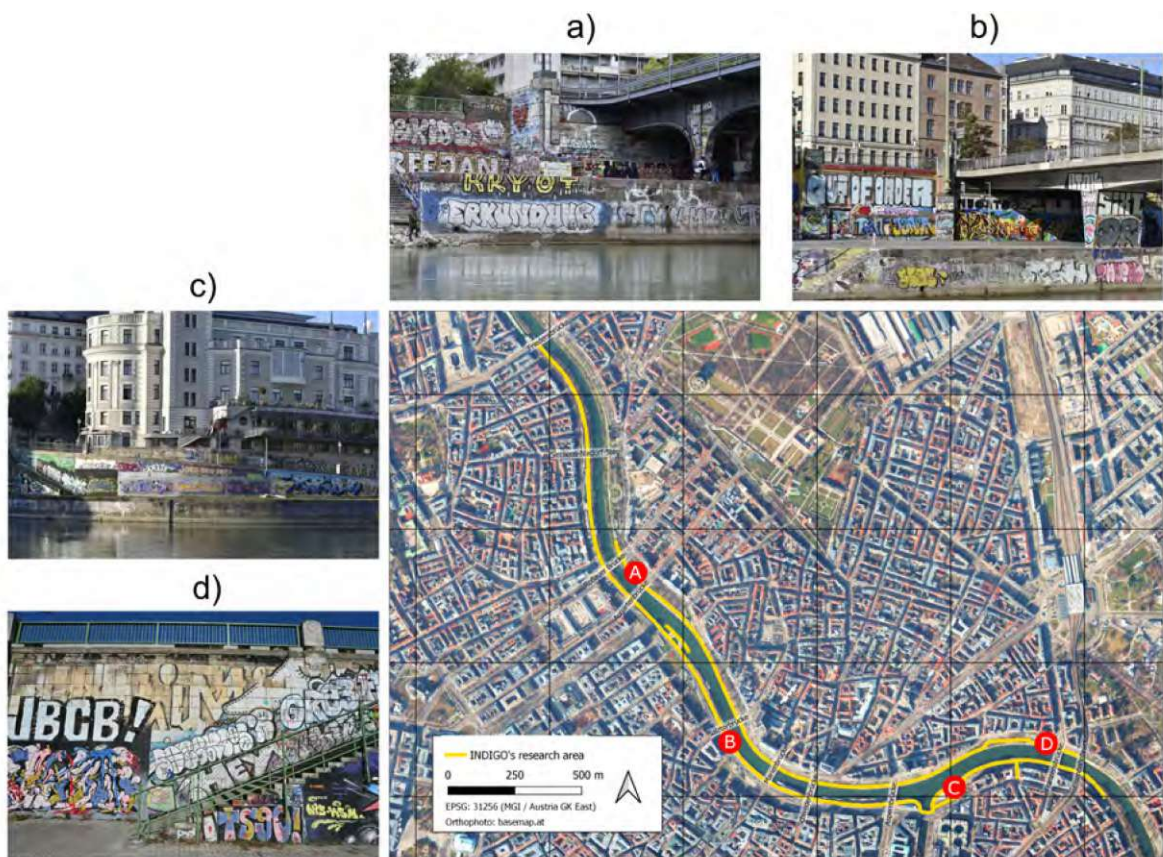


**Figure 2.1:** a)-d): Example images of the graffiti-covered surfaces at the Donaukanal and their respective approximate location along Donaukanal.

Since the early 1980s, large portions of the Donaukanal have undergone significant textural changes [66]. The once gray concrete walls have largely been replaced by a vast array of graffiti, making the Donaukanal one of the largest, if not the largest, consecutive graffiti areas in the world. This continuous stretch of graffiti is roughly bounded by two bridges: the *Verbindungsbahnbrücke* in the southeast and the *Friedensbrücke* in the northeast. While graffiti is also present outside this core area, the presence of parks that do not offer suitable surfaces for graffiti has led to these zones being less connected and generally less active. Consequently, this thesis focuses on the approximately 3.3 km stretch of the Donaukanal that is now almost entirely covered with graffiti. Figure 2.1 depicts overview photos of different parts along Donaukanal, highlighting the diversity and complexity of the graffiti-scape today.

The above-mentioned 3.3 km refers to an imaginary line, measured along the central waterway. The graffiti landscape of the Donaukanal can be further divided into a left and right bank, with left and right being relative to the flow direction of the Danube. Each bank has upper and lower sections: the upper parts refer to the walls adjacent to the walking and cycling paths, while the lower parts refer to the walls that border the actual waterway [10].

Quantifying the size of the graffiti-covered surfaces is challenging due to the complexity of the area [10]. However, a full photogrammetric survey conducted in 2021 (detailed in Chapter 2.2.1) revealed that the combined length of all graffiti-covered surfaces, including vertical walls, ramps, bridge pillars, and staircases, is approximately 13 km [10]. While this method of quantification has its limitations, it is crucial from an organisational perspective to estimate the approximate paths that need to be covered during surveys.

## 2.2 Objectives and Achievements of Project INDIGO

This chapter introduces the graffiti-focused research project INDIGO. Large parts of the work presented in this thesis was conducted within the framework of INDIGO. Chapter 2.2 and 2.2.1 are largely based on Verhoeven et al. (2022) [10] published under CC BY 4.0 license.

Project INDIGO (IN-ventory and DI-sseminate G-raffiti along the D-O-naukanal) was a two-year research initiative that began in September 2021, funded by the Austrian Academy of Sciences (ÖAW) under the Heritage Science Austria programme. The project focused on documenting, monitoring, and analysing graffiti along Donaukanal in Vienna, between *Friedensbrücke* and *Verbindungsbahnbrücke*. This stretch, although mostly unauthorised<sup>1</sup>, features a variety of fully graffiti-covered urban structures such as walls, staircases, bridge pillars, and embankments (Figure 2.1). The main goal of Project INDIGO was to establish a comprehensive approach for systematic graffiti documentation. This documentation involves detecting and capturing graffiti, processing the collected data to derive high-quality digital graffiti surrogates, and disseminating the collected records. A visual representation of the documentation process can be seen in Figure 2.2.

[66]: Ringhofer et al. (2018), 'Die Kunst der Straße–Graffiti in Wien'

[10]: Verhoeven et al. (2022), 'Project INDIGO: document, disseminate & analyse a graffiti-scape'

[10]: Verhoeven et al. (2022), 'Project INDIGO: document, disseminate & analyse a graffiti-scape'

1: only approximately 300m of the ca. 13km graffitied surfaces are designated legal graffiti surfaces



The documentation aspect of the project focused on gathering detailed information about the graffiti's geometric, spectral, geographic, temporal, and contentual characteristics. This included 3D surface mapping, high-resolution photography, and metadata collection, such as graffiti themes, types and styles. The aim was to create a detailed digital record that accurately reflects the graffiti as a dynamic form of urban cultural heritage.

The second major focus was the development of an open-access online platform, which would allow users to explore the graffiti-scape interactively. This platform was designed to support researchers and the public, enabling queries on the graffiti's temporal and spatial changes. The platform was planned to incorporate 2D and 3D visualizations of the graffiti and their surrounding, and standardised metadata, ensuring a consistent approach to recording and presenting graffiti information. A prototype of this platform was developed and is discussed as part of Chapter 4.6.

In terms of analysis, the project aimed to set the basis for analysing graffiti in unprecedented detail and comprehensiveness. By studying where, when, and how different types of graffiti appeared and were overwritten, the project, for example, aimed to provide insights into the broader socio-political aspects of urban graffiti. This can analysis can then support our understanding graffiti's role in the urban environment and its evolution over time.

To achieve these goals, project INDIGO was organised around five key activities: data acquisition, processing, management, dissemination, and analysis. Data were gathered through regular photo documentation and metadata collection. High-resolution photography was used to capture both new and changing graffiti, with attention to accurate colour representation [67]. The collected data were then processed, tagged with metadata, corrected for geometric distortions using 3D models, and converted into standardised formats. A controlled vocabulary was also developed to maintain consistency in classifying graffiti types and styles. The open-access platform should allow users to explore the graffiti-scape through interactive 3D views, browse images, and query metadata, with future plans for augmented reality features and citizen science initiatives. Eventually a prototype of this platform did go live (discussed in Chapter 4.6).

Project INDIGO successfully laid the groundwork for future research and public engagement. Significant progress was made in developing methods for documenting the graffiti-scape, including the creation of software tools and collaborative efforts that resulted in several peer-reviewed publications and open-source resources. Although not all initial objectives were fully realised, the project established a strong foundation for continued study and preservation of graffiti as an important element of urban culture, with potential for further development in a follow-up project.

### 2.2.1 INDIGO's photogrammetric backbone

In September and October 2021 a complete photographic coverage was conducted along INDIGO's designated research area (marked in violet

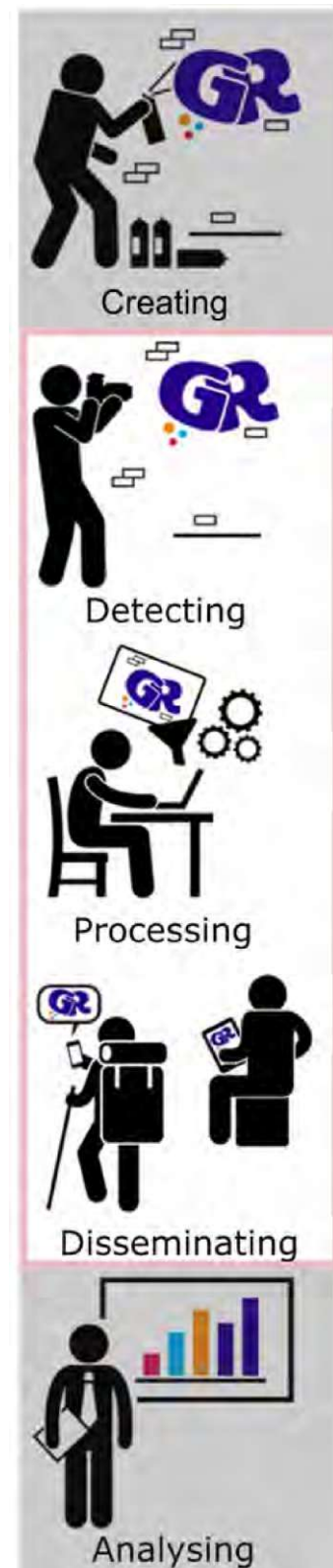


**Figure 2.2:** Overview of project INDIGO's main objectives highlighted in the red frame: detection, processing, and dissemination of graffiti.

[67]: Molada-Tebar et al. (2024), 'Practical RGB-to-XYZ Color Transformation Matrix Estimation under Different Lighting Conditions for Graffiti Documentation'

in Figure 2.3). This full photogrammetric coverage ultimately serves as INDIGO's photogrammetric backbone, which has three main purposes:

1. Creating a detailed record of the graffiti landscape at a specific time.
2. Setting the base for future photogrammetric processing, such as an incremental bundle block adjustment.
3. Constructing a comprehensive, continuous 3D surface mesh of the Donaukanal, enabling the placement of graffiti (ortho-)photographs in their native, albeit digital, environment.

As a result, the entire research area was documented through several photography campaigns (see Table 2.1) leading to the establishment of a photogrammetric backbone. An unexpectedly low water level in the Donaukanal in late September 2021 provided an opportunity to capture graffiti on surfaces that are usually submerged or located just above the waterline. Efforts were made to minimise any alterations to the graffiti during the process, but the large area covered and suboptimal weather conditions in October 2021 led to some delays. Although some changes were inevitable, this photographic campaign marks a key moment in documenting Donaukanal's graffiti-scape.

### Image Acquisition Strategy

The primary goal of the first image acquisition was to document the lower parts of the concrete embankment channelling much of the Donaukanal in the INDIGO study area (see examples in Figure 2.1). These photographs were taken from the opposite bank using an 85 mm lens on a Nikon D750 24-megapixel full-frame DSLR camera. With an approximate average distance of 50 m between the camera and embankment, the resulting mean Ground Sampling Distance (GSD) was 3.6 mm, ranging from 2.9 to 4.8 mm depending on separation distance (42 m to 68 m).

A higher resolution approach was used for urban structures adjacent to the embankment, employing a 20 mm lens on a 45-megapixel full-frame Nikon Z7 II. This setup produced an average GSD four times smaller than the embankment images. Details of both image acquisition campaigns are summarised in Table 2.1.

**Table 2.1:** Full photographic coverage acquisition parameters. Adopted from [10].

Date	Camera	Lens	Mean GSD	Acquisition Time	Image Count
30/09/2021	Nikon D750	85mm @ f/5.6	3.6 mm	3h 45min	2,065
01/10/2021	Nikon D750	85mm @ f/5.6	3.6 mm	3h 20min	2,544
26/10/2021	Nikon Z7 II	20mm @ f/5.6	0.9 mm	7h	6042
27/10/2021	Nikon Z7 II	20mm @ f/5.6	0.9 mm	7h 45min	6,591
28/10/2021	Nikon Z7 II	20mm @ f/5.6	0.9 mm	3h 40min	2,856
29/10/2021	Nikon Z7 II	20mm @ f/5.6	0.9 mm	7h	6608
<b>Total</b>				32h 30min	26706

The choice of GSD was dictated by the type of surface: weathered graffiti on the embankments just above the water surface were only photographed from the opposite bank and thus with less detail (3.6 mm GSD), while urban structures were documented at a higher resolution (0.9 mm GSD) using the Z7 II setup. In total 26,706 images were acquired on six days in autumn 2021.

## Photogrammetric Protocol and Challenges

To optimise image acquisition for SfM processing, specific protocols were followed. Every day, the focusing ring was immobilised with cellophane tape at a focus distance of circa 4 m (for the Z7 II) and 50 m (for the D750). Both portrait and landscape orientations were employed, with images taken both perpendicularly and at various angles to maximise 3D coverage of the scene. Vibration reduction was disabled, as it is prone to jeopardise the accuracy in photogrammetric processing results [68]. Lastly, the very high image count ensures redundancy, and therefore high accuracy in the resulting exterior and interior orientation parameters [69].

Despite these precautions, long linear scenes are prone to drift issues in camera pose estimations [70]. To counter this, INDIGO explicitly sought after bridging the channel during the photo acquisition (Figure 2.3) and, with tie points established even across the 20 mm and 85 mm sets despite substantial GSD disparities (Figure 2.5).

## Introducing Graffiti-scape Control Points

To minimise accumulation of drift effects in the estimated camera orientations and to express the SfM results in a real-world coordinate system, it was necessary to constrain the image network with external photo control data. This approach involved gathering 3D coordinates for numerous Graffiti-scape Points (GPs)<sup>2</sup> using measurements with a Leica TS16 total station. GPs were measured at distinctive scene points that are easily identifiable across multiple photos, even if they have been painted over, and that are presumed to have stable long-term positions (see Figure 2.4). These GPs were organised into 21 clusters: L1 to L9 for the left bank and R1 to R12 for the right bank of the Donaukanal.

[68]: Nocerino et al. (2022), 'GOOD VIBRATIONS? HOW IMAGE STABILISATION INFLUENCES PHOTOGRAMMETRY'

[69]: Fraser (2013), 'Automatic Camera Calibration in Close Range Photogrammetry'

[70]: Barazzetti (2017), 'NETWORK DESIGN IN CLOSE-RANGE PHOTOGRAMMETRY WITH SHORT BASE-LINE IMAGES'

2: It is to be noted that a distinction between Graffiti-scape Points (GP) and Graffiti-scape Control Points (GCP) is made. GPs are 3D point measured in the the research area and GCPs are GPs which were used in the photogrammetric processing.

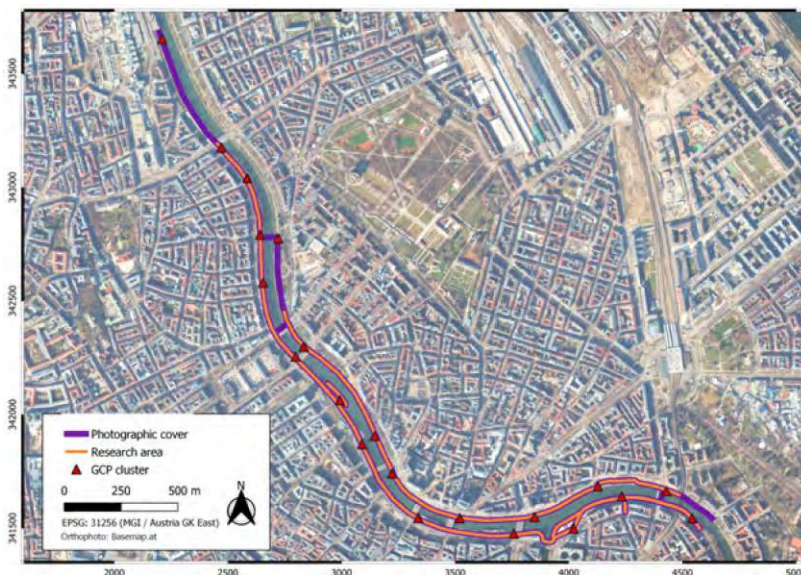


**Figure 2.3:** Overview of the prime research zone (orange line) the extent of the total photographic coverage (violet line) and the location of the twenty Graffiti-scape Control Point (GCPs) clusters. Adopted from [54].



Cluster	$\sigma_{xy}$ [mm]	$\sigma_z$ [mm]	CNPs Used	Used GCPs
L0	9	5	9	28
L1	8	11	10	17
L2	13	8	7	27
L3	12	25	5	20
L4	8	12	8	21
L5	N/A	N/A	N/A	N/A
L6	10	15	5	23
L7	8	14	7	30
L8	7	10	8	26
L9*	3	7	10	21
R1	8	8	4	30
R2	10	13	6	23
R3	5	15	7	29
R4	7	24	5	30
R5	12	7	4	26
R6	8	6	7	26
R7	4	9	8	32
R8	9	14	5	27
R9	6	22	6	29
R10	5	14	7	27
R11	12	6	4	30
R12*	3	7	10	23
<b>Minimum</b>	3	5	4	17
<b>Maximum</b>	13	25	10	32
<b>Mean</b>	8	12	7	26
<b>Total</b>	N/A	N/A	N/A	545

**Table 2.2:** Cluster-specific metrics: The first two columns show precision metrics for the derived TS16 centres, calculated using the number of CNPs listed in column three. The last two columns present the counts of measured GPs and GCPs (Graffiti-scape Control Points used to constrain the bundle adjustment). The table is adopted from [10]. \*Measurements were taken from the same total station position.

For each TS16 location, distances and bearings were recorded to a minimum of four and, on average, twelve visible Control Network Points (CNPs). These CNPs are part of an extensive control point network developed by the City of Vienna as part of a comprehensive terrestrial surveying initiative. Typically associated with man-made features such as drainage covers, wall edges, or bridge pillars, the coordinates of these points are available in the MGI/Austria GK East coordinate reference system (EPSG:: 31256)<sup>3</sup>. Table 2.2 provides precision statistics for surveyed clusters.

**Table 2.3:** Accuracy metrics for the full photographic coverage. Adopted from [10].

Metric	Value
RMSE <sub>x</sub>	1.1 cm
RMSE <sub>y</sub>	1.1 cm
RMSE <sub>xy</sub>	1.6 cm
RMSE <sub>z</sub>	0.8 cm
RMSE <sub>xyz</sub>	1.8 cm

3: The coordinates are available under a CC BY 4.0 license and can be accessed at <https://www.wien.gv.at/ma41datenviewer/public/start.aspx>.

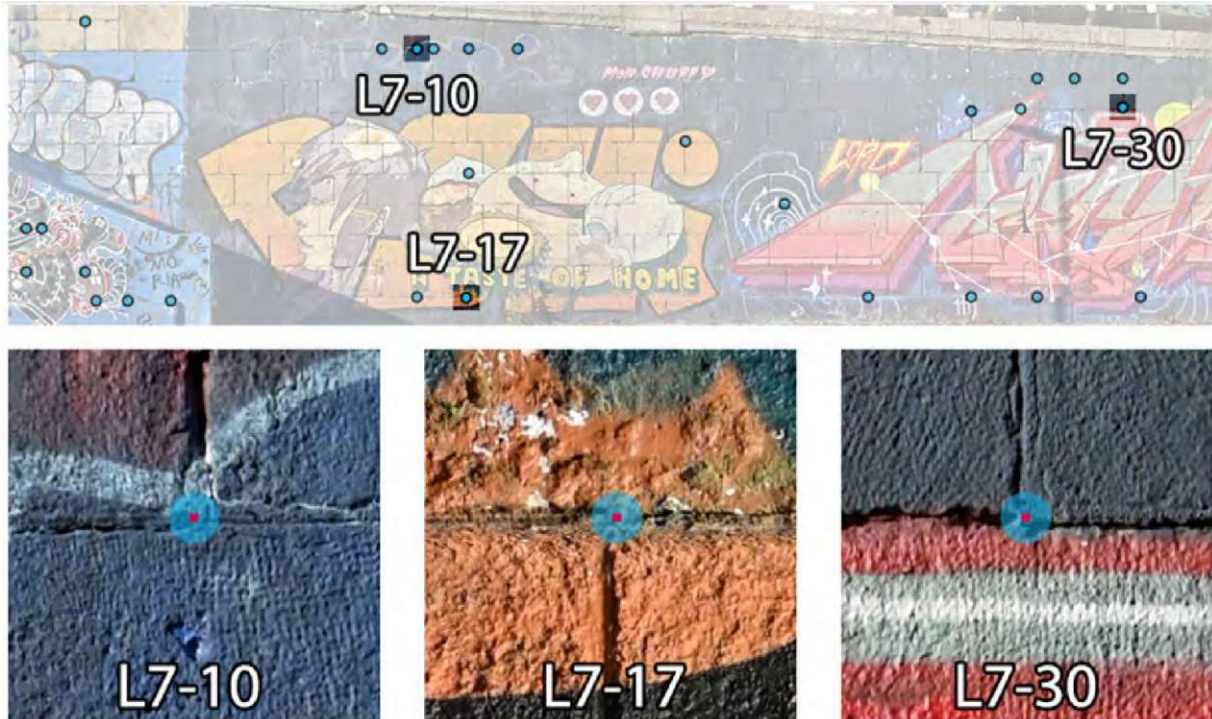


**Figure 2.4:** Three typical GPs out of the thirty that constitute cluster L7 on the left Donaukanal bank. Adopted from [10].

Most of the collected GPs serve then as Graffiti-scape Control Points (GCPs) constraining a self-calibrating bundle block adjustment, leading to a georeferenced photogrammetric model. The photogrammetric data processing is explained in more detail in the following chapter.

### Photogrammetric processing

All photographs were processed using Agisoft Metashape Professional 1.7.5, with a maximum of 25.000 feature points and 3.000 tie points per image. Manual adjustments were required to create two camera groups for the 85 mm images and three for the 20 mm images, as the software grouped cameras by focal length alone. The 20 mm images initially shared one group over the first two days due to a fixed focus, but cleaning was needed after graffiti paint sprayed on the lens on day three. Five sets of interior orientations were calculated, showing consistent principal distances: 85.155 mm and 85.184 mm for 85 mm, and 20.412 mm, 20.410 mm, and 20.402 mm for 20 mm images. Only four images estimation of exterior orientation parameters failed, despite scene changes, lighting differences, and geometry variations over four weeks. Interestingly, it was even possible to establish tie points between photographs acquired from opposite sides of the Donaukanal (see Figure 2.5).

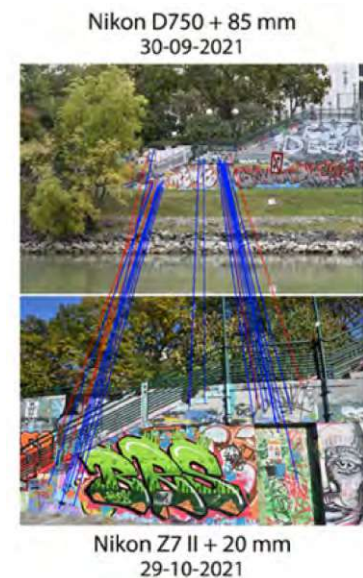


**Figure 2.5:** Example of tie points established between images taken from opposite sides of Donaukanal. Adopted from [10].

The 14.5 million 3D tie points (Figure 2.6) were visually checked for artefacts. GPs were marked cluster by cluster, with high-residual GPs ( $\geq 3\text{ cm}$ ) typically located at edges or cluster borders, resulting from less accurate reflector-less measurements of the total station. Of 593 GPs, 545 were kept. The average (3D) precision of the GCPs is estimated to be approximately 1 cm 2.2. Accounting for an additional 5 mm uncertainty for indicating GPs in the the images yields a precision of about 1.5 cm

for the introduced GCPs, which was used for weighting them in Agisoft Metashape to refine the final bundle block adjustment. This step stabilised camera positions and georeferenced the ca. 26,000 images, with final accuracy metrics shown in Table 2.3.

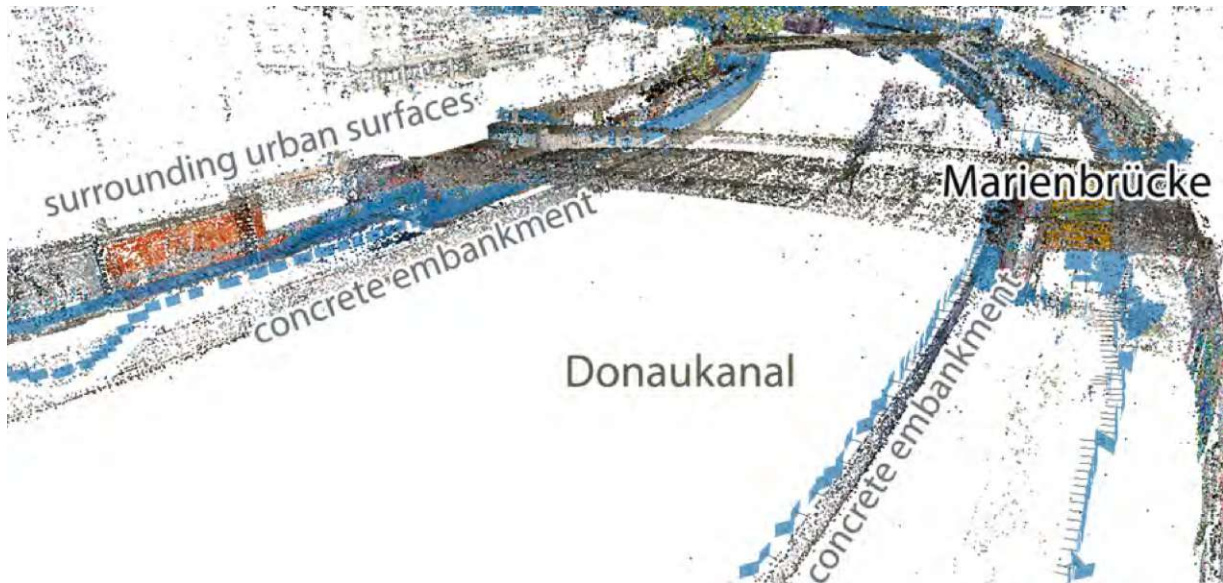


**Figure 2.6:** Locations of all photographs taken near Marienbrücke (Marien Bridge). The scene's structure is illustrated using a cleaned 3D tie point cloud. Adopted from [10].

This photogrammetric backbone serves as basis for the subsequent photogrammetric method development and documentation along Donaukanal.

## 2.2.2 Ethical considerations surrounding INDIGO's objectives

Documenting and disseminating graffiti presents specific ethical challenges, particularly around issues of consent, creator intent, and the impact of sharing the records digitally. All these topics were discussed between member of project INDIGO during a meeting with TU Wien's Pilot Research Ethics Committee<sup>4</sup>.

One primary consideration during these and other discussions were whether the creator has consented to having their work documented and distributed online. While some argue that graffiti is created in public space and meant to be seen by the public making it inherently open for documentation, it can also be argued that a creator may intend for their work to remain local and viewable only by people in the immediate area and not world wide through an online database [1]. For example, a creator might place a graffiti in a secluded spot, expecting a limited audience. Sharing this work widely online could increase its visibility beyond what the creator intended, potentially misrepresenting their purpose or attracting unwanted attention. From a legal perspective the so-called *Panoramafreiheit*, which generally allows a dissemination of photographs which are taken in and of the public, might be applicable in this context, but this view is debated. Through multiple discussions with creators, it became clear that most not only support INDIGO's activities but also explicitly wish for their creations to be shared, provided there

4: A general protocol of this meeting and a preparatory meeting can be found at the following links [https://drive.google.com/file/d/1Q8WkojnCfvLTb8lErwLtQBM6jyJJ0U\\_g/view](https://drive.google.com/file/d/1Q8WkojnCfvLTb8lErwLtQBM6jyJJ0U_g/view) and <https://drive.google.com/file/d/18miSsQheilYsd9UioFkmWUpHsaUjxVw/view>

[1]: Merrill et al. (2023), "Different Folks, Different Strokes": goINDIGO 2022's Creators vs Academics Discussion Round'



is no financial profit for the project involved. However, these views are not universal, and opposing perspectives likely exist. A possibility to mitigate this concern could be to give creators a means to request the removal of specific images granting control over their work's visibility while supporting academic interest in graffiti. However, offering such a tool involves also the risk of being misused. This misuse could for example result in a form of cancel culture, where certain views, symbols or creators are systematically reported for personal reasons or to support a political agenda. Such an approach would necessitate a moderation and transparent guidelines, leaving it hardly feasible for a research project to maintain.

Handling graffiti depicting sensitive, controversial, or clearly illegal content adds complexity, as it requires balancing the principle that research should objectively present the world as it is with ethical responsibility. This balance is further influenced by legal constraints, which may limit how such content can be documented, shared, or studied. This concern is aggravated by the fact that many graffiti use languages and codes unknown to those documenting them. It is a fact that most graffiti along the Donaukanal were created illegally. Although enforcement has not been strict in recent years, the question remains whether the collected data could be used as a law enforcement tool. Another relevant factor is the gender imbalance in graffiti culture, which is severely male-dominated. Documenting predominantly male-created works could inadvertently minimise the visibility of female creators, who often face additional barriers to recognition. This imbalance can lead to limited perspectives in the documented graffiti, reinforcing certain biases in how graffiti is perceived by the public.

# 3 An automated framework for graffiti change detection

This chapter is largely based on the following two peer-reviewed publications which are both published under the CC BY 4.0 license.

- ▶ Wild, B., Verhoeven, G., Muszyński, R. & Pfeifer, N. (2024). Detecting change in graffiti using a hybrid framework. *The Photogrammetric Record*, 00, 1–28. <https://doi.org/10.1111/phor.12496>
- ▶ Wild, B., Verhoeven, G. J., & Pfeifer, N. (2023). Tracking the urban chameleon - towards a hybrid change detection of graffiti. In *Volume X-M-1-2023, 2023 | 29th CIPA Symposium "Documenting, Understanding, Preserving Cultural Heritage. Humanities and Digital Technologies for Shaping the Future"* (pp. 285–292). ISPRS, Copernicus Publications. <https://doi.org/10.5194/isprs-annals-X-M-1-2023-285-2023>

## 3.1 State-of-the-art in graffiti change detection

A potential method for automating the identification of new graffiti along the Donaukanal involves the deployment of permanent cameras to monitor relevant areas. Previous research on graffiti change detection [19, 71, 72] has effectively utilised such techniques, primarily focusing on detecting the act of graffiti creation rather than explicitly identifying newly created graffiti. For instance, Angiati et al. (2005) [71] developed a multi-step approach that included extracting video frames, reducing image noise, performing feature extraction, and tracking features across consecutive frames. This methodology enabled the successful identification of individuals in front of frequently graffitied walls, thereby indirectly detecting changes in graffiti with a high success rate. Despite its potential for near-real-time detection, this approach is impractical for widespread application, particularly along the Donaukanal, due to significant logistical and financial constraints, as well as legal and ethical concerns related to large-scale public surveillance.

Given these limitations, a more viable alternative may involve the use of a single camera system mounted on a mobile platform, allowing for rapid and repeatable photo acquisition, which can then be analysed for graffiti-related changes. The foundation of image-based change detection techniques, which have been extensively developed since the advent of satellite remote sensing and NASA's Landsat program in the 1970s, supports this approach. The change detection process typically involves several stages: image preprocessing (such as co-registration and denoising), the application of a specific change detection algorithm, and the segmentation of the detection results to produce a binary change map [73]. The selection of an appropriate change detection algorithm

3.1	State-of-the-art in graffiti change detection . . . . .	29
3.2	Challenges in Image-Based Graffiti Change Detection . . . . .	31
3.3	Change detection data and methods . . . . .	33
3.4	Image acquisition at test site . . . . .	34
3.5	Image co-registration . . . . .	38
3.6	Generating reference change maps . . . . .	42
3.7	Hybrid change detection framework . . . . .	44
3.7.1	Pixel-based change maps . . . . .	44
3.7.2	Introducing image feature descriptors as change indicators . . . . .	47
3.7.3	Change map merging and threshold optimisation . . . . .	50
3.8	Results and discussion . . . . .	51
3.8.1	Pixel-based results . . . . .	51
3.8.2	Descriptor-based results . . . . .	54
3.8.3	Threshold optimisation and change map merging . . . . .	54
3.8.4	Hybrid change detection assessment . . . . .	55

[19]: Tombari et al. (2008), 'Graffiti detection using a time-of-flight camera'

[71]: Angiati et al. (2005), 'A novel method for graffiti detection using change detection algorithm'

[72]: Di Stefano et al. (2008), 'Graffiti detection using two views'

[73]: Asokan et al. (2019), 'Change detection techniques for remote sensing applications: A survey'

is highly dependent on the specific application and the nature of the available image data. In their comprehensive review, Tewkesbury et al. (2015) [74] categorised these tasks based on the unit of analysis (e.g., pixel, kernel, or object) and the comparison technique employed (e.g., arithmetic differencing, change vector analysis, or transformation-based methods). In recent years, also the integration of deep learning techniques into change detection has gained popularity, showing promising results [75–78]. However, these approaches often require extensive labelled data and can present challenges in their application to specific domains [79]. Parts of this work and the underlying data have also been used for a study on deep learning based detection. The results from this study will be outlined in Chapter 6.

Within project INDIGO, one of the three INDIGO photographers patrolled the Donaukanal to document new graffiti using a camera once a week (see [59] for further details). During each graffiti tour, any graffiti that had appeared since the previous graffiti tour had to be recorded. The identification of new graffiti primarily relied on two strategies. First, the experience and memory of Stefan Wogrin, a key project member who has been documenting graffiti for his *SprayCity* archive (<https://spraycity.at>) for many years. His extensive knowledge of the Donaukanal graffiti-scape allowed him to detect changes with far greater accuracy than other photographers, which is why he became INDIGO's lead photographer. The second approach involved a detection system capable of flagging newly added graffiti within the monitored graffiti-scape, thus aiding in the creation of a more thorough record. For this, the project team also kept a close eye on Instagram, where many individuals who regularly create graffiti along the Donaukanal post photos of their latest creations. Using a mobile GIS app (ESRI's ArcGIS Field Maps<sup>1</sup>), the team tracked these updates, gaining valuable information about new graffiti. To strengthen this social-media monitoring, INDIGO launched the #INDIGODonaukanal hashtag, encouraging graffiti creators to use it when posting their work. Images tagged with this hashtag were easily filtered and often revealed previously unseen graffiti. The online data gathered via social media supplemented the manual, memory-based documentation during the weekly tours.

However, both methods presented notable challenges. First, they were time-intensive, as the photographer had to navigate the entire area and observe each wall carefully. This is physically demanding due to the long distances covered and sometimes difficult weather conditions, and mentally challenging, requiring close attention to detail in spotting new or altered graffiti. Despite these efforts, many graffiti pieces still went unnoticed. Some were missed because they were too small or subtle, while others were created and subsequently covered up in between the photo tours. While the fluctuating nature of graffiti adds to its appeal [6], this lack of comprehensive digital documentation makes it difficult to conduct complete and unbiased research on graffiti, which is as outlined in Chapter 1.2.2. In INDIGO's case, the digital archive tended to emphasise larger and more visually prominent pieces, which conflicted with the project's goal of capturing the full spectrum of graffiti along the Donaukanal [10]. This revealed the need for more effective and precise techniques to track changes in the graffiti-scape.

The INDIGO project has developed significant expertise in the photogra-

[74]: Tewkesbury et al. (2015), 'A critical synthesis of remotely sensed optical image change detection techniques'

[75]: Ting Bai Le Wang et al. (2023), 'Deep learning for change detection in remote sensing: a review'

[76]: Parelus (2023), 'A Review of Deep-Learning Methods for Change Detection in Multispectral Remote Sensing Images'

[77]: Jiang et al. (2022), 'A Survey on Deep Learning-Based Change Detection from High-Resolution Remote Sensing Images'

[78]: Dong et al. (2024), 'ChangeCLIP: Remote sensing change detection with multimodal vision-language representation learning'

[79]: Shi et al. (2020), 'Change detection based on artificial intelligence: State-of-the-art and challenges'

[59]: Verhoeven et al. (2023), 'Facing a chameleon - how project INDIGO discovers and records new graffiti'

1: <https://www.esri.com/en-us/arcgis/products/arcgis-field-maps/overview>

[6]: Blanché (2015), 'Street Art and related terms'

[10]: Verhoeven et al. (2022), 'Project INDIGO: document, disseminate & analyse a graffiti-scape'

phy and processing of large collections of graffiti images [59], making photographs a logical choice as the primary data source for change detection. By equipping a mobile platform, such as a bicycle, with cameras, it would be possible to photograph the entire research area within approximately one hour. Orientation parameters for photos taken at different time intervals can be determined using an incremental SfM method. With the exterior orientation established for each photo, various methods can be applied to generate nearly pixel-perfectly co-registered images from photographs of two different epochs. Although this strategy of photo acquisition and co-registration is complex and requires substantial expertise, careful planning, and appropriate hardware, previous research [59] indicates that the primary challenge in developing an effective graffiti change detection framework lies in the automated identification of graffiti-related changes from these preprocessed images. The subsequent chapter will discuss the specific challenges involved in developing an algorithm capable of effectively distinguishing graffiti-related changes from other image variations in co-registered images.

[59]: Verhoeven et al. (2023), 'Facing a chameleon - how project INDIGO discovers and records new graffiti'

### 3.2 Challenges in Image-Based Graffiti Change Detection

Change detection, as defined by Singh (1989) [80], involves identifying differences in the state of an object or phenomenon by observing it at different times. This principle is critical in various applications of remote sensing and image analysis, including graffiti monitoring. An essential constraint of this definition is that changes can and usually must be distinguished between *important* and *unimportant* [81]. Figures 3.1a and 3.1b illustrate almost pixel-perfect co-registered images of the same graffiti scene taken on different days which differ substantially in terms of visual appearance, however only exhibit subtle difference in terms of graffiti-related changes (Figure 3.1d). An effective change detection process aims to identify significant alterations between these images, such as new graffiti or modifications to existing works.

[80]: Singh (1989), 'Review Article Digital change detection techniques using remotely-sensed data'

[81]: Radke et al. (2005), 'Image change detection algorithms: a systematic survey'

Detecting changes in graffiti through images presents several unique challenges (Figure 3.2):

- **Weather-related** Variations in lighting conditions between image capture times can produce significant radiometric differences that are not indicative of actual graffiti changes. For example, the differences shown in Figure 3.1c are influenced more by lighting conditions than by changes in the graffiti itself. Ambient light variations due to changing cloud cover and the angle of the sun can cast shadows or reflections that complicate the distinction between real graffiti modifications and irrelevant radiometric differences [81]. Weather conditions such as rain can also alter the appearance of graffiti, leading to inconsistencies between images taken on different days. For instance, wet walls from rain can reflect light differently, creating significant pixel value differences that may be misinterpreted as changes in graffiti [82].
- **Acquisition-related** Differences in camera settings, such as exposure time and ISO sensitivity, can affect image quality and create

[82]: Bruzzone et al. (2013), 'A novel framework for the design of change-detection systems for very-high-resolution remote sensing images'



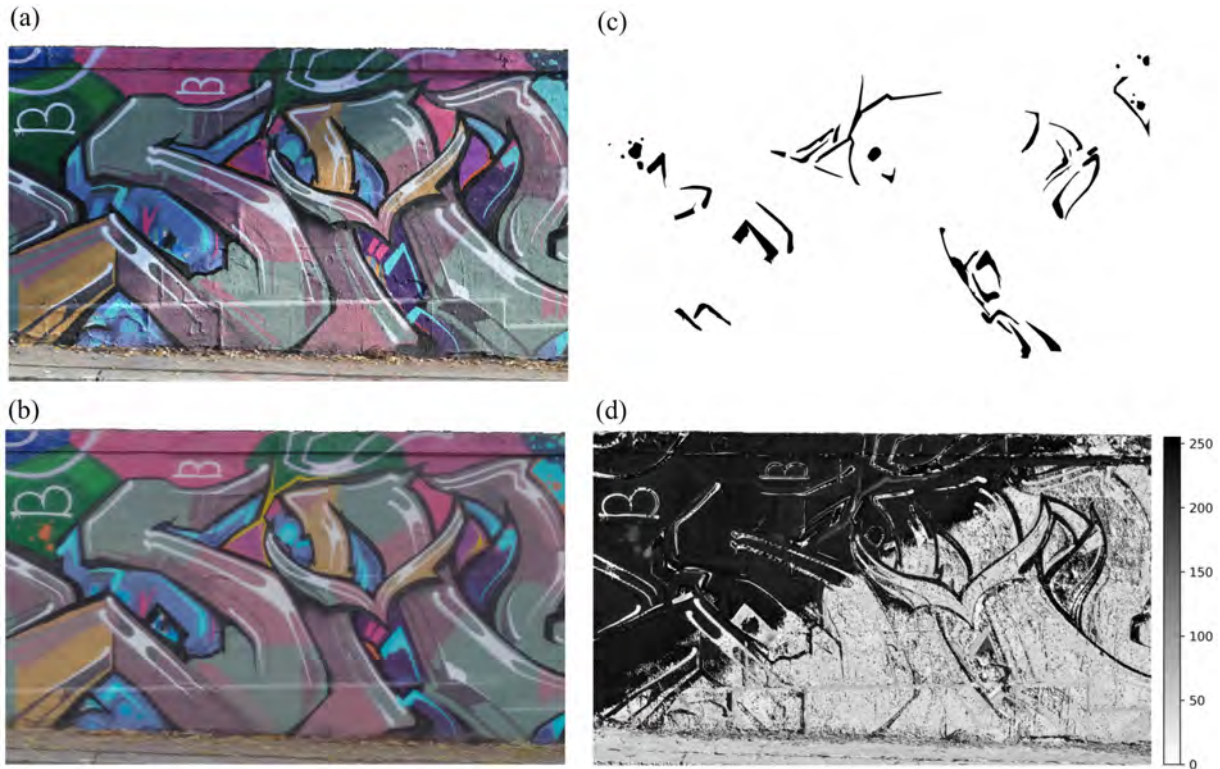


**Figure 3.1:** (a, b) Co-registered image pair of a scene depicting (parts of) a slightly altered graffiti. (c) Manually generated change map of (a) and (b). (d) Absolute grey-value differences between (a) and (b). Adopted from [54].

variations between image captures. Motion blur from kinematic platforms or variations in camera orientation can further distort image comparisons. These factors contribute to radiometric differences that do not necessarily reflect changes in graffiti but rather changes in image capture conditions.

- **Co-registration-related:** Minor misalignments between co-registered images can lead to significant pixel-level differences, especially in areas with high textural contrast. Accurate co-registration is crucial to ensure that detected changes are truly indicative of graffiti modifications rather than artifacts of misalignment.
- **Object-related:** Small noise-like structures and transient environmental factors, such as moving vegetation, can create variations in pixel values that do not correspond to actual graffiti changes. This usually does not trick the human visual system [83] but complicates the process of distinguishing between significant changes and irrelevant fluctuations in the data [84].

In summary, detecting graffiti through image-based methods requires overcoming several obstacles, such as variations in lighting, weather conditions, camera settings, co-registration errors, and image noise. Effectively tackling these challenges is essential for accurate graffiti monitoring. Additionally, automating the data acquisition process to a high degree is vital for ensuring rapid and frequent data collection and minimising observation gaps.

[83]: Arnheim (1954), *Art and visual perception: A psychology of the creative eye*

[84]: Bitelli et al. (2004), 'Image change detection on urban area: the earthquake case'



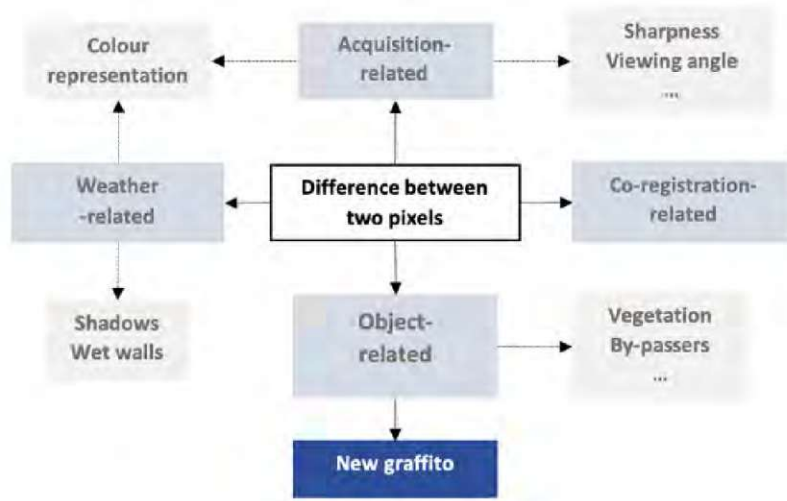


**Figure 3.2:** Challenges in image-based change detection of graffiti. Adopted from [55].

### 3.3 Change detection data and methods

The following two chapters will discuss: a) a workflow for an automated image acquisition and data processing pipeline, tested on a designated test-wall at Donaukanal, and b) how the resulting co-registered images can be efficiently transformed into reliable information about newly appeared graffiti compared to previous acquisitions. An overview of the developed and implemented workflow is depicted in Figure 3.3.

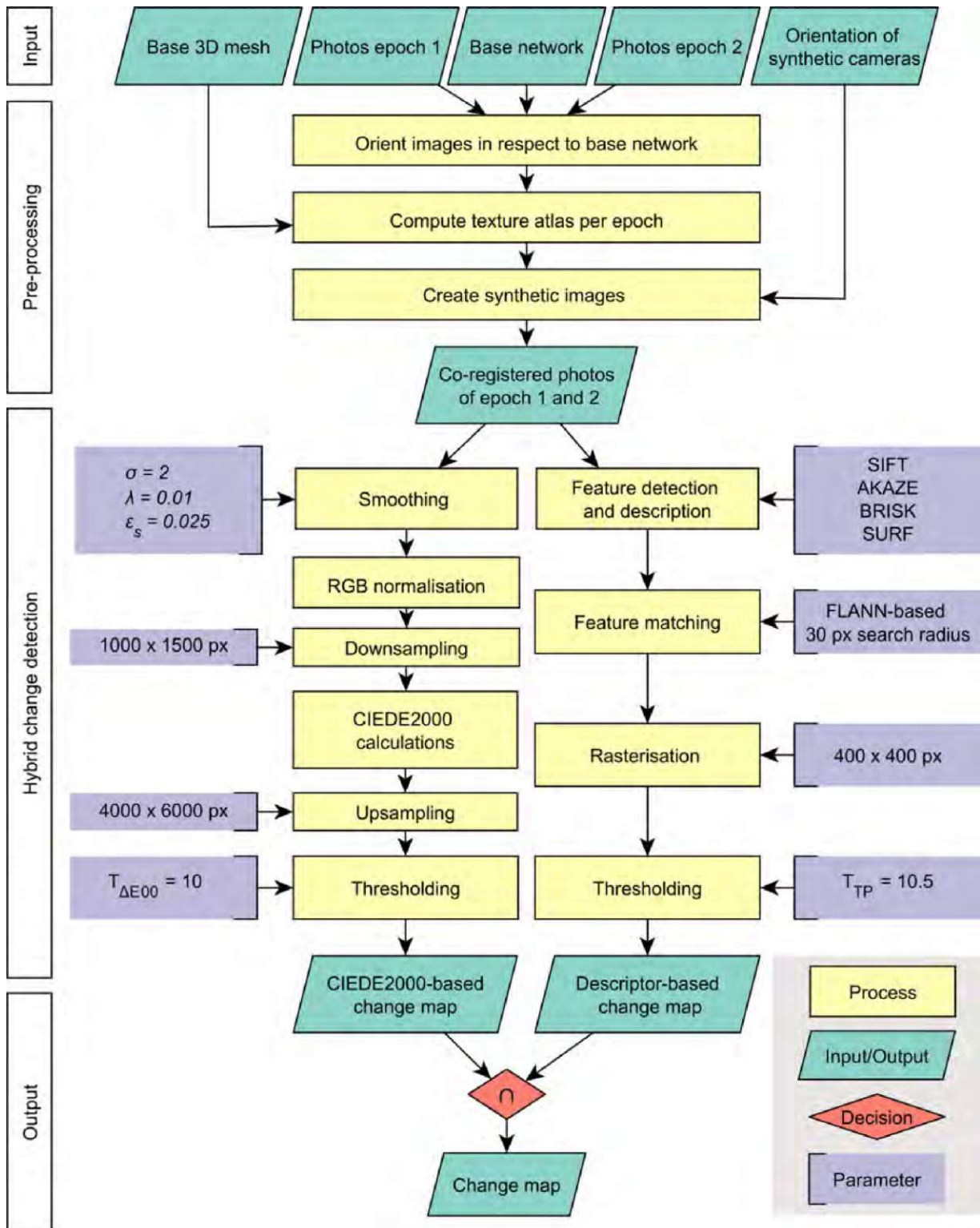


Figure 3.3: Workflowchart of the main steps in the hybrid change detection approach. Adopted from [54].

### 3.4 Image acquisition at test site

An image dataset was collected to develop and comprehensively evaluate the change detection workflow. This dataset focused on a test zone within INDIGO's research area, covering approximately 250 meters

along the Donaukanal, which is known for its high graffiti activity. The area included one of the three legal walls (*Wienerwände*; Figure 3.4), making it an ideal area for method developing and testing for this research. Limiting the image acquisition to this smaller yet dynamic section allowed for efficient data collection, as new graffiti or changes to existing pieces occur on a day-to-day basis. Imagery of both unchanged and altered graffiti could be captured at regular, short intervals, requiring minimal resources for continuous monitoring. This targeted approach provided a solid foundation for testing and refining the change detection process, enabling accurate tracking and analysis of graffiti changes over time.

The three colour setting options exploited during the data acquisition process are explained in the Community Support<sup>2</sup> by GoPro as follows:

- ▶ **GoPro:**<sup>3</sup> This setting enhances saturation, resulting in vivid colours for a visually striking effect, minimising the need for post-processing.
- ▶ **Natural:** This profile aims to accurately represent colours as perceived by the human eye, offering a realistic depiction of the scene.
- ▶ **Flat:** A neutral colour profile that captures greater detail in shadows and highlights. This setting provides flexibility for colour correction in post-production, enabling better integration with footage from other equipment.

2: <https://community.gopro.com/s/article/Advanced-Protune-Controls-Explained>, last accessed: October 4 2024

3: Recently the *GoPro* colour profile has been renamed to *Vibrant*

According to this description *Flat* appears the most promising option. However, as no experience with the usage of these colour profiles regarding change detection is available all three profiles were tested.

The collected data comprises 29 individual photo collections (see Table 3.1), acquired over 11 days between October 21, 2022, and December 1, 2022, using two different camera setups. The first two datasets (ID1 and ID2) were captured with a Nikon Z 7II camera, featuring a 45.4 MP resolution, paired with a Nikon NIKKOR Z 20 mm f/1.8 S lens. These photographs were part of INDIGO's second total coverage survey, aimed at creating a detailed 3D surface model of the entire research area. Their inclusion in the change detection dataset was intended to enhance both the graffiti and camera variability.

**Table 3.1:** The protocol for the 29 photo collections states the date, camera (and settings), and if shadows were present during the image acquisition. Note that photos acquired on the same day were shot simultaneously but with varying camera settings.

ID	Date	Camera	Sharpness	Colour	Shadows
1	21 October 2022	Nikon Z 7II	N.a.	N.a.	No
2	2 November 2022	Nikon Z 7II	N.a.	N.a.	Yes
3	12 November 2022	GoPro HERO10 Black (A)	High	Natural	Yes
4	12 November 2022	GoPro HERO10 Black (B)	High	GoPro	Yes
5	12 November 2022	GoPro HERO11 Black	High	Flat	Yes
6	13 November 2022	GoPro HERO10 Black (A)	High	Natural	Yes
7	13 November 2022	GoPro HERO10 Black (B)	High	Flat	Yes
8	13 November 2022	GoPro HERO11 Black	High	GoPro	Yes
9	14 November 2022	GoPro HERO10 Black (A)	High	Flat	No
10	14 November 2022	GoPro HERO10 Black (B)	High	GoPro	No
11	14 November 2022	GoPro HERO11 Black	High	Natural	No
12	17 November 2022	GoPro HERO10 Black (A)	Medium	Flat	No
13	17 November 2022	GoPro HERO10 Black (B)	Low	Flat	No
14	17 November 2022	GoPro HERO11 Black	High	Flat	No
15	19 November 2022	GoPro HERO10 Black (A)	Medium	Flat	No
16	19 November 2022	GoPro HERO10 Black (B)	Low	Flat	No
17	19 November 2022	GoPro HERO11 Black	High	Flat	No
18	22 November 2022	GoPro HERO10 Black (A)	Medium	GoPro	No
19	22 November 2022	GoPro HERO10 Black (B)	Low	GoPro	No
20	22 November 2022	GoPro HERO11 Black	Low	Natural	No
21	25 November 2022	GoPro HERO10 Black (A)	Low	GoPro	Yes
22	25 November 2022	GoPro HERO10 Black (B)	Medium	Natural	Yes
23	25 November 2022	GoPro HERO11 Black	High	Flat	Yes
24	27 November 2022	GoPro HERO10 Black (A)	Medium	Natural	No
25	27 November 2022	GoPro HERO10 Black (B)	High	Natural	No
26	27 November 2022	GoPro HERO11 Black	Medium	Natural	No
27	1 December 2022	GoPro HERO10 Black (A)	Medium	GoPro	No
28	1 December 2022	GoPro HERO10 Black (B)	Low	Natural	No
29	1 December 2022	GoPro HERO11 Black	Medium	GoPro	No



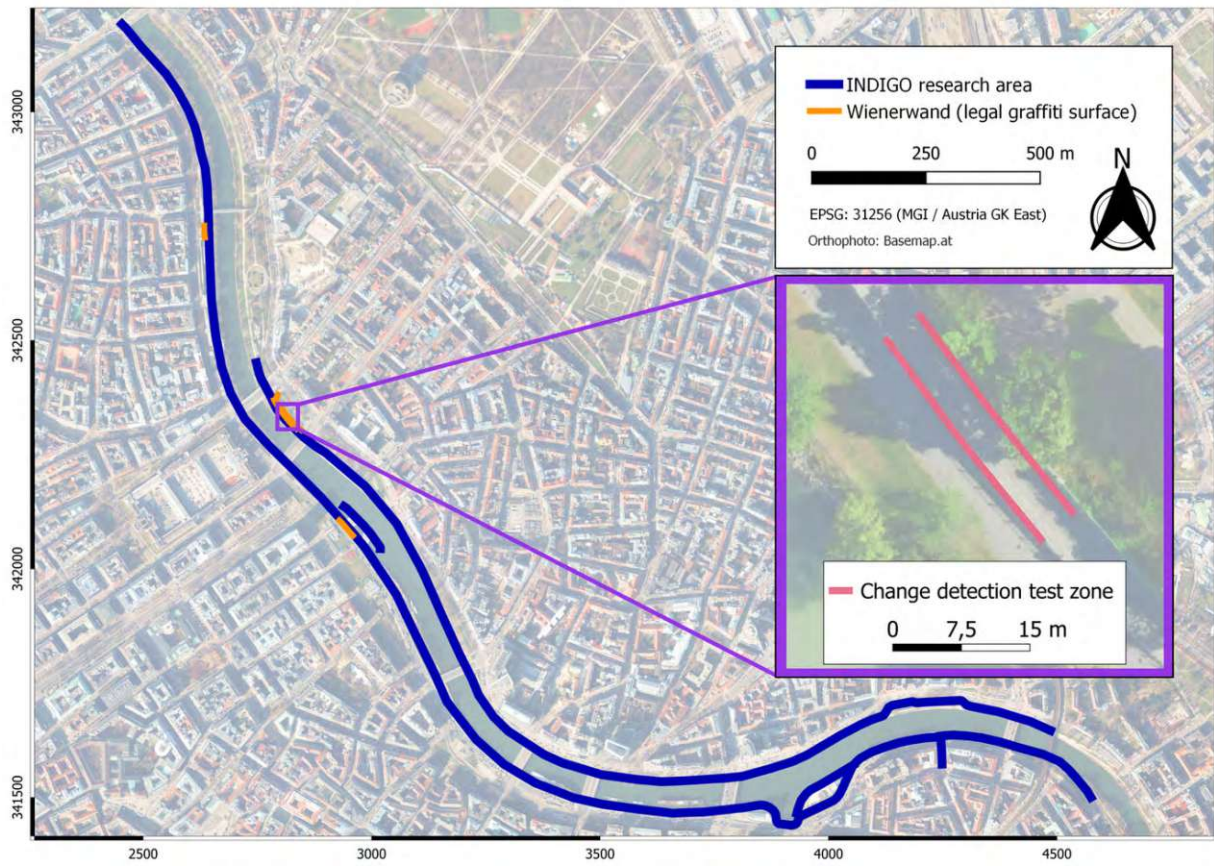


**Figure 3.4:** INDIGO’s research area, along Vienna’s Donaukanal with the designated change detection test zone depicted in the smaller inset. The legal graffiti surfaces (i.e., Wienerwände) are highlighted in orange. Adopted from [54].

The remaining 27 datasets (ID 3–29) were specifically acquired for the change detection analysis, utilising a triple GoPro camera setup. This setup consisted of three GoPro cameras, two GoPro HERO10 Blacks and one GoPro HERO11 Black, mounted in a frame (Figure 3.5) to ensure that their optical axes were parallel and their centers of projection were as close together as possible. The specifications of this GoPro camera setup are as follows:

- GoPro Camera Setup
  - Two GoPro HERO10 Blacks
  - One GoPro HERO11 Black

This configuration was employed on 9 days, resulting in a total of 27 datasets (9 days x 3 cameras). The strategic combination of these two setups aimed to optimise the quality and diversity of the captured images, thereby facilitating more effective change detection.

At a walking pace of approximately 5 km/h, each GoPro camera captured two images per second using its built-in intervalometer, resulting in a capture interval of roughly 0.7 m. The Nikon Z 7II camera followed a stop-and-go pattern, with a similar baseline. Both camera setups primarily used landscape orientation, positioning the optical axis perpendicular to the graffitied walls. Occasionally, convergent images (with an inclined optical axis) and rotated images, either flipped 180°, rotated 90° clockwise, or 90° counterclockwise around the optical axis, were also taken. In the GoPro setup, at least one camera was consistently positioned upside down. Additionally, some images were taken at an increased object distance. These variations were integral to enhancing the network geometry of the camera setup, especially for such elongated networks, and improving camera orientation estimation [85–87]. Each of the 29 image datasets maintained a high longitudinal overlap between images (ca. 80%), essential for the subsequent SfM pipeline.

Images were intentionally captured in various weather conditions to assess the sensitivity of the change detection approach. Additionally, distinct camera settings were applied to the three GoPro cameras (see Table 1) for two main purposes. Due to the significant influence of camera settings on the final images, each simultaneous capture can be considered a separate epoch, with the expected outcome (empty change maps) known a priori. Having a substantial number of image pairs without any changes is also critical for enhancing and validating the algorithm's specificity.

### 3.5 Image co-registration

The cameras' orientation parameters were calculated using an incremental SfM method in Agisoft Metashape Professional 1.8.4. This incremental SfM approach first estimates the interior and exterior orientations for a base network, then incrementally orients each new image from subsequent epochs to this established network. This workflow has already been successfully implemented in multiple studies within the INDIGO project (e.g., [54, 59]). For this approach to be effective, it's essential to establish stable tie points across images from different epochs. Therefore,



Figure 3.5: (a) The three GoPro cameras mounted in a frame. Adopted from [54].

[85]: Luhmann et al. (2016), 'Sensor modelling and camera calibration for close-range photogrammetry'

[86]: Nocerino et al. (2014), 'Accuracy of typical photogrammetric networks in cultural heritage 3D modeling projects'

[87]: Stamatopoulos et al. (2014), 'Automated Target-Free Network Orientation and Camera Calibration'

[54]: Wild et al. (2024), 'Detecting change in graffiti using a hybrid framework'

[59]: Verhoeven et al. (2023), 'Facing a chameleon - how project INDIGO discovers and records new graffiti'

the photographic coverage extended beyond the graffiti walls, which may have undergone complete texture changes, to include stable elements like building façades, street lamps, and bridge pillars with consistent geometry and texture.

The Nikon Z 7II images served as the base network. The interior and exterior orientations were estimated using 179 graffiti-scape points, based on the MGI/Austria GK East coordinate reference system (EPSG: 31256), as constraints for the bundle adjustment (see [10] for details). This placed the test zone's images and graffiti-scape points within a broader image network, likely resulting in more accurate orientation values. A depth-map-based surface mesh was then created from around 3,100 images of the test zone. Vegetation, trash cans, and street lamps were removed from this mesh in Geomagic Wrap 2021 (<https://oqton.com/geomagic-wrap>), which also corrected mesh errors like small holes and non-manifold areas. A 25 m section was then extracted from this 250 m mesh. Due to the high facet density, the mesh geometry was simplified using a 1 cm tolerance-based decimation in Atango Balancer nPro (<https://www.atango.com/buy/nPro>). After applying Wrap's geometry correction tools to this decimated mesh, an artefact-free, two-manifold triangular 3D surface mesh of just over 51,000 facets was achieved (Figure 3.6). This surface mesh will now be referred to as the change detection test zone mesh.

This change detection test zone mesh was reimported into Metashape Professional to compute photographic textures for each epoch (Figure 3.7). Before texturing a 3D surface mesh, each mesh vertex requires associated 2D texture coordinates,  $u$  and  $v$ . These UV texture coordinates are computed through UV parametrisation, or a *UV unwrap*, which essentially lays out each mesh facet on the 2D texture map or texture atlas [88]. Each pixel in the texture atlas is then assigned an RGB value based on photos capturing that location on the 3D surface mesh (Figure 3.7). The resulting 2D RGB image is then applied to the 3D mesh as a diffuse texture. While manual UV mapping software exists, Metashape offers an automatic, non-interactive *generic* parametrisation. Because these UV coordinates remain usable for all subsequent texturing operations, a single 3D surface mesh with UV coordinates served as the base for all diffuse texture atlases. Following analysis of various sizes, texture atlases of  $16,384 \times 16,384$  px were computed for each of the 29 photo sets (Figure 3.6), resulting in 29 geometrically identical 3D models, each textured differently (i.e., their texture atlases had identical layouts but differing RGB values; see Figure 3.7).

While theoretically feasible, using the 29 co-aligned texture atlases directly for change detection poses three main challenges: First, each image exceeds 200 MP, complicating processing. Second, the layout and seams within and between texture atlases may negatively affect the change detection algorithm. Third, co-registered texture atlases assume static geometry over time. While this is true for the custom change detection dataset, it is unrealistic for dynamic environments like the Donaukanal, where infrastructure is continuously modified. Failing to update geometry and UV parametrisation would lead to erroneous textures. However, updating them disrupts the alignment of texture atlases.



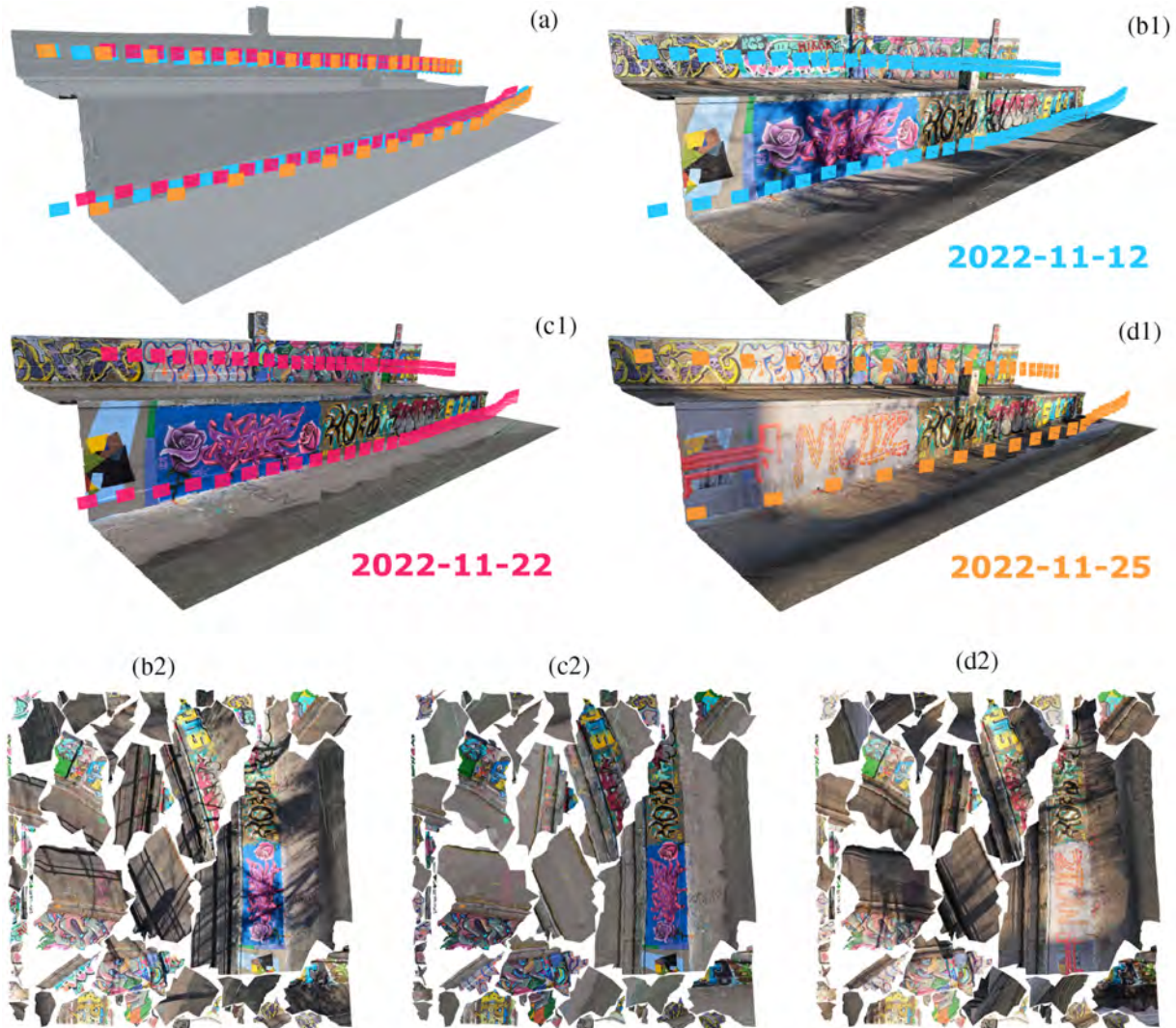


**Figure 3.6:** (a) The base surface mesh of the change detection test zone with the exterior camera orientations of three explanatory image datasets indicated by rectangles. The colours indicate different epochs. (b1, c1, d1) The base mesh textured using the photographs of the three different epochs (ID3, ID19 and ID22). (b2, c2, d2) The texture atlases used to generate (b1, c1 and d1), respectively. Adopted from [54].

To address these challenges, 17 synthetic cameras, each with a distortion-free 50 mm lens, were introduced along the test zone, positioned at approximately equal distances from the walls (Figure 3.7). Each synthetic camera rendered a 24MP image for every available textured 3D model, generating a total of 493 ( $17 \times 29$ ) synthetic images via a custom Python script. The ground sampling distance (GSD) of these synthetic images varies between 0.5 and 0.9 mm, depending on the distance from the synthetic camera to the 3D model. However, this GSD does not fully describe spatial resolution, as it also depends on texture atlas detail, which itself is influenced by pixel count, mesh size, and UV parametrisation (determining empty texture space and distortion). For this 25 m test zone mesh, textures sized  $16,384 \times 16,384$  px provided optimal results. Textures of  $8,192 \times 8,192$  lacked detail, while those at  $32,768 \times 32,768$  showed minimal quality gain but required substantially higher processing and storage resources.

To conclude this chapter, several key aspects of the workflow merit atten-



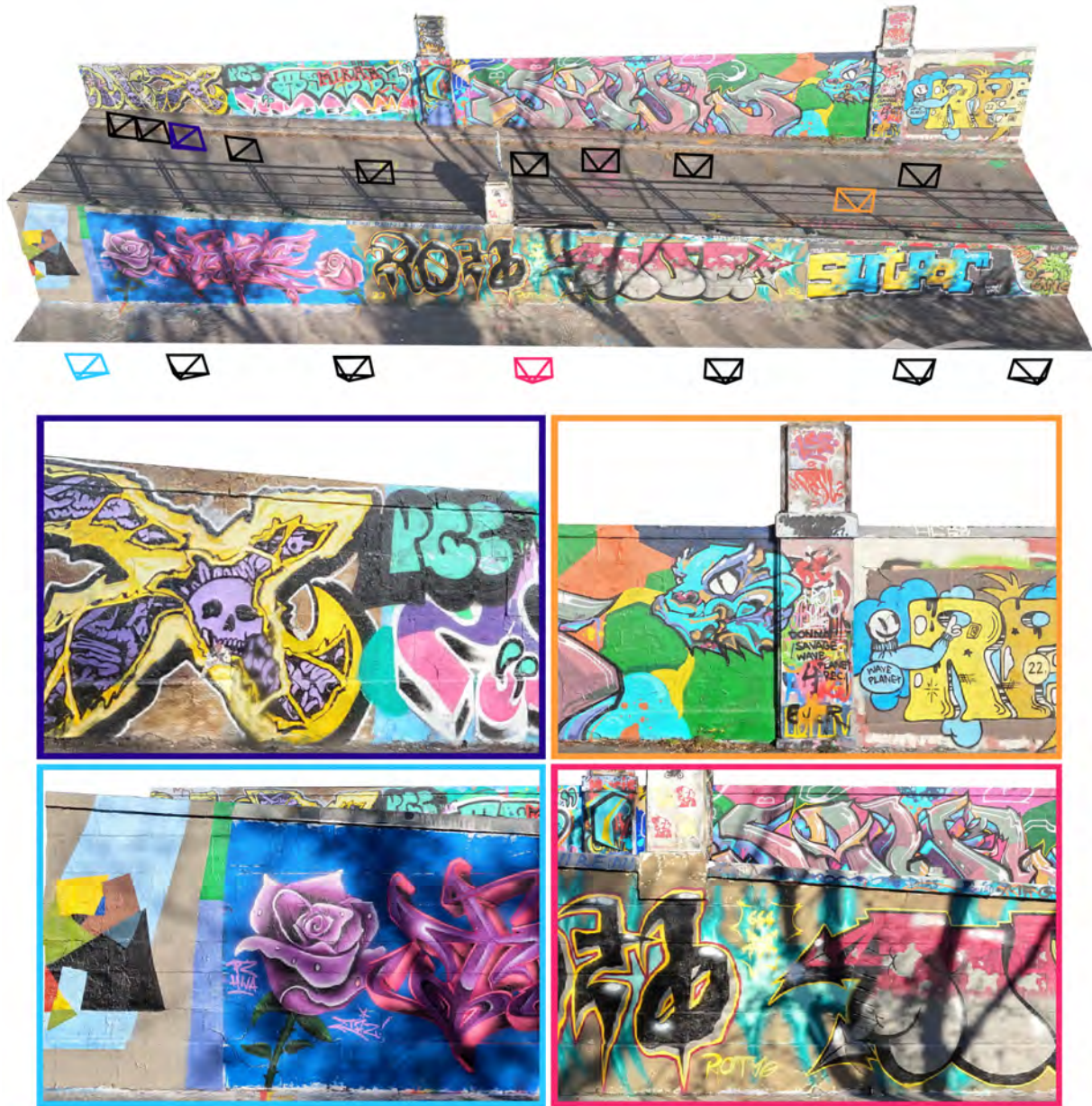


**Figure 3.7:** (Top) 3D surface mesh of the change detection test zone textured using the imagery acquired on 12 November with the GoPro HERO10 Black (epoch ID4). The manually placed synthetic cameras are symbolised by the black wireframe pyramids. (Below) The corresponding rendered images for the colourised synthetic cameras. To facilitate file organisation, these synthetic cameras were systematically numbered from 1 to 17. The numbering sequence commences at 1, located in the lowermost section of the first row, and proceeds until 17 in the upper right corner. For instance, the blue, pink, violet and orange rectangles correspond to synthetic cameras 1, 4, 10 and 16, respectively. Adopted from [54].

tion. First, though synthetic camera placement could be automated by positioning cameras at equal intervals along a predefined line, this might reduce the benefits of manually reducing blind spots and ensuring comprehensive scene coverage. Second, creating the base mesh and manually placing synthetic cameras is a one-time task, and investing time here is worthwhile. Third, the textures and synthetic images include occasional ghost-like appearances of passersby and, in rare cases, graffiti creators due to the intervalometer's automatic capture, making such occurrences hard to avoid. While masking people is an option, it risks leaving gaps in the texture. Finally, slight errors in camera orientations or in the geometric surface model can affect pixel alignment accuracy, but overlaying images

from the same synthetic camera setup reveals an average misalignment of just a few pixels. These minor discrepancies, which could trigger false positives along sharp texture edges, are manageable by applying a morphological opening operation (Chapter 3.7.3).

### 3.6 Generating reference change maps

To optimise and validate the proposed change detection method, reference change maps were generated to capture all graffiti-related changes occurring between pairs of epochs. This generation process involved evaluating not only consecutive epochs but also all other possible epoch combinations, maximising the utility of the synthetic images. Given a dataset of 29 epochs across 17 synthetic cameras, there are a total of 13,804 potential image pairs, calculated as follows:

$$17 \times 29 \times 28 = 13,804 \quad (3.1)$$

Since a pair  $AB$  is equivalent to  $BA$  in terms of detected change, only unique pairs were considered, reducing the number to 6902.

A semi-automated approach was employed to generate reference change maps for each unique pair. The process started by organising all images from each synthetic camera into 17 folders, where each folder corresponds to one synthetic camera and contains 29 images sorted chronologically. Not all epochs show graffiti changes compared to the previous epoch. To account for this, a table was created to log epochs with detected changes relative to their preceding epochs. Consecutive epochs with observed changes were noted, as indicated by the coloured numbers in the *ID* column of Figure 3.8.

To capture graffiti-scape changes across highlighted change epochs and their preceding epochs, black polygons were used to mark differences within each image pair. This manual annotation was performed using the open-source software Inkscape (<https://inkscape.org>) and GIMP (<https://www.gimp.org>). This process was conducted according to a protocol developed for consistency in generating change maps.

#### The guideline specified:

*Indicate all differences on the surface which originate from added graffiti between two epochs. This indication is done by generating polygons which cover all changed regions in the images. Because of the co-registration accuracy of the two images and potential blurriness, a positional accuracy of ca. 20 pixels is expected. The indication should start with the area-wise biggest changes and end with smaller changes and not take more than 30 minutes per image pair.*

This process yielded 43 unique binary change maps. Using these manually generated maps, a custom Python script automated the creation of change maps for all possible synthetic image pairs (see Figure 3.8). This script took the unique maps and their corresponding IDs as input, outputting change maps for each possible combination. To streamline data management,



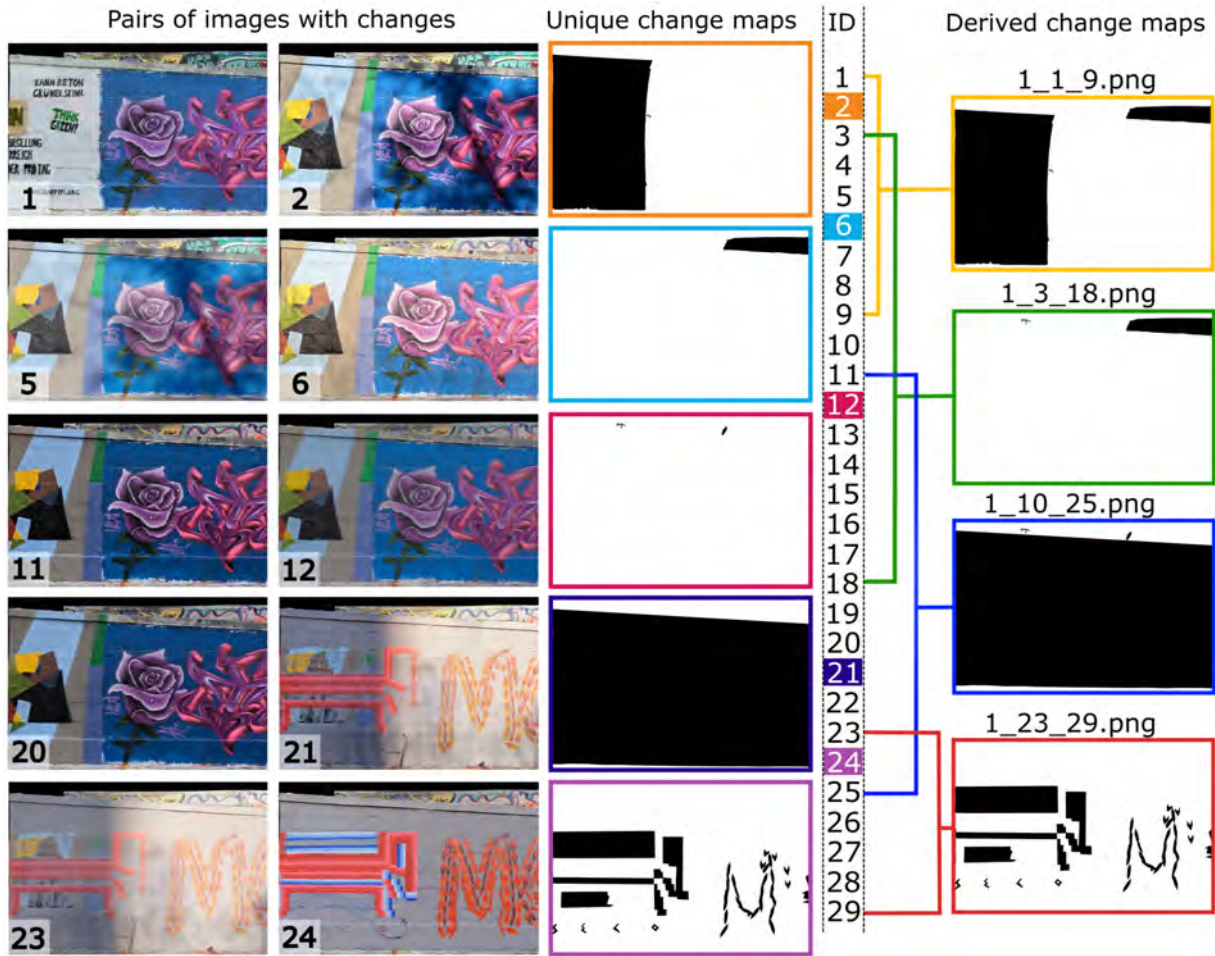


**Figure 3.8:** Exemplary depiction of the change map creation process for images rendered from the same synthetic camera. The first two columns depict image pairs between which graffiti-related change occurred. The numbers indicate the epoch IDs (Table 3.1). Unique change maps (third column) were manually generated for epochs where change occurred with respect to the previous one. The coloured IDs in the fourth column indicate these epochs with change. The fifth column depicts selected change maps automatically derived from the five unique change maps. The coloured lines indicate for which epochs the change map was computed (e.g., the yellow-framed change map depicts the automatically derived graffiti-scape change between the epochs with IDs 1 and 9). The change map filenames reflect this organisational structure. Adopted from [54].

each change map was saved under a unique filename formatted as  $X\_Y\_Z.png$ , where  $X$  denotes the synthetic camera number (1–17),  $Y$  the reference epoch ID (1–28), and  $Z$  the new epoch ID (2–29).

Additionally, 34 binary masks were created to exclude irrelevant image areas: 17 masks identified *no data* regions, while the other 17 masked out irrelevant pixels from background elements like ground or façades. Areas covered by these exclusion masks were excluded from the performance analysis of the change detection approach.

The complete change detection reference dataset, which includes all 6,902 synthetic image pairs, corresponding change maps, and exclusion masks, is publicly available under the following link: <https://doi.org/10.48436/ayj4e-v4864> [89].

[89]: Wild et al. (2023), *INDIGO Change Detection Reference Dataset*

### 3.7 Hybrid change detection framework

As previously discussed, implementing effective image-based change detection for graffiti presents a range of challenges. Initial tests with existing solutions and available open-source software—which are limited relative to the numerous methods developed—revealed that a single-method approach would not suffice for the task’s complexity.

This hybrid change detection method is presented as follows: the *Pixel-based Change Maps* Chapter outlines a new pixel-based approach, while the *Descriptor-based Change Maps* Chapter reviews a recently introduced descriptor-based method [55]. These approaches are then combined within a hybrid change detection pipeline (see the *Change Map Merging* Chapter for details, with further discussion in the *Threshold Optimisation* Chapter).

[55]: Wild et al. (2023), ‘TRACKING THE URBAN CHAMELEON - TOWARDS A HYBRID CHANGE DETECTION OF GRAFFITI’

#### 3.7.1 Pixel-based change maps

##### Image smoothing

As discussed in *Status Quo in Graffiti Change Detection*, a significant challenge in image-based graffiti change detection is the presence of noise-like structures on graffiti-bearing surfaces. These structures can cause small but noticeable shadows under certain solar altitudes and azimuths. Reducing this noise before applying pixel-based graffiti change detection methods could improve change detection results. While conventional smoothing techniques, such as mean filtering or Gaussian blurring, can effectively reduce noise, they also blur all edges in the image, an undesirable effect given that many graffiti contain sharp, thin lines (e.g., Figures 3.2).

To address this, the present study employed the edge-aware smoothing algorithm introduced by Xu et al. (2012) [90]. This algorithm uses a relative total variation metric to quantify spatial differences along the x and y axes within specified windows, distinguishing between an image’s structural components (representing larger objects) and textural details (fine-scale patterns, often with some periodicity) without relying on prior assumptions about pattern regularity or symmetry [90]. This technique allows for smoothing of fine details while preserving edges, enabling more refined analysis in subsequent steps. Four key parameters control texture-structure separation and smoothing [90]:

[90]: Xu et al. (2012), ‘Structure Extraction from Texture via Relative Total Variation’

- ▶ **Scale parameter ( $\sigma$ ):** Determines the maximum size of texture elements and the algorithm’s capability to distinguish texture from structure. The recommended range for  $\sigma$  is [0, 8]. Lower  $\sigma$  values increase processing time and retain more spatial detail.
- ▶ **Smoothness parameter ( $\lambda$ ):** Controls the overall smoothness. Higher values yield smoother results but increase processing time. The recommended range is [0.01, 0.03].
- ▶ **Sharpness parameter ( $\varepsilon_s$ ):** Influences the final sharpness. Smaller values produce sharper results but require more processing time. The recommended range for  $\varepsilon_s$  is [1e-3, 0.03].
- ▶ **Number of iterations:** Larger values increase processing time and smoothing, though the effect diminishes per iteration.



Of these, the scale and strength parameters are most important relative to image size. After testing various parameter combinations and assessing their impact, detailed in the *Pixel-based Results* Chapter the final parameters selected were  $\sigma = 2$ ,  $\lambda = 0.01$ ,  $\varepsilon_s = 0.025$  and two iterations. These settings provided satisfactory smoothing with acceptable processing times for images of  $1000 \times 1500$  pixels, yielding runtimes of approximately 2–4 seconds on a fast processor using Xu et al.'s (2012) MATLAB code. However, applying edge-aware smoothing to a full 24 MP synthetic image ( $4000 \times 6000$  pixels) would extend processing to over 30 seconds.

Therefore, a downsampling and upsampling approach was incorporated. Each 24 MP synthetic image was downsampled by a factor of 16 using nearest-neighbour interpolation, resulting in a 1.5 MP image for smoothing, which was eventually again upsampled to 24 MP using nearest-neighbour interpolation. Nearest-neighbour interpolation was chosen because common alternatives, such as bicubic interpolation, may produce pixel values outside the original range. Although bilinear interpolation reduces jagged edges compared to nearest-neighbour, it can make small features appear fainter. Both methods yield similar values for large regions of quasi-identical pixels generated by the smoothing algorithm. While the influence of interpolation methods on change detection outcomes was not assessed here, the slight differences in edge and feature handling make it unlikely that using another interpolation would meaningfully alter results.

### RGB normalisation

Another key challenge lies in managing inter-epoch illumination variations, which can introduce substantial differences in the image data even in the absence of graffiti-related changes. To achieve approximate illumination invariance efficiently, the smoothed synthetic images were RGB normalised by dividing each red (R), green (G), and blue (B) channel by the combined sum of all three channels for each pixel [91, 92]:

$$R_n = \frac{R}{R + G + B}, G_n = \frac{G}{R + G + B}, B_n = \frac{B}{R + G + B} \quad (3.2)$$

The resulting normalised red ( $R_n$ ), green ( $G_n$ ), and blue ( $B_n$ ) pixel values are the RGB chromaticity coordinates, which sum is always equal to 1. Figure 3.9 shows the RGB-normalised version of the same scene under direct sunlight (top row) and diffuse lighting (bottom row). This normalisation step effectively removes shadows while preserving colour chromaticity. However, it does not adjust for the dominant colour of the illumination-specifically, the correlated colour temperature of the light source. The upper right inset of Figure 3.9 illustrates this: shaded areas contain a higher proportion of blue light compared to direct sunlight, resulting in bluer pixels in shaded regions following RGB normalisation.

[91]: Finlayson et al. (1998), 'Comprehensive colour image normalization'

[92]: Kampel et al. (2010), 'Improved motion segmentation based on shadow detection'

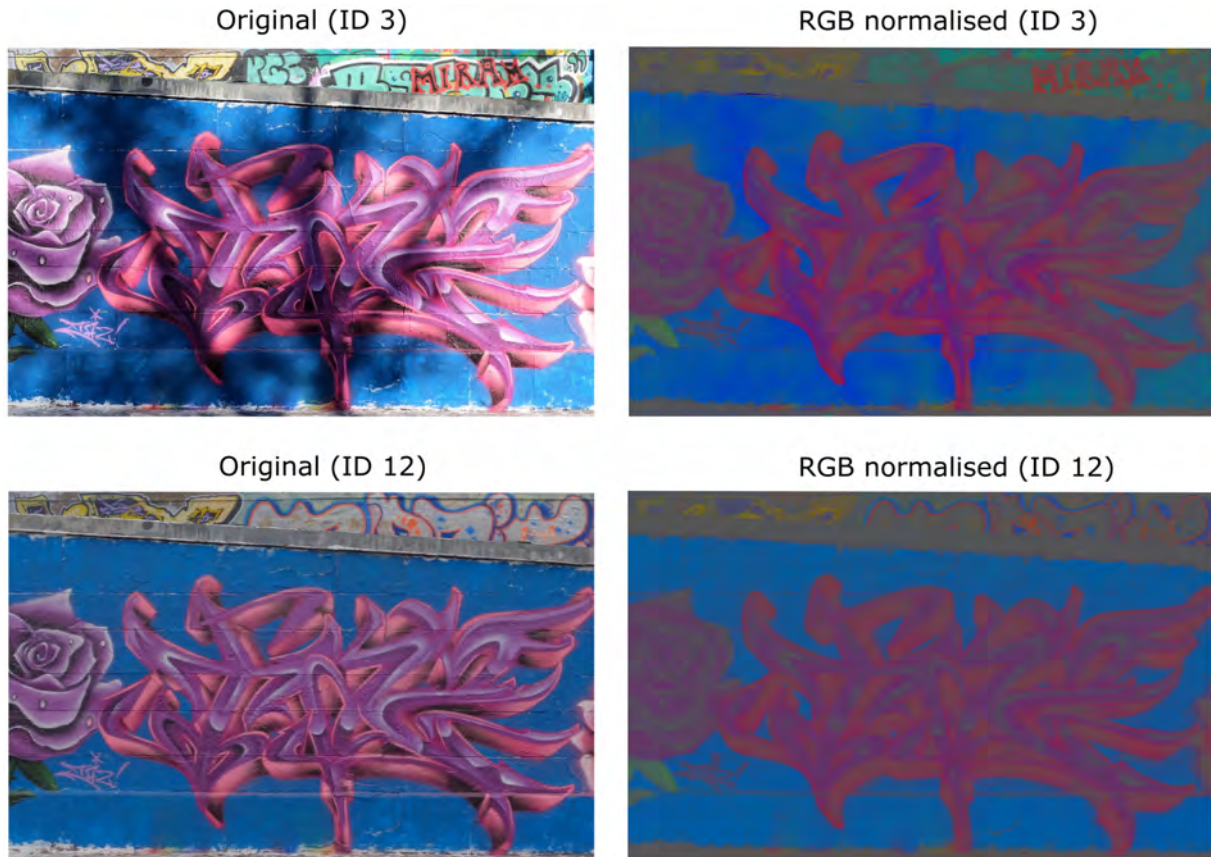


**Figure 3.9:** Results from RGB normalisation. The first column depicts input images recorded under strongly differing illumination conditions: direct sunlight resulting in strong shadows due to trees in front of the wall (upper left; ID3) and cloudy conditions (lower left; ID12). The corresponding RGB-normalised images are shown in the second column. Adopted from [54].

### CIEDE2000 colour differences

After smoothing and RGB normalising all images, pairwise image changes were calculated using CIEDE2000-based colour differencing. This technique, allows for determining deviations from target colours (e.g., digital photos vs. real-world objects, or screen vs. print colours), and typically employs the CIE 1976  $L^*a^*b^*$  (CIELAB) colour space, adopted in 1975 by the Commission Internationale de l'Éclairage (CIE; Eng. International Commission on Illumination; [93]). CIELAB is a three-dimensional colour space that decomposes colour into luminance (lightness,  $L^*$ ) and chrominance (hues on  $a^*$  and  $b^*$  axes, representing red-green and yellow-blue hues, respectively) components (<https://www.iso.org/standard/74166.html>; last accessed April 15, 2025). Since it is perceptually uniform, every unit change in  $L^*$ ,  $a^*$ , or  $b^*$  represents a just noticeable difference to human vision [94]

A colour difference in the CIE  $L^*a^*b^*$  colour space is represented by the symbol  $\Delta E$ . Here,  $\Delta$  denotes a change in the variable  $E$ , which is linked to the German term *Empfindung*, meaning *sensation* in English. The method for calculating this difference varies according to the chosen colour-difference formula, each offering slightly different interpretations of  $\Delta E$ . The original  $\Delta E_{ab}$  formula dates back to 1975 [93] and defines the colour difference as the 3D Euclidean distance between the  $L^*a^*b^*$  coordinates of the sample and the reference. However, this approach

[93]: McLaren (1976), 'XIII—The development of the CIE 1976 ( $L^* a^* b^*$ ) uniform colour space and colour-difference formula'

struggled with highly saturated colours, where CIELAB fails to remain perceptually uniform. To address these perceptual inconsistencies, instead of creating a new colour space, the CIE introduced updated weighted colour-difference formulas based on CIELAB: CIE94 (1995) and the current standard, CIEDE2000 (2001), which was later adopted as the joint ISO/CIE 11664–6:2022 International Standard (<https://www.iso.org/standard/74166.html>, last accessed April 15, 2025). Compared to CIE94, CIEDE2000 introduced five corrections to better align with human visual perception. Due to the complexity and length of the CIEDE2000 equations, a detailed description is omitted for brevity, but complete information is available in official CIE and ISO publications.

This change detection approach uses CIEDE2000-based colour differencing by first converting smoothed, illumination-normalised images from sRGB to CIE  $L^*a^*b^*$  space, referencing the CIE D65 standard illuminant as white. Then, pixel-wise  $\Delta E_{00}$  (CIEDE2000 colour difference) is computed between paired images. Finally, a binary change map is generated from these continuous colour differences using an optimised threshold, detailed in Chapter 3.8.3.

### 3.7.2 Introducing image feature descriptors as change indicators

In his highly influential work, David G. Lowe (1999, p. 1) [95] writes:

*Object recognition in cluttered real-world scenes requires local image features that are (...) partially invariant to illumination, 3D projective transforms, and common object variations.*

Replacing *object* with *change* yields a statement closely aligned with the aims of this study. In particular, illumination invariance is an essential feature in the context of this study. Therefore, it is logical that the key result from Lowe's work, the Scale Invariant Feature Transform (SIFT), offers a promising foundation for image-based graffiti change detection. Specifically, the objective is to transform both images into a collection of local features (not limited to SIFT features), each represented by a descriptor vector. Similar descriptors at similar positions in the co-registered images suggest unchanged regions around these points, and conversely, differing descriptors indicate change. Different studies experimented with various feature descriptors as change indicator (e.g., [96, 97]). They found good performance of descriptor-based change maps, which generally contained less noise than pixel-based approaches but had problems detecting change on featureless objects. This principle has been tested in several variants for detecting changes in satellite imagery obtained from optical sensors [97, 98] and Synthetic Aperture Radar [99, 100], with results confirming its applicability, although mainly restricted to feature-rich areas such as cities. To the best of the authors' knowledge, the transferability of this concept to conventional (terrestrial) images and other applications such as the detection of new graffiti remains unexplored. However, given the generally texture-rich nature of graffiti, this approach seems worth exploring.

The descriptor-based approach implemented in this study consists of three main steps (see 3.10):

[95]: Lowe (1999), 'Object recognition from local scale-invariant features'

[96]: Pillai et al. (2017), 'Descriptors based unsupervised change detection in satellite images'

[97]: Seo et al. (2022), 'Feature-based approach to change detection of small objects from high-resolution satellite images'

[97]: Seo et al. (2022), 'Feature-based approach to change detection of small objects from high-resolution satellite images'

[98]: Liu et al. (2019), 'A contrario comparison of local descriptors for change detection in very high spatial resolution satellite images of urban areas'



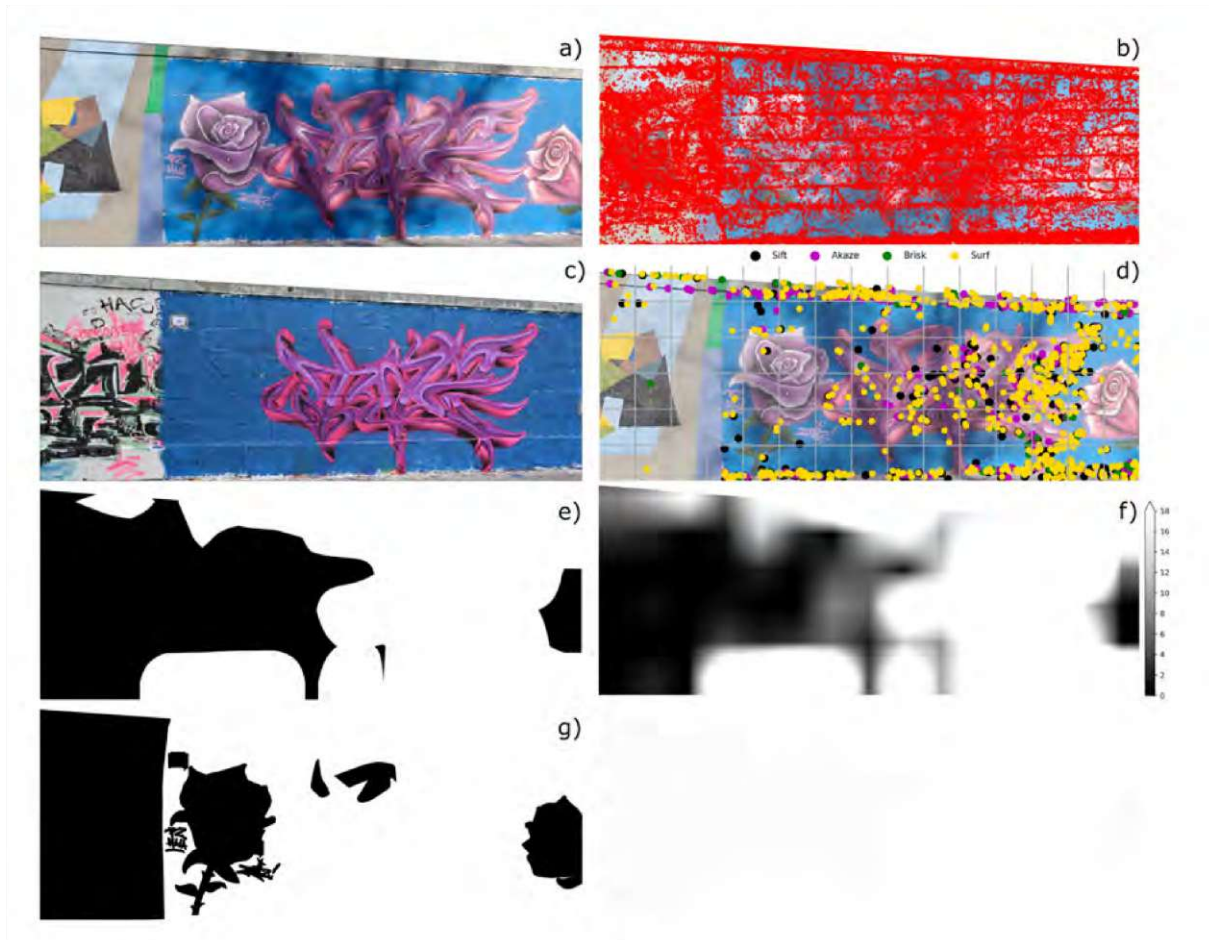


**Figure 3.10:** a) and c) input images from two different epochs. b) Detected feature points in a using all detectors (SIFT, SURF, AKAZE, BRISK) d) Matched and filtered feature points between the image pair. f) Bi-linear interpolated density map of the rasterised matched feature points. e) Final descriptor-based change map. Black denotes change. g) Manually generated reference change map. Subfigures adopted from [55].

1. Detection of distinctive features and computation of descriptor vectors in both images using well-established feature detectors and descriptors (Figure 3.10b).
2. Matching of features based on their proximity in both feature and image space (3.10d).
3. Rasterisation of the matched feature points (Figure 3.10d) and binary classification into changed/unchanged pixels based on the density of the matched feature points (Figure 3.10f and 3.10e).

The following Chapters will detail the individual steps in more depth:

#### Feature point detection and description:

First, feature points are detected in the input images. These points are typically located at edges, corners, or blobs<sup>4</sup> (Figure 3.10b; [101]). This is advantageous, as graffiti often exhibit sharp transitions between the layers specific to the graffiti. In the subsequent step, the detected feature points are described based on the unique patterns within their neighbouring pixels, a process referred to as feature description. This step results in a fixed-length descriptor vector for each detected interest point.

4: Areas within a digital image that stand out due to distinct characteristics, such as luminance or colour, compared to their neighbouring areas.

[101]: Tareen et al. (2018), 'A comparative analysis of SIFT, SURF, KAZE, AKAZE, ORB, and BRISK'



In this work, the respective OpenCV [102] implementations of the following four well-established detectors and descriptors are used: SIFT [95], SURF [103], AKAZE [104], and BRISK [105]. The rationale for employing multiple feature detectors and descriptors lies in their varying properties and sensitivities, which can provide partly independent and complementary information [101], thereby enhancing the reliability of the method. Each detector employed the corresponding algorithm for feature description (i.e., feature points detected by SIFT were also described using SIFT).

### Feature matching

To match the detected features between the two images, a FLANN-based matching method was utilised. FLANN, short for Fast Library for Approximate Nearest Neighbours, comprises algorithms tailored for efficiently identifying nearest neighbours within high-dimensional datasets [106]. In this process, for each feature point detected in image A, FLANN locates the corresponding feature point in image B that has the smallest Euclidean distance between their descriptor vectors. However, this technique often results in numerous false matches, as many features may only appear in one image or be due to background noise, making them insufficiently distinctive (Lowe, 2004).

To effectively reduce false matches, the precise co-registration of the images is leveraged by only accepting matches where points are close in image space. Specifically, a 20-pixel threshold was applied, roughly translating to a real-world distance of about 3 cm. Matches exceeding this distance were considered incorrect.

For image pairs with less precise co-registration, the maximum allowed distance between matched features could be increased, paired with an additional Lowe Ratio Test [107]. In Lowe's ratio test, each feature point from the first image is paired with multiple potential feature point from the second image. For each feature point, the two closest matches (i.e., those with the smallest distance) are retained. The test then assesses whether the distance between these two best matches differs substantially. A difference is considered substantial when the following condition holds:

$$d_1 < d_2 \cdot a \quad (3.3)$$

where  $d_1$  represents the distance between a feature point and its best match,  $d_2$  denotes the distance to its second-best match, and  $a$  is known as *Lowe's ratio*. A commonly recommended value for  $a$  is 0.7 [107], which was also adopted in this work. If the condition is not met, indicating that the match may be ambiguous or unreliable, the feature point is discarded and not included in further analysis.

### Rasterisation

The resulting matched feature points, often called tie points, serve as a proxy for unchanged image regions. To visualise this, a quadratic grid with a cell size of 400 pixels is overlaid on the image, resulting in 150

[95]: Lowe (1999), 'Object recognition from local scale-invariant features'

[103]: Bay et al. (2006), 'Surf: Speeded up robust features'

[104]: Fernández Alcantarilla (2013), 'Fast Explicit Diffusion for Accelerated Features in Nonlinear Scale Spaces'

[105]: Leutenegger et al. (2011), 'BRISK: Binary robust invariant scalable keypoints'

[101]: Tareen et al. (2018), 'A comparative analysis of SIFT, SURF, KAZE, AKAZE, ORB, and BRISK'

[106]: OpenCV (2024), *Feature Matching with FLANN*

cells, calculated as  $(6000/400) \times (4000/400)$ . Each grid cell is assigned the number of tie points within its boundaries. These values are then upsampled using bilinear interpolation to match the original pixel count of  $6000 \times 4000$  pixels. A binary change map is derived by applying a threshold to the tie point density. The selection of suitable thresholds is discussed in Chapter 3.8.3.

### 3.7.3 Change map merging and threshold optimisation

Up to this point, two preliminary outcomes have been generated for each synthetic image pair: the smoothed and RGB-normalised CIEDE2000 colour differences  $\Delta E_{00}$ , calculated on a pixel-by-pixel basis, and the tie point density image. The former serves as a strong indicator of change, while the latter identifies areas with no change. However, appropriate thresholds must be established to convert these outcomes into a binary change map, a crucial step discussed in the following chapter. After creating binarised versions of the pixel-based ( $CM_{pix}$ ) and descriptor-based ( $CM_{des}$ ) change maps, they were combined using a logical AND operation to produce a single merged binary change map ( $CM$ ):

$$CM = CM_{pix} \wedge CM_{des} \quad (3.4)$$

This ensured that only regions marked as changed in both maps were considered graffiti-related alterations in the final change map. Finally, a morphological opening was applied with a  $15 \times 15$  pixel kernel to reduce any residual noise and eliminate artifacts caused by minor co-registration errors.

Finally, thresholds must be applied to create binary change maps from the intermediate results. Specifically, a threshold for the CIEDE2000 differences ( $T_{\Delta E_{00}}$ ) and for the tie point densities ( $T_{TP}$ ) must be set. A training dataset of 50 synthetic image pairs, selected randomly from all 6,902 pairs, was used to systematically determine the most suitable thresholds. The resulting threshold-specific change maps were systematically evaluated against the corresponding reference change maps using the following standard metrics:

$$\text{Precision} = \frac{TP}{TP + FP} \quad (3.5)$$

$$\text{Recall} = \frac{TP}{TP + FN} \quad (3.6)$$

$$\text{F1-Score} = 2 \cdot \frac{\text{Precision} \cdot \text{Recall}}{\text{Precision} + \text{Recall}} = \frac{2TP}{2TP + FP + FN} \quad (3.7)$$

$$\text{Specificity} = \frac{TN}{TN + FP} \quad (3.8)$$

$$\text{CCR} = \frac{TP + TN}{TP + TN + FP + FN} \quad (3.9)$$

where true positives (TP) and true negatives (TN) represent correctly classified pixels, while false positives (FP) and false negatives (FN) denote misclassified pixels. These metrics were computed for every pair of threshold-specific and reference change maps. Subsequently, the median value for each metric was computed across different thresholds to facilitate threshold optimisation. Ultimately, the parameter  $T_{\Delta E_{00}}$  was set to 10, and  $T_{TP}$  was set to 10.5. Details on the procedure that led to those choices can be found in Chapter 3.8.3.

## 3.8 Results and discussion

This chapter elaborates on the rationale behind the chosen parameter values for the pixel-based and feature-based change detection components, discussed in chapters 3.8.1 and 3.8.2. Following this, Chapter 3.8.3 explains the process of optimising thresholds and merging change maps. Finally, Chapter 3.8.4 evaluates the overall performance of the hybrid change detection process.

### 3.8.1 Pixel-based results

The effect of edge-aware smoothing was evaluated visually by comparing the smoothed outputs with the original input (Figure 3.11). This comparison highlights the method's capability to improve change detection results by reducing noise from complex geometric details on the walls. The degree of smoothing depends significantly on the image resolution and the algorithm's parameter settings, particularly the scale parameter  $\sigma$  and the strength parameter  $\lambda$ . Figure 3.11 presents the algorithm's output using two distinct parameter configurations. With the *weak smoothing* approach, some finer structures remain visible, whereas they are almost completely removed in the *strong smoothing* version. However, it becomes clear that *strong smoothing* can also remove certain textural details, like thin lines, leading to undetected features by the change detection algorithm.

To identify optimal smoothing parameters for the change detection task, a quantitative analysis comparing RGB-normalised CIEDE2000 change maps with reference change maps from a randomly generated sample of 50 synthetic image pairs was performed. The results showed that smoothing had a modest but positive effect on pixel-based change detection (Table 3.8.1). The *weak smoothing* approach consistently produced the best results, except for specificity, where the original input performed slightly better. Although the differences were minor, they indicate that smoothing generally improves change detection outcomes. Additionally, the enhanced interpretability due to reduced noise and the negligible increase in processing time justify using *weak smoothing* for all subsequent analyses. For this parameter evaluation, the CIEDE2000 threshold  $T_{\Delta E_{00}}$  was set to 21, which provided visually pleasing results for the training dataset.

A visual inspection of the exemplary results (Figure 3.12) reveals promising outcomes regarding the RGB-normalisation following the smoothing process. The smoothed, RGB-normalised synthetic images (Figure 3.12

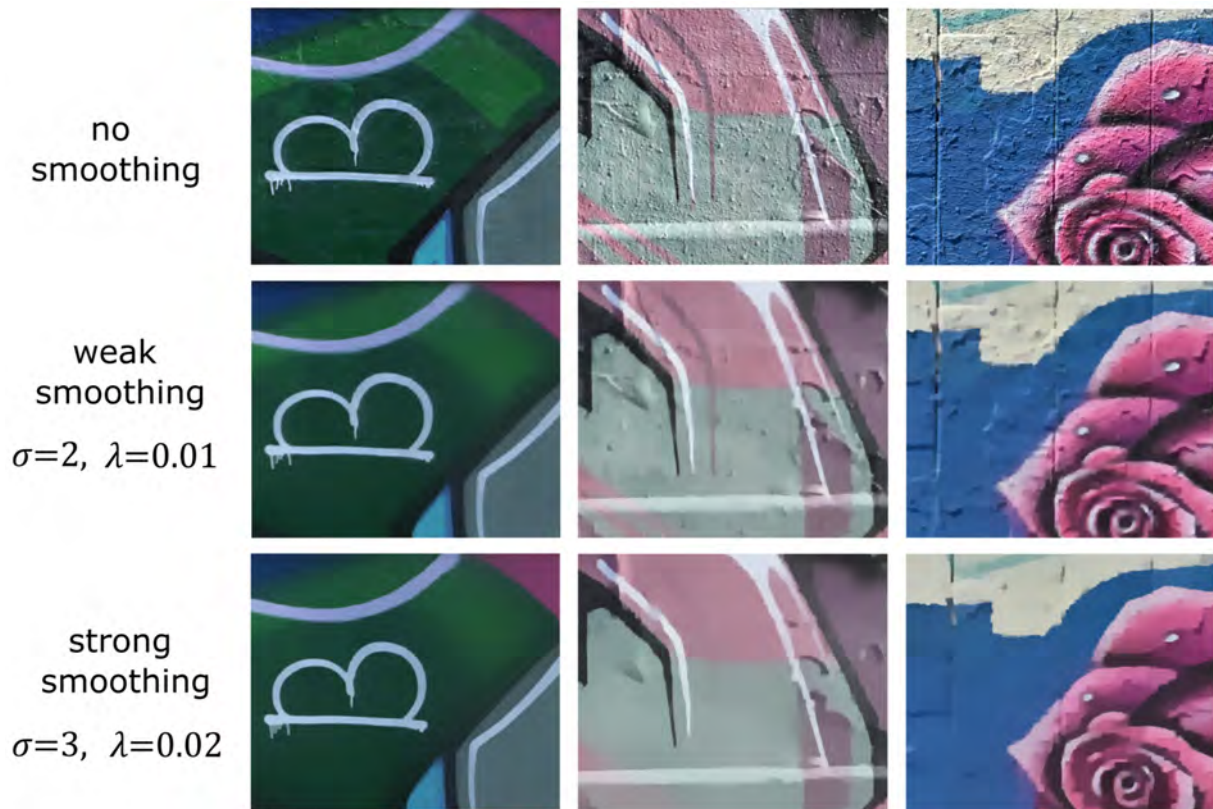


**Figure 3.11:** First row: three 1,200×1,000 pixel snippets extracted from different synthetic images. Second and third rows: the same snippets after applying edge-aware smoothing with different values for the scale parameter and the smoothness parameter  $\lambda$ . Both sets used  $\epsilon = 0.025$  for two iterations. In agreement with image smoothing, these snippets were downsampled by a factor of 16 before smoothing. The smoothed results were then upsampled to reach the initial pixel count again. Both resizing processes applied nearest neighbour interpolation. Adopted from [54].

**Table 3.2:** Results from the pixel-based change detection with different parameters used for the edge-aware smoothing. All metrics are based on the 50 randomly selected synthetic image pairs.

Smoothing	Parameters used	F1-Score [%]	Recall [%]	Precision [%]	CCR [%]	Specificity [%]
No smoothing	N.a.	65	73	73	85	89
Weak smoothing	$\sigma = 2 \lambda = 0.01$	69	76	78	87	88
Strong smoothing	$\sigma = 3 \lambda = 0.02$	67	74	75	88	88

b1 and b2) display strong illumination invariance while effectively retaining the chromatic characteristics of the graffiti. These features indicate that this simple colour space transformation can successfully address illumination variations. However, a limitation of RGB-normalisation has been identified: pixels with similar proportions of R, G, and B (such as white, grey, and black pixels) become nearly indistinguishable in the RGB-normalised space, making them prone to being overlooked [108]. This issue is illustrated in Figure 3.12, where the black facial elements in the upper right corner show similar RGB-normalised values to the surrounding white and grey backgrounds.

Despite this, the resulting CIEDE2000 differences (shown in Figure 3.12c) remain relatively large at that location due to the vivid colours used in

[108]: Kender (1976), *Saturation, hue, and normalized color: Calculation, digitization effects, and use*



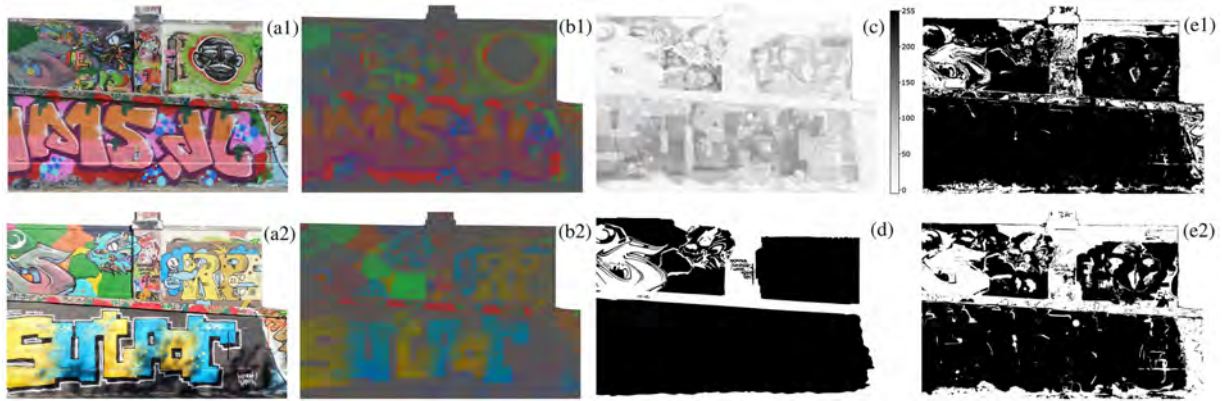


**Figure 3.12:** Pixel-based processing chain example. (a1, a2) Input image pair (epoch ID1 and ID3). (b1, b2) Respective smoothed and RGB-normalised variants. (c) Colour differences based on CIEDE2000. (d) Reference change map. (e1, e2) Pixel-based change maps derived using two different thresholds:  $T_{\Delta E_{00}} = 10$  (e1) and  $T_{\Delta E_{00}} = 21$  (e2). Adopted from [54].

the new graffiti. However, such a change might have gone unnoticed if the original black graffiti had been covered with white, grey, or black paint. Achromatic areas like these can negatively affect change detection results. Colours with lower chromaticity are often used as base layers in graffiti, making up a significant portion of the graffiti. While one could argue that failing to detect changes in the background is less critical, as it typically does not alter the graffiti's intended meaning, this viewpoint may not be universally accepted by graffiti creators and scholars. From a graffiti documentation perspective, overlooking background changes due to RGB normalisation is generally likely to be more acceptable than missing the central part of the graffiti as new graffiti can still be identified, albeit not in its full extent.

Moreover, Figures 3.12e1 and e2 illustrate that the binary pixel-based change maps vary significantly depending on the CIEDE2000 difference threshold  $T_{\Delta E_{00}}$ . Selecting an appropriate  $T_{\Delta E_{00}}$  involves balancing the detection of excessive changes against the risk of missing actual changes. This trade-off is quantified using recall, precision, and F1-score, as described in Chapter 3.8.3. An optimal threshold was identified using a training set of 50 synthetic image pairs and their reference change maps. This process involved testing 16 integer thresholds from 9 to 24, generating binary change maps for each synthetic image pair. The median metrics for each threshold were calculated based on these change maps and their corresponding reference data. The metrics revealed predictable trends: higher values for  $T_{\Delta E_{00}}$  reduced false detections (improving precision) but led to missed detections (lowering recall). The optimal  $T_{\Delta E_{00}}$  for this analysis was set at the point where recall and precision intersected. For the training data, this intersection occurred at a threshold where both precision and recall reached 77% (as shown in Table 3.3).

**Table 3.3:** Results from the pixel-based change detection.

Method	Threshold	F1-Score [%]	Recall [%]	Precision [%]	CCR [%]	Specificity [%]
RGB-norm	$T_{\Delta E_{00}} = 21$	69	77	77	87	88

### 3.8.2 Descriptor-based results

The descriptor-based approach proves most effective for objects with significant textural variations, enabling the extraction of numerous feature points (see Figure 3.13). For instance, matching two synthetic images featuring graffiti with fine text elements can be done efficiently, leading to a dense distribution of tie points and a higher probability of detecting areas labelled as *no change*. However, these areas also carry the risk of masking real changes, as illustrated in the upper middle section of Figure 3.13c. This issue can be addressed by modifying the grid cell size or lowering the threshold  $T_{TP}$ . Adjustments like these, however, may increase the number of FPs, making the selection of an optimal threshold essential. Importantly, evaluating and selecting such a threshold should be done alongside the pixel-based approach, as the descriptor-based change detection method alone is insufficient for identifying changes in regions with minimal or no texture.

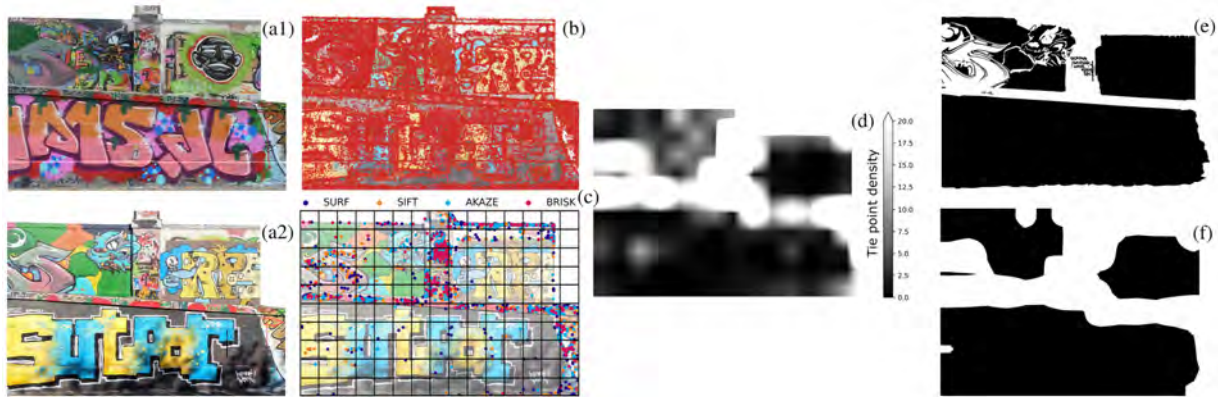


**Figure 3.13:** Descriptor-based processing chain example. (a1, a2) Input image pair (epochs ID1 and ID3). (b) Image A1 overlaid with extracted feature points (using SURF, SIFT, AKAZE and BRISK). (c) Matched and filtered tie points overlaid with a grid for tie point density calculations. (d) Tie point densities derived from panel (c) using linear interpolation. (e) Reference change map between a1 and a2. (f) Descriptor-based change map using a tie point density threshold ( $T_{TP}$ ) of 11. Adopted from [54].

### 3.8.3 Threshold optimisation and change map merging

Chapters 3.8.1 and 3.8.2 highlighted the necessity of applying thresholds to generate binary change maps from intermediate pixel- and descriptor-based change detection outcomes. Although a suitable threshold  $T_{\Delta E_{00}}$  for the pixel-based component of the graffiti change detection approach was established in the *Pixel-based Results* chapter, this value did not incorporate descriptor-based data. Therefore, creating an optimal combined binary change map  $CM$  requires determining a new threshold  $T_{\Delta E_{00}}$  for the pixel-based results and identifying an appropriate threshold  $T_{TP}$  for the descriptor-based results.

Following the method described in Chapter 3.12, 16 integer CIEDE2000 thresholds ranging from 9 to 24 were used to produce pixel-based change maps for each of the 50 synthetic image pairs in the training dataset. For the descriptor-based results, 12 threshold values between 3 and 14 were tested. Combining all possible pairs of thresholds yielded 192 (i.e.,  $16 \times 12$ ) binary hybrid change maps for each image pair. Each map was evaluated against its corresponding reference change map using precision, recall, F1-score, specificity, and CCR metrics. Metric-specific

medians were then calculated and compiled into a matrix for all 192 threshold combinations (see Figure 3.14).

The optimal thresholds were found to be 10 or 11 for the tie point density limit and 10 for the CIEDE2000 colour difference. With  $T_{TP} = 10.5$  and  $T_{\Delta E_{00}} = 10$ , the combined change maps achieved a precision and recall intersection at 83%, with the F1-score peaking at 79%.

Figure 3.14 showed two expected primary trends:

1. Increasing  $T_{TP}$  results in higher recall but lower precision.
2. Increasing  $T_{\Delta E_{00}}$  produces the opposite effect, with lower recall and higher precision.

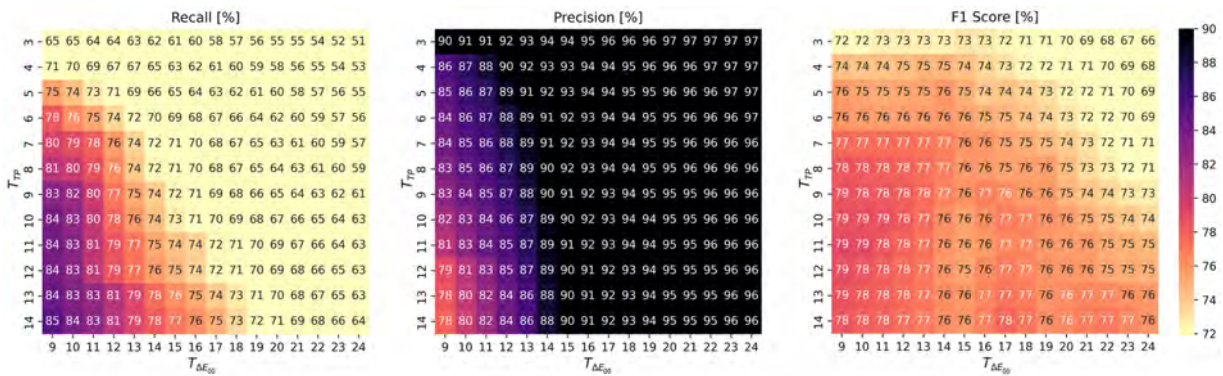


**Figure 3.14:** The tested tie points ( $T_{TP}$ ) and CIEDE2000 ( $T_{\Delta E_{00}}$ ) thresholds with their corresponding assessment values. These assessment values represent metric-specific median values computed via the thresholds-specific hybrid change maps and their reference change maps for the 50 image pairs of the sample dataset. Adopted from [54].

The analysis of the threshold evaluation highlighted the advantages of the descriptor-based approach. When using a very low  $T_{TP}$  threshold, the recall and F1-score experienced significant decreases. For instance, with  $T_{TP} = 3$ , the maximum F1-score achieved was only 73%, and the recall dropped to 65%. Setting thresholds naturally requires a balance between detecting excessive changes and failing to detect real changes. The main aim of this study was to strike an equilibrium between these conflicting objectives. As more experience is acquired, it may become necessary to adjust the threshold values to prioritise the identification of true positives, even if it results in accepting more false negatives, or vice versa.

### 3.8.4 Hybrid change detection assessment

The evaluation of the entire image-based graffiti change detection method was conducted using two approaches. First, the hybrid change detection pipeline, optimised with all parameter values and thresholds, was applied to 6902 pairs of synthetic images. Reference change maps for each pair allowed for a quantitative assessment of the results using the metrics described in Chapter 3.8.3. Second, the performance metric values were compared with those derived from the Iteratively-Reweighted Multivariate Alteration Detection (IR-MAD; [109]), a commonly used change detection method [74].

IR-MAD is an extension of the Multivariate Alteration Detection (MAD; [110]) method and is widely used for change detection in multi-spectral

[109]: Nielsen (2007), 'The regularized iteratively reweighted MAD method for change detection in multi-and hyperspectral data'

[74]: Tewkesbury et al. (2015), 'A critical synthesis of remotely sensed optical image change detection techniques'

[110]: Nielsen et al. (1998), 'Multivariate alteration detection (MAD) and MAF postprocessing in multispectral, bitemporal image data: New approaches to change detection studies'



remote sensing imagery. MAD effectively identifies uncorrelated information between input images, which is a strong indicator of change. It is based on canonical correlation analysis (CCA), which finds linear combinations of the input bands ( $2 \times 3$ ) that maximise correlation [111]. For bitemporal multi-band images, the canonical correlations are subtracted from each other, highlighting potential changes in the image [109]. A threshold is applied to the resulting differences (MAD components) to distinguish between change and no change. This threshold is typically determined dynamically per image pair using k-means clustering (with  $k=2$ ), which results in two clusters with minimal within-cluster variance. A key advantage of MAD is its invariance to linear scaling, making it robust to variations in illumination and sensor settings.

[111]: Hotelling (1992), 'Relations between two sets of variates'

[109]: Nielsen (2007), 'The regularized iteratively reweighted MAD method for change detection in multi-and hyperspectral data'

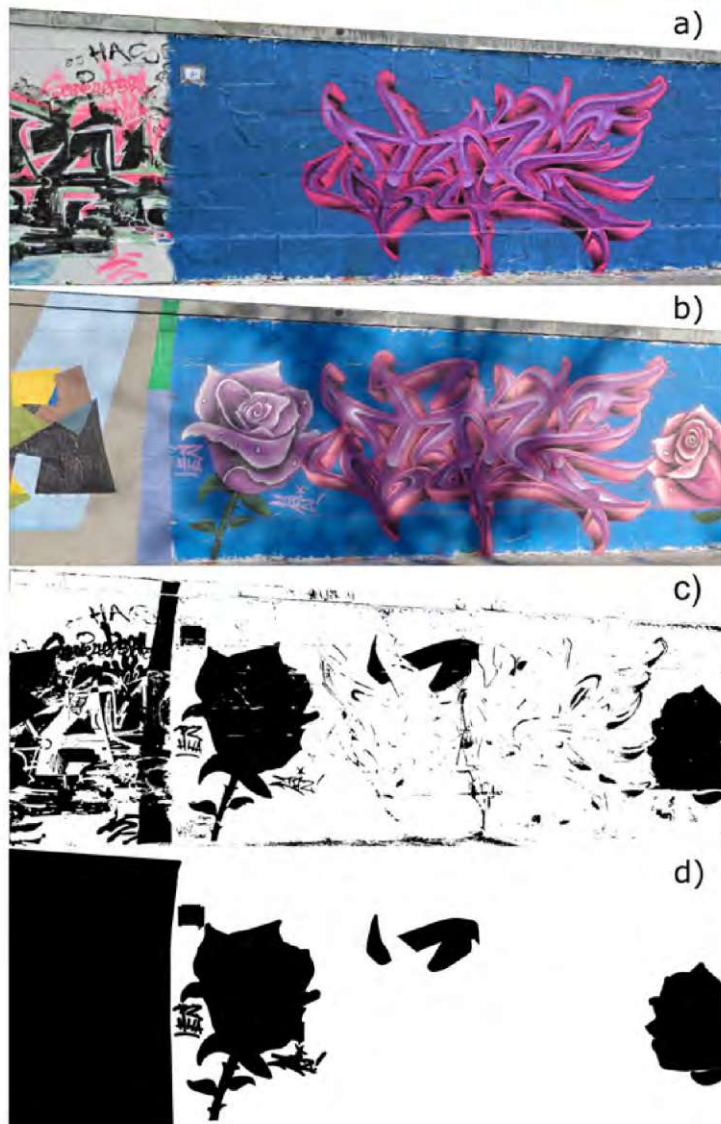


**Figure 3.15:** a) and b): co-registered images from the same graffiti scene at the Donaukanal taken on 12-10-2022 and 12-11-2022, respectively. c) Results from IR-MAD using the images from a) and b) as input where black denotes change and white no change. d) Manually generated reference data. Adopted from [55].

In addition to standard MAD, IR-MAD iteratively assigns weights to pixels based on the change magnitude detected in the previous iteration (i.e., pixels with minor change are given higher weights). This iterative process enhances the robustness of the change detection [109]. The iteration stops when the maximum difference in the

[109]: Nielsen (2007), 'The regularized iteratively reweighted MAD method for change detection in multi-and hyperspectral data'



canonical correlation drops below a threshold,  $\epsilon$ . Tests suggest  $\epsilon = 0.1$  is suitable for graffiti change detection. Larger values of  $\epsilon$  lead to more false positives, while smaller values may result in false negatives and increased runtime. This study uses the IR-MAD implementation from ChenHongruixuan's ChangeDetectionRepository on GitHub (<https://github.com/ChenHongruixuan/ChangeDetectionRepository>; [112]).

Running IR-MAD on the images in Figures 3.15a and b produces the change map shown in 3.15c, which highlights graffiti cover changes, demonstrating the applicability of IR-MAD for this use case. However, while visually effective, IR-MAD alone is insufficient for graffiti change detection due to the noisy nature of the resulting change map, which includes several false positives, particularly at edges (e.g., between sandstone bricks or transitions between graffiti layers). This noise is a common issue with pixel-based approaches, largely caused by image co-registration errors and differences in illumination between the acquisitions [74]. Additionally, IR-MAD struggles in completely changed or unchanged scenes, as its k-means clustering expects two classes and fails when only one is present. Thus, two sets of IR-MAD based reference change maps were created:

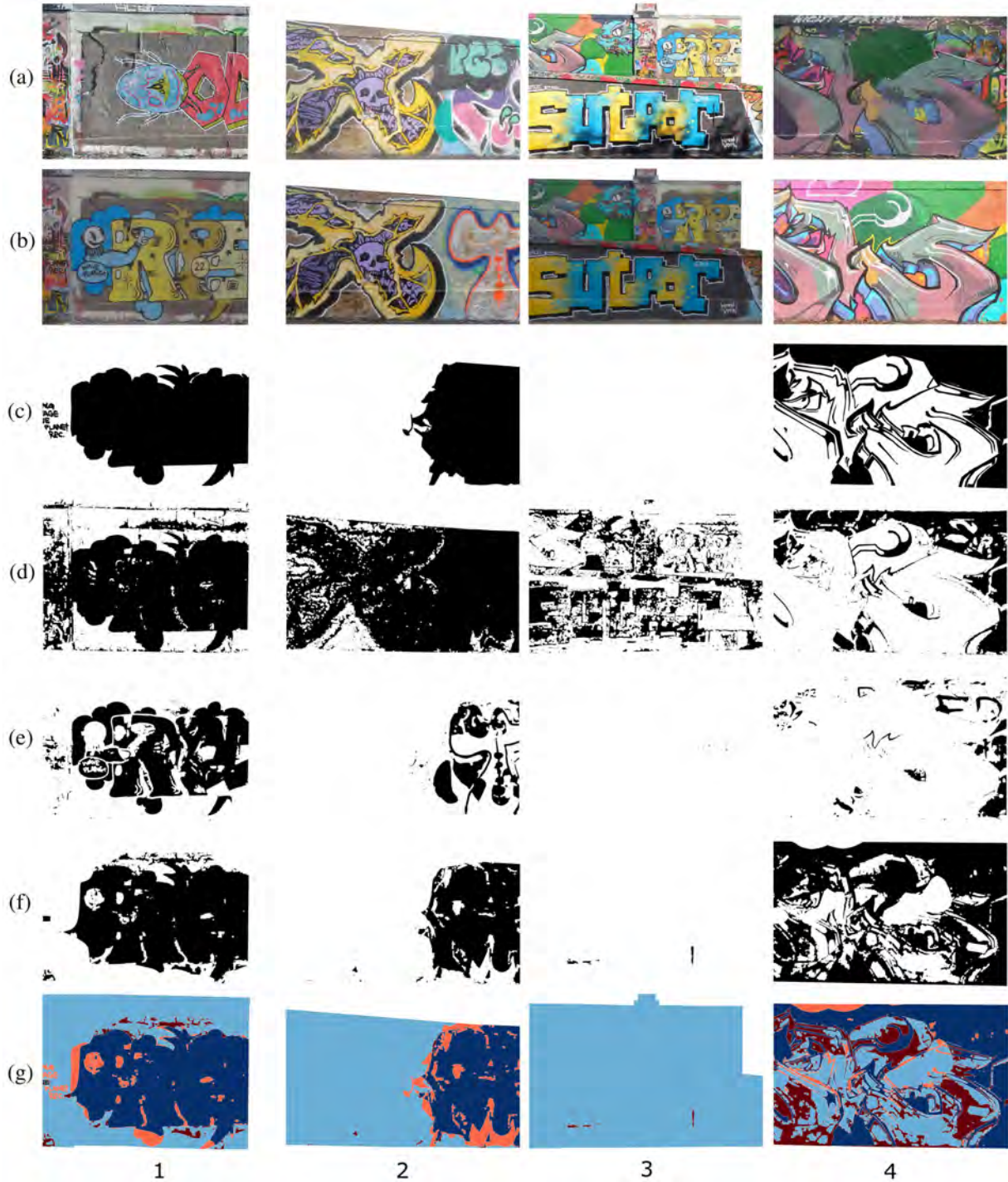
- The first set of IR-MAD change maps was generated using a dynamic per-image threshold, determined by K-means clustering ( $K = 2$ ), distinguishing between change and no change.
- The second set used a static threshold, with its optimal value determined through the procedure outlined in the *Pixel-based Results* chapter. The same 50 image pairs training dataset was employed for both the static threshold optimisation and the hybrid approach optimisation.

Table 3.4 presents the relevant metrics for the three change detection approaches and shows that the newly developed hybrid method achieves high overall performance with relatively low variability, especially when compared to the results from IR-MAD. When comparing these metrics to those for the training dataset (Figure 3.14), there is a slight decrease in recall, a small increase in F1-score, and a slight improvement in precision. However, these metric values remain close to those obtained during threshold tuning, suggesting that the training dataset is representative. The exceptionally high CCR and specificity values further confirm the method's general applicability, which is supported by the visual representation of the exemplary results (3.16).

**Table 3.4:** Optimised thresholds, average runtime (on a 16-core INTEL i9-12900K processor) and metric-specific median results (with their median absolute deviations) for the three tested change detection algorithms. All metrics are based on the entire synthetic image set of 6902 pairs.

Method	Threshold(s)	F1-Score [%]	Recall [%]	Precision [%]	CCR [%]	Specificity [%]	Average time per Pair [s]
Hybrid	$T_{TP} = 10.5$ $T_{\Delta E_{00}} = 10$	$80 \pm 13$	$77 \pm 11$	$87 \pm 13$	$95 \pm 5$	$98 \pm 2$	16.3
IR-MAD	Dynamic (K-means)	$51 \pm 25$	$69 \pm 17$	$81 \pm 17$	$64 \pm 14$	$66 \pm 14$	17.1
IR-MAD	$T_{IR-MAD} = 28$	$48 \pm 32$	$81 \pm 19$	$81 \pm 17$	$98 \pm 1$	$99 \pm 0$	7.2

[74]: Tewkesbury et al. (2015), 'A critical synthesis of remotely sensed optical image change detection techniques'



**Figure 3.16:** Four exemplary results (columns 1–4) with the respective synthetic input pairs (a and b), reference change maps (c), IR-MAD results with K-means thresholding (d), IR-MAD results with a static threshold of  $T_{IR-MAD} = 28$  (e), hybrid change detection results (f) and colourised comparison of the hybrid results with the reference map (g); (light) blue denotes true (negatives)/positives and (light) red denotes false (negatives)/positives. Adopted from [54].

However, there are some limitations. The visual quality of the results does not always align with the metrics, emphasising that the obtained metrics must be interpreted with caution for individual examples (e.g., Figure 3.16f4). Due to the coarse initial tie-point-based change map, smaller graffiti, such as tags, are sometimes missed (e.g., Figure 3.16f1). On the other hand, the hybrid approach performs exceptionally well on

completely unchanged scenes (e.g., Figure 3.16f3), as reflected in the high specificity values (Tables 3.4 and 3.5).

**Table 3.5:** Exemplary results from the hybrid change detection approach.

Method	Example #	F1-Score [%]	Recall [%]	Precision [%]	CCR [%]	Specificity [%]
Hybrid	1	84	88	81	83	77
IR-MAD (K-means)	1	79	66	99	81	99
IR-MAD	1	87	95	81	85	75
Hybrid	2	86	76	98	91	99
IR-MAD (K-means)	2	49	33	99	75	99
IR-MAD	2	57	95	41	49	23
Hybrid	3	N.a.	N.a.	N.a.	99	99
IR-MAD (K-means)	3	N.a.	N.a.	N.a.	66	66
IR-MAD	3	N.a.	N.a.	N.a.	99	99
Hybrid	4	72	87	61	69	55
IR-MAD (K-means)	4	75	61	96	81	98
IR-MAD	4	29	17	99	63	99

Comparison with the established IR-MAD method revealed that the hybrid approach outperformed IR-MAD when using K-means dynamic thresholding (Table 3.4). All metrics were significantly worse for this IR-MAD binarisation variant, and its variability was higher. This can be attributed to the limitations of K-means thresholding in completely unchanged image pairs, as shown in Figure 3.1 d3. However, when applying an optimised IR-MAD threshold, determined through the same threshold optimisation process used for the pixel-based approach, performance between IR-MAD and the hybrid method was similar, particularly for recall, precision, CCR, and specificity. Notably, IR-MAD showed much higher variability, as reflected in the large median absolute deviations for recall, precision, and F1-score. This variability contributed to the significant difference between F1-score and recall/precision.

In terms of computational efficiency, the hybrid approach (16.3 s per image pair where 11.6 s is for the generation of  $CM_{pix}$  and 4.7 s for  $CM_{des}$ ) required more processing time than the IR-MAD variant with a static threshold (7.2 s per image pair). This difference is mainly due to the additional steps in the hybrid method, such as smoothing, feature point extraction, matching, and the computational complexity of the CIEDE2000 formulas. However, the processing time for the hybrid approach remains reasonable for the intended task.

To contextualise this, consider that each image pair covers roughly 5 meters of graffiti-covered wall, with around 13 km of such surfaces in the Donaukanal study area [10]. Factoring in about 10% redundancy in image pairs, this results in 2,860 pairs, or approximately 13 hours of processing to generate a complete change map for the entire research

area, assuming consistent surface geometry for reuse of the base surface mesh. This estimate excludes the time needed for photo acquisition and co-registration (image orientation and synthetic image generation), which depends on the number of photos and the incremental SfM implementation. With a good base photo network, about 1 hour of image acquisition (using 3 GoPro cameras mounted on a bike helmet, capturing 24,000 photos at 2 photos per second, resulting in 8,000 photos per camera) and 2 hours for transport and data management, all synthetic images could likely be generated in about a day on a powerful computer. It is reasonable to expect that a dedicated team could monitor changes in the 13 km-long graffiti-scape on a two-day, maximally three-day basis.

In summary, this chapter introduced an efficient and largely automated process for generating co-registered synthetic graffiti images from overlapping photographs. This approach was successfully applied to a test zone along Vienna's Donaukanal. Using these synthetic images, binary reference change maps were created, resulting in a comprehensive dataset of 6092 co-registered image pairs with corresponding change maps, all of which have been made publicly available. A more thorough summary and further conclusions and an outlook related to this work can be found in Chapter 6 including an outlook how this change detection can be integrated in an automated documentation workflow.



# 4 An automated framework for generating rectified and georeferenced graffiti images

As noted in the Introduction, preserving the spatio-temporal context in graffiti documentation is essential for capturing the dynamic, multi-layered nature of graffiti's creation, modification, and interaction over time. While a static photograph alone might fail to convey the full cultural and societal significance of graffiti, absolutely georeferenced photographs not only address the spatial context but also lay the groundwork for understanding the temporal evolution of graffiti. By generating georeferenced graffiti images, it would also become possible to conduct more quantitative spatial analysis. Such an analysis could, for example, be the simple question of which colours are dominating at a certain point in space and time. By having the RGB information, and the approximate extent of each pixel, this question could be easily automated. As anticipated by Project INDIGO, every photograph of a graffito should be annotated with metadata [52]. By enriching the photos with metadata, such as graffiti styles, topics, and motifs, georeferenced images can lay the groundwork for geospatially analysing graffiti in unprecedented detail [58].

Chapter 4.1 first explores image distortions as a major challenge in photographic graffiti documentation, drawing primarily from the conference proceedings contribution from Wild et al. (2023) [58].

Subsequently, planar rectification (Chapter 4.2) is proposed and evaluated as a potential method for georeferencing and correcting image distortions. Small portions of this chapter were initially introduced in [10] but were substantially extended for this thesis.

Chapter 4.3 and 4.4 expands this idea by introducing orthophotos as potential solution for above mentioned problems. These Chapters can be seen as core part of Chapter 4 as they introduce and evaluate the developed software AUTOGRAF. Chapter 4.3 and 4.4 is largely based on the following peer-reviewed article which is published under CC BY 4.0 license:

Wild, B., Verhoeven, G. J., Wieser, M., Ressler, C., Schlegel, J., Wogrin, S., Otepka-Schremmer, J., & Pfeifer, N. (2022). AUTOGRAF—AUTomated Orthorectification of GRAffiti Photos. *Heritage*, 5(4), 2987–3009. <https://doi.org/10.3390/heritage5040155>

Chapter 4.5 explores an approach to enhancing the AUTOGRAF workflow by incorporating data from an RTK-GNSS device mounted on a camera. This integration enables the direct collection of georeferencing information, a solution previously presented in a conference proceedings contribution by Wieser et al. (2024) [57].

4.1	Image distortions . . . . .	62
4.2	Planar rectification . . . . .	63
4.2.1	Quality assessment of the planar rectification approach . . . . .	64
4.2.2	Considerations regarding the large scale applicability of planar rectification . . . . .	65
4.3	AUTOGRAF - AUTomated Orthorectification of GRAffiti Photos . . . . .	66
4.3.1	The orthophoto principle . . . . .	66
4.3.2	Acquiring and managing graffiti photos . . . . .	69
4.3.3	Initial SfM and quality checks . . . . .	69
4.3.4	Incremental SfM approach . . . . .	70
4.3.5	Creation of the 3D Model and determination of a custom projection plane . . . . .	71
4.3.6	Orthophoto creation and graffito segmentation . . . . .	73
4.3.7	Orthorectification experiment . . . . .	74
4.4	Results from the orthorectification experiment . . . . .	76
4.4.1	Initial local and incremental SfM . . . . .	76
4.4.2	Derivation of the 3D surface model and the projection planes . . . . .	77
4.4.3	Quantity and quality of the derived orthophotos . . . . .	77
4.4.4	Feasibility of the workflow . . . . .	79
4.5	The potential of incorporating highly-accurate direct georeferencing . . . . .	81
4.6	Potential dissemination of the results . . . . .	83

Chapter 4 ends by discussing a potential dissemination via web maps method for the collected and processed graffiti images. This last Chapter 4.6 summarises the results of the Master thesis by Baumann (2024) [47].

## 4.1 Image distortions

Improving how new graffiti can be detected is one central challenge tackled using photogrammetric techniques. Another key challenge in photographic documentation are distortions. Although often barely noticeable, every photo is affected by image distortions caused by three key factors:

- **Perspective distortions** arise when the object being photographed is not a single plane aligned parallel to the camera's focal plane. The effect of perspective is visualised by the red line in Figure 4.1.
- **Topographic distortions** arise from the uneven relief of the photographed object. Graffiti-covered surfaces often feature protruding or receding elements, such as doors, ventilators, or other infrastructural components that contribute to the graffiti canvas. Even the concrete walls themselves, which serve as the primary backdrop for graffiti, may display significant variations in surface topography. Such irregularities create varying distances between the camera and different parts of the surface, leading to topographical displacements of these elements and resulting in a distorted or misleading representation of the overall object.
- **Lens distortions** are geometric imaging errors of optical systems that cause local changes in image scale. These distortions typically appear as inward or outward curving of straight lines, particularly when lenses with very short focal lengths are used. While for utilised camera lenses, these distortions are generally less significant compared to other types of distortions, they are still noticeable and should be taken into consideration when photogrammetrically documenting graffiti [58].



**Figure 4.1:** Semi-transparent photograph of a graffiti, captured around Halloween in November 2021, demonstrating common distortions found in conventional photography. Perspective distortion is illustrated by two converging dashed red lines, while the orange rectangle highlights topographic displacement caused by a door embedded in the wall. Adopted from [58].

This chapter explores two photogrammetric methods to address the challenges mentioned earlier. It begins with a straightforward solution: planar rectification, examining its accuracy and limitations. Next, the orthophoto concept is introduced, highlighting its potential for documenting graffiti. Following this, an automated software framework for large-scale orthorectification of graffiti is presented, with its performance evaluated using a dataset of 826 photographs capturing 100 graffiti along the Donaukanal.

## 4.2 Planar rectification

The image of a planar object (e.g., a vertical wall) taken with a camera is a so-called projective transformation [113]. Where the image of the object is located in the image plane and how strong the perspective distortions are depends on the location of the planar object, where the camera is, the angular attitude of the camera, and the camera parameters themselves, i.e., primarily the focal length. Under the condition that the camera produces an exact central projection (the so-called pinhole camera model), this transformation has eight parameters ( $a_1, a_2, a_3, b_1, b_2, b_3, c_1, c_2$ ). It describes the relationship between the object coordinates ( $X, Y$ ) and image coordinates ( $x, y$ ) [113]:

$$X = \frac{a_1x + a_2y + a_3}{c_1x + c_2y + 1} \quad (4.1)$$

$$Y = \frac{b_1x + b_2y + b_3}{c_1x + c_2y + 1} \quad (4.2)$$

The eight parameters can be determined from (at least) 4 control points, which are measured in both the image and the object space. Once these parameters are known, the planar rectified image can be generated. This is a new digital image that has the same image content as the central perspective image, but it is scaled (i.e., distances measured in the image space can be translated to distances in the object space) and does not suffer from perspective distortions. This means that, in theory, all pixels have the same size at the object, e.g., 1mm. If the planar object is known with its coordinates in a superior coordinate system, the rectified image can also be transformed into this system, which can be used, e.g., for visualisation.

Above, several assumptions were given: the object is planar, and the camera produces a central perspective image. In realistic cases, these assumptions do not hold entirely. Firstly, images from real cameras suffer from lens distortion, which causes the image to deviate from an exact central projection. Lens distortion effects usually increase from the image centre to the image borders and can be limited by using large focal lengths and largely eliminated in post-processing, for example, by correcting the image using Brown's distortion model [49]. Correcting the images for lens distortion leads to slightly improved results. However, it also requires more (computational) effort.

Another assumption that seldomly holds in real-world scenes is the planarity of the object. At Donaukanal, most objects are human-made (e.g., walls, bridge pillars, etc.). Visually, these objects often exhibit plane

[113]: Kraus (2012), *Photogrammetrie: Geometrische Informationen aus Photographien und Laserscanneraufnahmen*

[49]: Brown (1996), 'Decentering distortion of lenses'



structures. However, it is fair to assume that even seemingly planar walls feature curvatures or other deviations from planarity, which might be hidden visually.

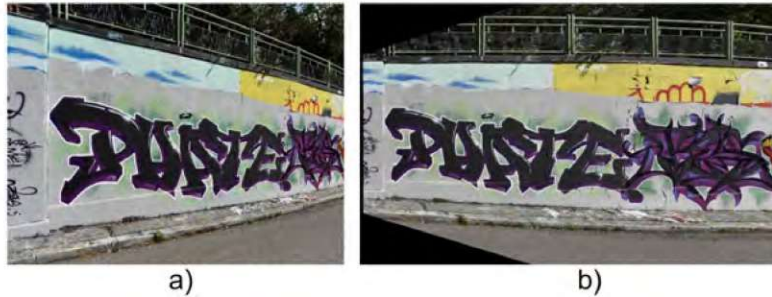


**Figure 4.2:** Example of a planarly rectified image depicting graffiti at the testing zone. a) the original image (Nikon D750 + Nikon AF-S NIKKOR 20mm f/1.8G ED @ f/5.6 - 1/1600 s - ISO 200). b): the planar rectification of the same image.

### Planar rectification workflow

To investigate the applicability and accuracy of this projective transformation approach, approximately 40 graffiti at the INDIGO testing zone were rectified using planar rectification. For each image, sometimes depicting several graffiti, four 3D points (i.e., control points) were measured in the SfM derived, textured, and georeferenced (EPSG:: 31256) 3D model from the photogrammetric backbone. The control points were measured at well-identifiable locations, preferably at the border of the graffiti/graffiti of interest. From these 3D coordinates, an adjusted plane was computed by minimising the orthogonal distances between the control points and the plane (orthogonal regression plane). By projecting the measured 3D points onto this adjusted plane, 2D coordinates of the control points were obtained. Using the corresponding 2D image coordinates, the eight parameters were determined, and a rectified image (Figure 4.2) was retrieved by inverting Eq. 4.1 and Eq. 4.2:

$$(x, y) = f^{-1}(X, Y) \quad (4.3)$$

The coordinates in the object space were picked in Agisoft's Metashape using the photogrammetric backbone. All further calculations were conducted in MATLAB (<https://de.mathworks.com/products/matlab.html>).

#### 4.2.1 Quality assessment of the planar rectification approach

For a quantitative evaluation of the rectification results, one image of a graffiti from the testing zone was selected (Figure 4.3a). Thirteen checkpoints were measured in both the 3D model and the rectified image. The measured 2D image coordinates were then transformed back into the superior coordinate system by inverting the transformation described above. The accuracy of the planar rectification was quantified as the Euclidean distance (hereafter referred to as *error*) between the 3D point measured in the 3D model and the 3D point derived from the planar rectification. To assess the impact of lens distortion, the rectification was performed and evaluated on both the original image



and an undistorted image, the latter generated using Brown's distortion model as implemented in Agisoft's Metashape.

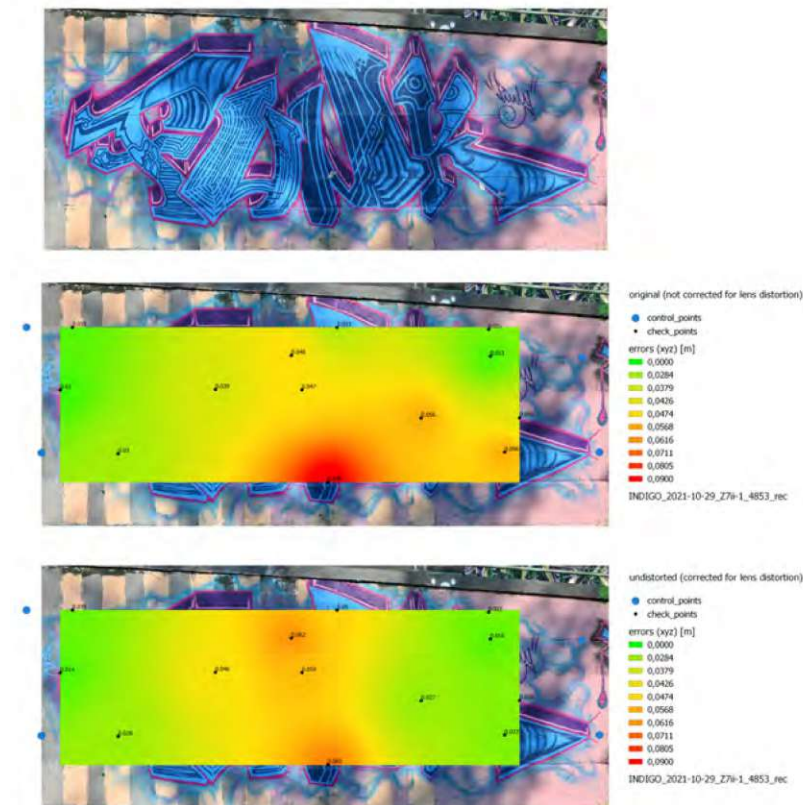


**Figure 4.3:** a) original image (Nikon Z 7II + Nikon NIKKOR Z 20mm f/1.8 S @ f/5.6 - 1/500 s - ISO 64). b) planarly rectified image of the graffiti (not corrected for lens distortion). c) planarly rectified image of the graffiti (corrected for lens distortion). The numbers beside the checkpoints denote the respective error. The color-coded overlay of b) and c) was generated in QGIS by applying an inverse distance interpolation on the retrieved residuals.

The evaluation of the rectified example image (Figure 4.3b and c) reveals that errors are largest in the center of the image and decrease towards the control points. The mean errors for the undistorted image are slightly smaller ( $3.5 \pm 1.8$  cm) compared to the original image ( $3.9 \pm 2.2$  cm), which was not corrected for lens distortion. The largest errors occur in the x-direction, which approximately corresponds to the normal of the plane used for the rectification. This suggests that the error is primarily driven by the curvature of the wall, which is not easily visible but is evident upon analysing the SfM-derived point cloud. While the effect of lens distortion is noticeable, it plays a secondary role.

It should be noted that these findings are based on a single example image, which cannot represent the full diversity of scenes and objects at the Donaukanal. Thus, the errors reflect the magnitude of potential errors rather than the average expected for all images along the Donaukanal. Nonetheless, the results suggest that, in certain cases, planar rectification can be a viable solution for georeferencing images and correcting perspective distortions.

#### 4.2.2 Considerations regarding the large scale applicability of planar rectification

The planar rectification approach described in Chapter 4.2 has the advantage that it can be implemented using very simple means (a single-lens reflex camera and simple computer programs that can be supplied

with very liberal licenses in python) and some effort to generate the control points in the superior coordinate system (total station or 3D model of cm-accuracy and -detail). However, the work effort must be considered too. For each image in total (a minimum of), four control point pairs (four on the object and four in the image) have to be measured and fed into the processing pipeline. Often, the search for well identifiable points is difficult and thus time-consuming. An average planar rectification process at the INDIGO testing zone took approximately 15 minutes. Given the large number of new graffiti that appear at Donaukanal each week, other options need to be considered as well.

One potential alternative is the usage of a 3D model of the scene (i.e. the Donaukanal) in combination with direct georeferencing of the image by exploiting the information (i.e., the exterior orientation parameters) gathered through GNSS/IMU sensors. For this method, the graffiti is in a first step segmented in the image space. These corner points of the graffiti can be intersected with the 3D model by combining the known interior orientation with the GNSS/IMU-derived exterior orientation. The intermediate result is a set of (control) point pairs which can in the next step be used to derive the projective transformation parameters from Equation 4.1 and 4.2. The advantage of this approach, especially compared to the planar rectification workflow discussed in Chapter 4.2, is the high degree of automation that can be achieved. At the same time, the software requirements can be kept low. On the other hand, this approach has the disadvantage of being very dependent on the measurement accuracy of the GNSS/IMU sensors. Even with high-quality hardware, the accuracy of this approach will, in the standard case, be lower than that in Chapter 4.2.1. Furthermore, this method likely fails at scenes where no exterior orientation parameters can be derived due to obstruction of the GNSS signals (e.g., beneath bridges). The topic of direct georeferencing will be revisited in Chapter 4.5.

Another solution to overcome the issues associated with planar rectification would be the usage of all the available structural (3D) information of the object, resulting in the creation of an orthophoto. The applicability of orthophotos, how they are created and how their creation can be automated for the large-scale applicability for extensive graffiti-scapes as the Donaukanal will be explored in the next chapter by introducing AUTOGRAF, a software tool for the AUTomated Orthorectification of GRAffiti Photos.

## 4.3 AUTOGRAF - AUTomated Orthorectification of GRAffiti Photos

### 4.3.1 The orthophoto principle

A well-known concept to remove distortions and georeferencing images is orthorectification. An orthophoto eliminates all three types of distortions by converting the photograph from its original central projection on the image sensor into an orthogonal projection onto a specified projection plane [114]. Achieving this orthorectification of digital photographs requires three types of auxiliary data (Figure 4.4):

[114]: Deng et al. (2015), 'Automatic true orthophoto generation based on three-dimensional building model using multiview urban aerial images'

- (a) The interior and exterior orientation parameters of the camera. The exterior orientation specifies the camera's position and orientation at the time of image capture, while the interior orientation defines the internal geometry of the camera, including lens distortion characteristics.
- (b) A complete, hole-free, and continuous 3D model of the surface where the graffiti is located (e.g., a wall, bridge pillar, or staircase);
- (c) A projection plane used to orthogonally project the texture information from the photograph(s), following its intersection with the 3D surface model.

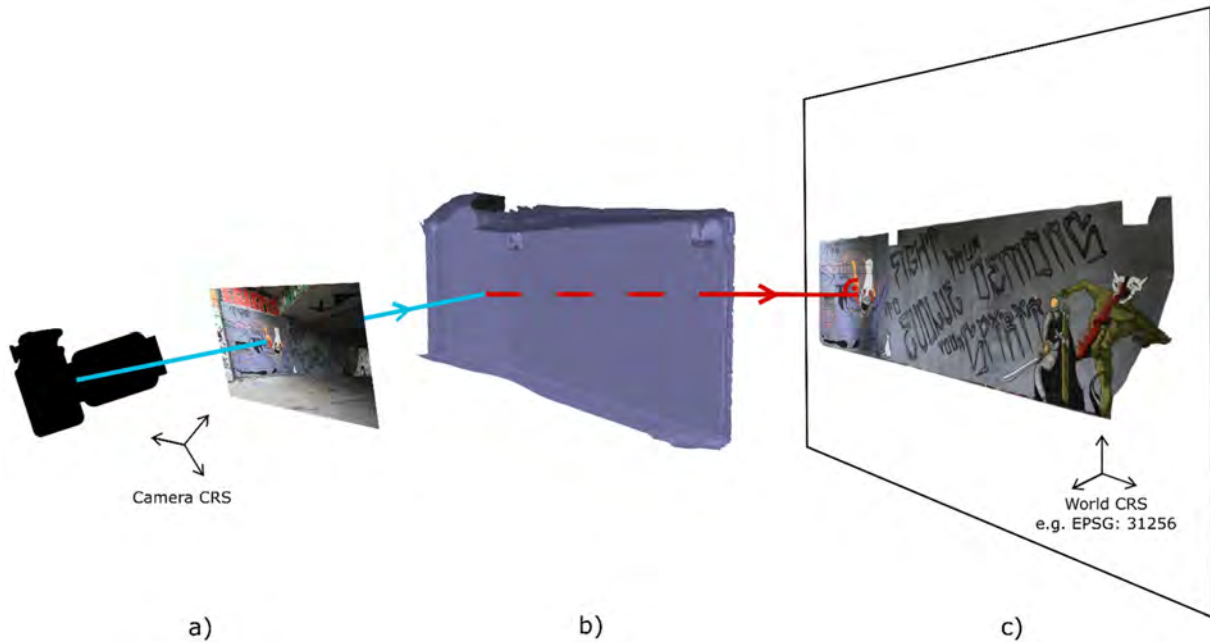


**Figure 4.4:** Overview of the orthophoto generation process with the three required data sources: (a) the camera's exterior and interior orientation parameters; (b) the hole-free 3D surface model of the scene; (c) the ortho-projection plane (including the projected orthophoto). CRS refers to Coordinate Reference System. Adopted from [53].

The following chapters present the conceptualisation, development, and evaluation of, AUTOGRAF (AUTomated Orthorectification of GRAffiti photos), a software tool that allows for the fully automated derivation of orthophotos from new graffiti that appear along Donaukanal. The tool facilitates the extraction of data from new graffiti photographs and an existing dataset of previously captured images, for which the interior and exterior orientation parameters have already been determined during the computation of the photogrammetric backbone (Chapter 2.2.1). Given the rapid emergence of new graffiti along the Donaukanal, a key requirement for AUTOGRAF is minimising manual intervention. To meet this need, INDIGO's photogrammetric pipeline (Figure 4.5) incorporates three primary processing steps that operate without human input:

- (1) Conducting initial quality and consistency checks on the graffiti images;
- (2) Estimating the interior and exterior orientation of the camera;
- (3) Generating a digital 3D model of the graffiti-covered surface, calculating the (ortho-)projection plane (also known as the reference plane), and producing the final orthophoto.

The initial checks (1) aim to indicate whether the input is likely to

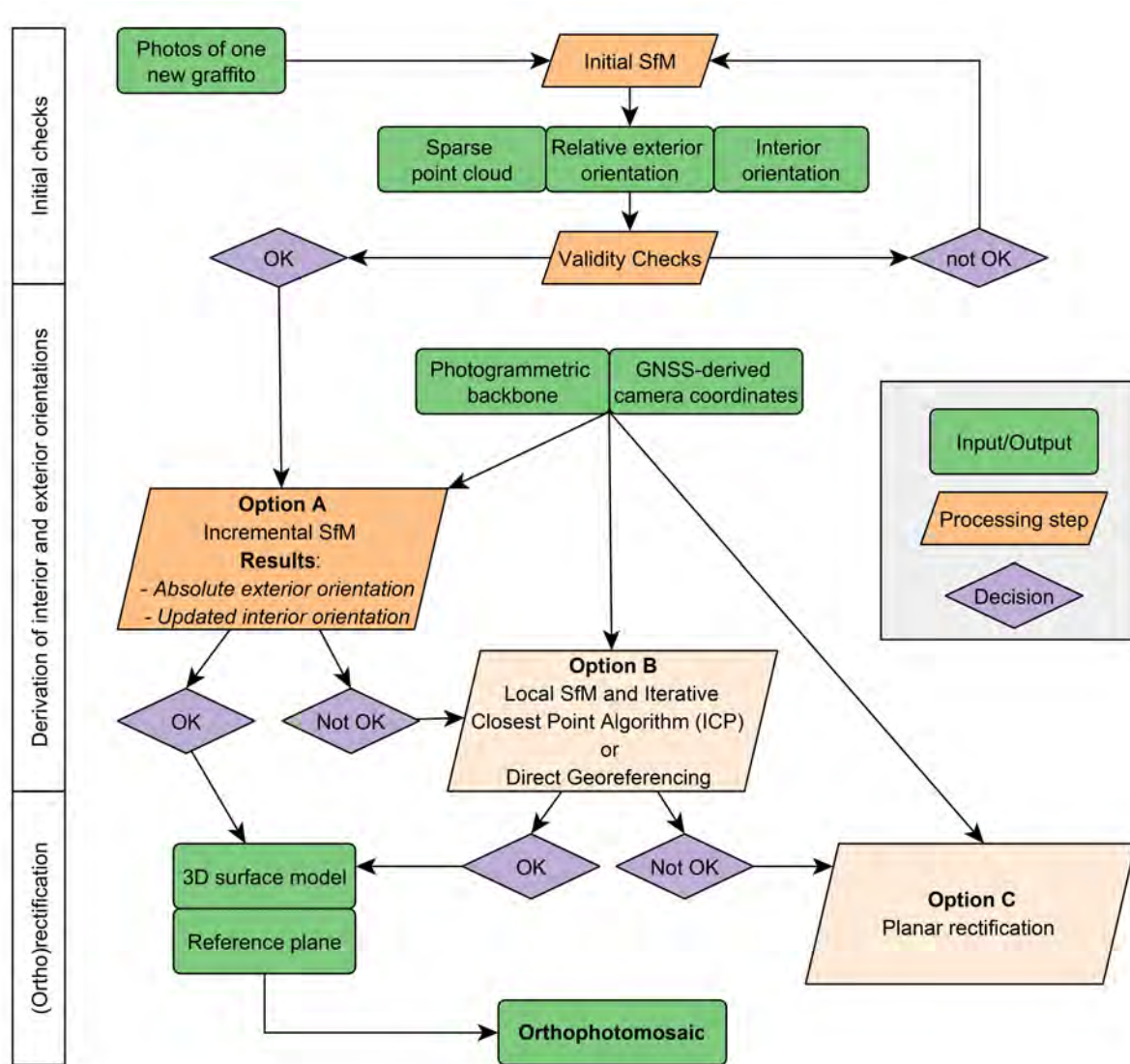


**Figure 4.5:** Photogrammetric workflow chart with the three main processing steps indicated on the right side of the chart. Grey boxes are alternatives to the incremental SfM approach and might be implemented in the future. However, they only serve as potential fallback solutions. A discussion on their applicability can be found in Chapter 4.5 and 4.2

provide reliable results or if parts of the input should be removed from the orthorectification process to increase reliability and decrease processing times. In the next step the cameras' interior and (absolute) exterior orientations are estimated. These parameters are retrieved using an incremental SfM approach [115] and require the availability of an existing network of images with known absolute exterior orientation parameters: INDIGO's photogrammetric backbone. Lastly, the newly oriented cameras are used to derive the 3D continuous surface model of the scene. The projection plane is approximated using the sparse point cloud, an intermediate result of the incremental SfM step. The pixel's RGB values are (orthogonally) projected onto this projection plane. The following chapters detail the intermediate processing steps and show how AUTOGRAF was designed, implemented and tested on real-world examples.



### 4.3.2 Acquiring and managing graffiti photos

When a new graffiti is identified, image acquisition must ensure the identification of common feature points (tie points) between the new graffiti's image set and previously captured photos at the same location within INDIGO's total coverage network. Often, changes to the graffiti scene and its surroundings occur between photography sessions. Therefore, in addition to photographing the new graffiti, its environment is also captured to establish tie points.

Photographers must adhere to guidelines aligned with the subsequent SfM processing, similar to those for total coverage acquisition. These include capturing photos with significant overlap and using both perpendicular and inclined optical axes relative to the scene. Perpendicular images are especially critical for orthophoto generation, as they ensure an approximately consistent spatial resolution (i.e., image scale). Photographers should also rotate the camera by 90° intervals to capture both portrait- and landscape-oriented images. During the session, the camera's focusing distance should remain fixed to maintain consistent interior camera orientation across the graffiti image block.

Before capturing an image sequence of a new graffiti, one photograph of an X-Rite (now Calibrite) ColorChecker Passport Photo 2 is taken, along with a spectrometer measurement of the incident illumination. The spectrometer measurement supports colorimetric processing, while the ColorChecker image acts as a backup and aids in photograph management [67]. These images can be automatically detected, facilitating the organisation of graffiti photos into uniquely identified, graffiti-specific folders.

Once these preparations are complete, AUTOGRAF can be initiated by providing the folder paths to the program. AUTOGRAF, a Python add-on for Agisoft's photogrammetric software Metashape, is available under the GNU General Public License v3.0 and can be downloaded from GitHub (<https://github.com/GraffitiProjectINDIGO/AUTOGRAF>, accessed on 29 September 2022).

[67]: Molada-Tebar et al. (2024), 'Practical RGB-to-XYZ Color Transformation Matrix Estimation under Different Lighting Conditions for Graffiti Documentation'

### 4.3.3 Initial SfM and quality checks

Once the images are passed to AUTOGRAF, an initial checking procedure is performed to enhance the reliability of results and optimise computation times by identifying and excluding images unsuitable for further processing. These checks specifically target photographs that are of low quality (e.g., blurry) or have been erroneously assigned to a graffiti image folder, causing them to mismatch with other images in the set. Such images may also lead to inaccurate estimations of the camera orientation parameters.

At the outset of these checks, an initial local SfM process is applied. This procedure calculates each image's interior and relative exterior orientation parameters. Images for which these parameters cannot be determined lack sufficient common feature points with the other images in the folder, indicating either poor quality or incorrect assignment to the folder. These images are excluded from the subsequent processing



Figure 4.6: Logo of AUTOGRAF

pipeline, thereby reducing computation times. Log-files are created to document such details and incidents.

For images successfully oriented by Metashape, an additional quality check is conducted. During this check, the *Reprojection Error* (RE) is calculated for each reconstructed 3D tie point. The RE is defined as the pixel distance between the measured location of a tie point in the image ( $P_{\text{measured}}$ ) and the 2D projection of its reconstructed 3D counterpart ( $P_{\text{projected}}$ ). To represent the RE for an individual image, the *Root Mean Square Error* (RMSE) of all REs within the image is computed as follows:

$$\text{RMSE}_{\text{img}} = \sqrt{\frac{1}{n} \sum_{i=1}^n (P_{\text{measured}} - P_{\text{projected}})^2}, \quad (4.4)$$

where  $n$  is the total number of tie points in the image.

The  $\text{RMSE}_{\text{img}}$  serves as a quantitative measure of the bundle block adjustment accuracy for a given image. While it is possible to discard images exceeding a specific  $\text{RMSE}_{\text{img}}$  threshold to improve workflow accuracy, doing so risks the creation of gaps in the final orthophoto. To avoid this, no images are removed based solely on their  $\text{RMSE}_{\text{img}}$ . Instead, the  $\text{RMSE}_{\text{img}}$  is recorded for each image, allowing for manual adjustments or further analysis of the achieved accuracy, if needed.

#### 4.3.4 Incremental SfM approach

An essential step in deriving the orthophoto is the computation of the absolute exterior camera orientations. This is achieved by applying an incremental SfM routine, where the new graffiti images that passed the initial quality checks are incrementally oriented and self-calibrated (i.e., solving for the interior orientation) by integrating them into the existing photogrammetric backbone of the entire Donaukanal. This method relies on tie points established between the existing and new images, emphasising the need for careful image acquisition that captures sufficient details of the invariant surroundings.

Figure 4.7 demonstrates the effectiveness of this approach: tie points were successfully identified between images taken on 27 October 2021 and 17 December 2021, despite most parts of the graffiti being covered during these 52 days. Valid matches were even found for an image taken on an island in the middle of the Donaukanal (Figure 4.7).

To accelerate the incremental SfM computation, Metashape preselects overlapping photo pairs from significantly downsampled images before conducting the image matching process, using a user-defined pixel count. While this *generic preselection* significantly speeds up processing, further limiting the search space is beneficial due to the large volume of image data that must be processed. This is achieved by using position data to filter out photos irrelevant to the currently processed graffiti image stack. An external GNSS receiver collects this position data, and the Solmeta GMAX geotagger is currently mounted on the Nikon Z7 II cameras to estimate the camera's location during image exposure. The GMAX is a dual satellite positioning system utilising GPS and BeiDou satellites,



**Figure 4.7:** Example of valid tie points (blue lines) established between one image of a new graffiti (Upper; 17 December 2021) and two images covering the same site but 52 days earlier and with significant differences in texture. The two lower photos were acquired during the full photographic coverage on 27 October 2021. Adopted from [53].

recording the camera station's WGS84 coordinates (EPSG:4326) as image metadata in standardised Exif (Exchangeable image file format) tags.

AUTOGRAF then converts these WGS84 coordinates into the coordinate reference system (CRS) used by the entire image network (EPSG:31256). These initial camera location estimates are employed to define a search radius, beyond which photos are excluded from the incremental SfM process. Since the estimated positions can be unreliable beneath bridges, and because the GMAX geotagger does not provide directly accessible accuracy estimates, the search radius is set sufficiently large to ensure the orientation of images acquired under bridges. Currently, a 30-meter search radius is used, as smaller radii occasionally result in photos not being oriented due to insufficient overlapping imagery. Ideas on how this can be further improved are presented in Chapter 4.5.

#### 4.3.5 Creation of the 3D Model and determination of a custom projection plane

Once the camera orientations for each graffiti photo set are derived, the 3D model of the graffiti scene and the projection plane can be computed. The 3D model is generated using depth-map-based multi-view stereo matching [116], which results in either a dense point cloud or a triangle-based polymesh, both of which digitally represent the surface. If the point cloud option is chosen, Metashape can interpolate (i.e., mesh) the dense collection of points into a polymesh. The advantage of this approach is that the point cloud can be filtered and classified before meshing. Metashape also provides basic tools for filtering facets of the polymesh, but the *isolated component filter* integrated into Metashape and executed via AUTOGRAF is specifically used to remove parts of the 3D meshed surface that are not connected to the main component. The main component is defined as the mesh containing the most vertices, which, in nearly all cases, corresponds to the graffiti-covered surface where the photographic coverage is most concentrated. This filtering removes isolated structures such as branches or street lamps that might obscure the graffiti in the final orthophoto.

However, deriving the projection plane requires a custom solution since graffiti-covered walls are arbitrarily oriented in space and are not neces-

[116]: Seitz et al. (2006), 'A comparison and evaluation of multi-view stereo reconstruction algorithms'

sarily ideal planes. They may be curved or contain extruding elements like pillars or doorframes. Thus, the reference plane, which is perpendicular to the orthogonal viewing direction, must be approximated to the graffiti surface. This is achieved by fitting an individual plane for each graffiti based on the previously derived tie point cloud. The concept is that most tie points are located on the graffiti-covered wall, allowing the derivation of a primary plane (the projection plane) through plane adjustment of the tie point cloud. Before adjusting the plane, outlier tie points are removed using the RANdom SAmple Consensus (RANSAC) method.

RANSAC is a robust outlier detection method introduced by Fischler and Bolles in 1981 [117]. It works by repeatedly and randomly subsampling the input data (e.g., the 3D tie point cloud) and using these subsamples to derive the parameters of a mathematical model (e.g., the parameters of a plane equation). Each subsample contains the minimum number of data points necessary to unambiguously determine the model parameters. The resulting model parameters are then tested against the remaining data, and points that fit the model well (within a specified threshold  $t$ , such as  $t = 10$  cm) are considered inliers. The final model is determined by the set of parameters that yield the largest consensus set. This consensus set can then be used to categorise the data into inliers and outliers (Figure 4.8). For this application, the number of subsamples ( $n$ ) and the uncertainty threshold ( $t$ ) were set to 1000 and 10 cm, respectively.

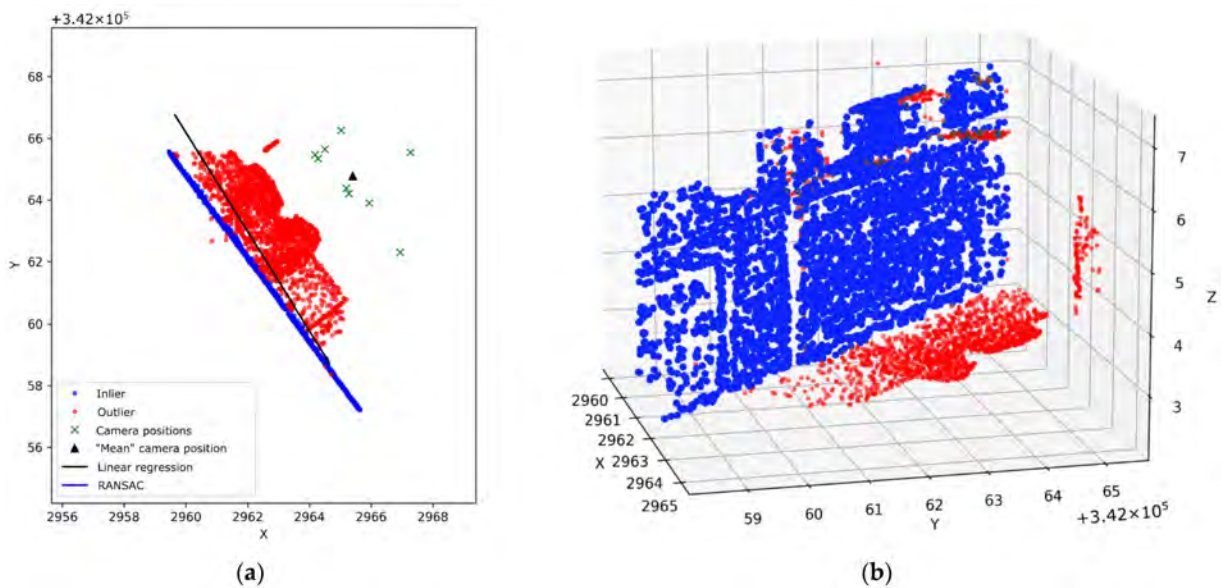


**Figure 4.8:** An example of a RANSAC-classified tie point cloud derived from the images depicted in Figure 4.8. (a) depicts the top view, including the projected camera positions and the derived RANSAC result. The result from an ordinary least square fitting (linear regression) before RANSAC classification is also shown for comparison. (b) shows a 3D representation of the classified tie point cloud. Adopted from [53].

Once the inlier points of the plane are detected, they are used to derive the plane parameters through least-squares minimisation of the orthogonal distances from the points to the plane. This can be solved by computing the eigenvectors of the matrix of centralised moments. The eigenvectors give the plane parameters as two normalised direction vectors parallel to the plane (**a**, **b**) and one perpendicular vector (**c**) to the plane. AUTOGRAF automatically calculates these three vectors and passes them to Metashape as a matrix  $M$ :





**Figure 4.9:** Example collection of nine images for one graffiti. The last image (lower right corner) was used for selecting the graffiti's outline as it covers the whole graffiti. Although overview images are now acquired at the beginning of an image sequence, they were acquired at the end of the first project months. Adopted from [53].

$$M = \begin{bmatrix} \mathbf{a}^T \\ \mathbf{b}^T \\ \mathbf{c}^T \end{bmatrix} = \begin{bmatrix} a_x & b_x & c_x \\ a_y & b_y & c_y \\ a_z & b_z & c_z \end{bmatrix} \quad (4.5)$$

where the subscripts  $a_x, b_y, c_z, \dots$  denote the individual (x-, y-, z-) components of the direction vectors.

#### 4.3.6 Orthophoto creation and graffiti segmentation

With the camera orientations, the 3D mesh of the graffiti surface, and the projection plane known, the orthophoto is generated. Metashape also supports orthophoto mosaicking, which enables the blending of orthophotos by stitching them along designated seamlines to produce a continuous and complete orthophoto, referred to as an orthophotomosaic. This technique's major advantage is that it allows the generation of an orthophoto for the entire graffiti, even when no single image covers the entire surface, enabling the representation of extensive areas. Additionally, it allows for higher spatial resolution analysis of the graffiti, as multiple close-range images can be combined into a single orthophoto.

Since the current approach relies on photos depicting large portions of the surrounding area, the graffiti of interest typically covers only a part of the resulting orthophoto. To exclude irrelevant areas, a graffiti outline is manually defined, which, along with image selection and assignment to the corresponding graffiti, is the only manual step in the entire orthophoto creation process. Boundary selection is currently performed using an overview image, taken right after the ColorChecker photo, which ideally covers most or all of the graffiti. The 2D coordinates of the graffiti's boundary are selected in the image space. By intersecting the image ray, passing through the camera's projection centre and the selected image coordinates, with the 3D model, the corresponding 3D world coordinates (EPSG:: 31256) are derived through a process known as monoplottting. If the 3D surface model is unavailable for a boundary point, the image ray is instead intersected with the RANSAC-derived

projection plane of the scene. The calculated 3D world coordinates are stored as a polygon in a vector file and serve as the georeferencing realisation. To facilitate this boundary selection a custom python script was developed which allows for a quick extraction of graffiti outlines from overview images.

Boundary selection is necessary to avoid including parts of the graffiti scene in the final orthophoto that are distorted, incorrectly textured, or contain gaps due to insufficient image overlap. These parts typically do not contribute value to the graffiti orthophoto but occupy significant disk space, so they are excluded. It is important to note that this boundary selection introduces a certain degree of subjectivity, as the boundaries of a graffiti are often unclear and difficult to define. However, this does not contradict the goal of placing the graffiti in its original context, which is achieved later when the georeferencing information allows positioning the graffiti (as an orthophoto or texture patch) within a virtual 3D environment, thus relating it to neighboring graffiti.

Finally, the orthophoto is exported at three different raster cell sizes: 1 cm, 1 mm, and its native Ground Sampling Distance (GSD), which typically ranges between 0.5 and 1 mm, primarily determined by the camera's distance from the graffiti during image acquisition. The georeferencing data, which includes the transformation parameters, is stored separately and allows the assignment of 3D world coordinates to each pixel in the 2D orthophoto.

### 4.3.7 Orthorectification experiment

#### Experimental setup

In order to evaluate how AUTOGRAF performs in a real-world scenario, 100 graffiti were randomly selected from the complete set of graffiti documented between November and December 2021. The images were divided into individual folders, with each folder containing all photos taken for a single graffiti. To store the 14-bit color data captured by the digital camera, the final workflow of INDIGO will rely on colorimetrically processed RAW photos, saved as 16-bit lossless compressed TIFF files. However, as the processing pipeline was not yet finalised at the time of the experiment, this test was conducted using minimally compressed JPEG files, which were in-camera generated from the RAW images. An example of one complete image set is shown in Figure 4.9. The experiment utilised a total of 826 images, occupying 27.0 GB of storage space. On average, each graffiti folder contained 8 images (with a minimum of 3 and a maximum of 63 images), captured from different positions and viewing angles. The wide variation in the number of images per graffiti can be attributed to one graffiti folder, which contains 63 images. This particular graffiti is located very close to the water, and to fully document it, 63 images with very short focusing distances were necessary (Figure 4.11b). On the other hand, a folder containing only three images is a side effect of initiating a documentation project, where team members were still learning how to capture an adequate image network.

## Experiment evaluation

The experiment primarily aimed to answer two questions: (A) Are the results of the expected quality? and (B) Does AUTOGRAF enable sufficiently fast processing of large amounts of graffiti images, which is essential for the continuous monitoring of the graffiti landscape along the Donaukanal? The second question (B) is relatively simple to address by measuring the time required to produce an average orthophoto and comparing this duration with the expected number of graffiti to be processed within a given period. However, assessing the quality of the orthophotos (A) is more complex due to the inherent subjectivity of the evaluation. To mitigate this, a classification scheme was introduced, allowing the categorisation of each orthophoto into four distinct classes (0, 1a, 1b, 2), as detailed in Table 1. To ensure replicability and transparency of the experiment evaluation, the resulting orthophotos, along with the code, were uploaded to the following GitHub repository: <https://github.com/GraffitiProjectINDIGO/AUTOGRAF> (accessed on 2 December 2024).

**Table 4.1:** Classification scheme for the quality assessment of the generated graffiti orthophotos.

Class	Short Explanation	Long Explanation
0	No orthophoto/Orthophoto with significant flaws	A graffiti for which no orthophoto could be generated or the orthophoto's quality is so poor that it cannot be used for a detailed analysis.
1a	Orthophoto with minor flaws (input data-related)	An orthophoto is generated, and the quality is sufficient for an overall inspection. However, smaller parts of the graffiti are cut off, occluded, distorted, underexposed or blurry. The reason is input data-related and cannot be fully resolved by manual intervention during the orthophoto generation process.
1b	Orthophoto with minor flaws (AUTOGRAF-related)	Same as 1a, but the flaws are AUTOGRAF-related. The problem can thus be (largely or entirely) solved by 3D model editing, manual selection of the input images or other manual interventions.
2	Orthophoto with no or marginal flaws	The orthophoto does not exhibit any or only marginal flaws, which do not disturb the graffiti analysis. Manual intervention would not improve the result.

To differentiate between issues related to AUTOGRAF and those primarily caused by input data, a distinction between classes 1a and 1b was made. This distinction clarifies the actual limitations of the developed methodology (classified as 1b) versus general challenges encountered during image acquisition (classified as 1a). Issues in class 1a might include areas of the graffiti not captured in the photographs or poor image geometry (e.g., when all images are taken from similar positions). In these cases, the problem could potentially be addressed by rephotographing or through manual intervention during orthorectification. However, such problems are classified as 1b (AUTOGRAF-related) in this experiment, as the goal was to compare AUTOGRAF's performance against that of a hypothetical manual operator. Furthermore, rephotographing can be time-consuming and may not always be feasible, particularly if the graffiti has already been covered. The accuracy of the georeferencing

for the resulting orthophotos was evaluated by comparing the derived boundary polygons with a vector map of infrastructure provided by the city of Vienna.

## 4.4 Results from the orthorectification experiment

### 4.4.1 Initial local and incremental SfM

During the initial SfM procedure, all images were oriented locally and self-calibrated within their respective graffiti subblocks. For 823 out of 826 images, the local SfM procedure was successfully completed, demonstrating both high performance in feature point extraction and subsequent bundle block adjustment, as well as thorough data acquisition and management. The mean  $RMSE_{img}$  for these 823 images was  $0.83 \pm 0.31$  pixels (Figure 4.10).

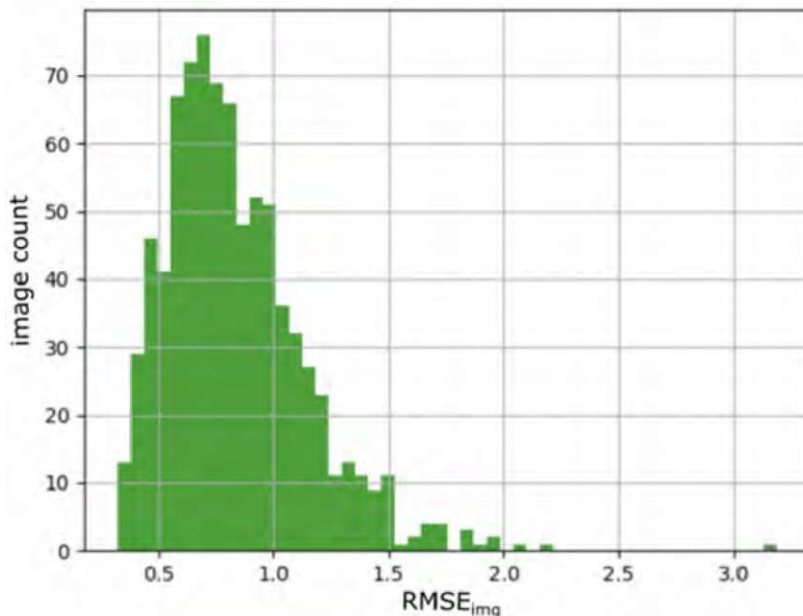


**Figure 4.10:** Histogram of  $RMSE_{img}$  for the 823 images, which were oriented locally in their respective graffiti block. The  $RMSE_{img}$  was obtained using Equation 4.3.3. Adopted from [53].

Concerning the derivation of absolute exterior and interior orientation parameters, the incremental SfM approach was successful for 752 out of the 823 images (91%). These 752 oriented images correspond to 97 graffiti for which the complete image set (i.e., all images assigned to the graffiti) was successfully oriented, and one graffiti image set for which only one image could be oriented. The 71 photos, which could not be added to the existing total coverage camera network, belong to three graffiti (Figure 4.11). The graffiti (Figure 4.11b), which was covered with 63 images, is among the failures. Only one of its 63 images was successfully oriented, explaining the diverging success rate between the number of oriented images and oriented graffiti blocks (91% oriented images vs. 97% successfully oriented graffiti blocks). The mean  $RMSE_{img}$  for the 752 incrementally oriented images is  $1.65 \pm 0.44$  pixels.

Inspection of the graffiti blocks that could not be oriented (Figure 4.11) shows that they hardly depict the surrounding environment, such as





**Figure 4.11:** Overview images of the three graffiti for which the incremental SfM approach failed. The graffiti depicted in (a,b) are located very close to the channel. The graffiti in (c) was covered with only three images with little coverage of the surrounding environment. Adopted from [53].

other graffiti or neighbouring infrastructure, making it impossible to establish tie points between these images and those of the existing total coverage photographs. This potentially could have been resolved in all three cases by rephotographing the scene. However, it is to be noted that in some cases (Figure 4.11a, b), the narrow operating space significantly complicates proper image acquisition. Certain imperfections in image acquisition will thus remain unavoidable or can only be mitigated with additional efforts such as the use of a very-wide angle lens (e.g., 10 mm) or crossing the Donaukanal to photograph the graffiti with a telephoto lens (e.g., 105 mm) to depict larger portions of the scene. Overall, the achieved success rate (97%) of the incremental SfM is highly satisfactory.

#### 4.4.2 Derivation of the 3D surface model and the projection planes

The results from the incremental SfM routine for every graffiti subblock (i.e., the exterior and interior camera orientations and tie points) are used to derive scene-specific 3D surface meshes and projection planes for each graffiti scene. For the 3D meshing, the implementations provided by Metashape are used. The quality of the resulting 3D models is highly dependent on the number of input images. For some graffiti, only three to five images were acquired, which suffices in most cases to derive a 3D representation of the graffiti-covered surface but in some cases leads to small artefacts in the retrieved mesh. For the tested graffiti, however, these artefacts hardly occurred on the parts of the mesh where the graffiti of interest is located, but mainly on the edges of the model, towards which the image coverage decreases. Overall, these imperfections did not notably influence the orthorectification results.

Concerning the projection plane derivation, no notable problems occurred. A visual examination of the classified point clouds confirms the robustness of the applied RANSAC method. The derived projection planes approximate the graffiti-covered surfaces well.

#### 4.4.3 Quantity and quality of the derived orthophotos

The orthophotos were classified based on the classification scheme introduced in Table 4.1. This classification (Table 4.2) shows that 95% of the tested graffiti were orthorectified without major flaws (class 1a,





1b, or 2). For 80% of the graffiti, orthophotos without or with only marginal flaws were generated (class 2). 15% of the orthophotos exhibited minor problems such as minor occlusions, distortions, blurriness, or underexposure (class 1a and 1b). Most minor flaws (10 out of 15) were related to the automated editing of the 3D model (class 1b). In some cases, parts of the model that occlude the graffiti were not removed and thus caused occlusions in the final orthophoto. The example for class 1b in Table 4.2 depicts such a case: a pile of broken wooden planks located in front of the graffiti causes part of the graffiti to be occluded. For this and for other graffiti, an improved image acquisition would most likely solve the issue, but this would be more time-consuming than manual editing of the 3D model and is likely not possible anymore due to the destruction of the graffiti. Thus, these flaws were still considered AUTOGRAF-related.

The deficits of the remaining 5% of orthophotos with minor flaws (class 1a) are primarily associated with inadequate or insufficient input data, which can only be resolved by rephotographing the graffiti and rerunning the orthorectification pipeline. The reasons for the partial failure in these cases were bad illumination conditions at the time of image acquisition (causing shadows or very dark areas), too few photographs, or unfavorable image acquisition geometry. The latter two caused some graffiti to be warped or blurry. The class 1a included in Table 4.2 depicts a graffiti that was photographed from five almost identical positions, causing poor measurement geometry, which leads to blurry parts in the orthophoto and a Ground Sampling Distance (GSD) of only 2.3 mm.

The average GSD of all derived orthophotos is 0.9 mm, indicating that, on average, spatial details of 2.0 mm should be well visible. It needs to be stressed again that the classification is subjective, as it is based on human interpretation.

Figure 4.12 illustrates the overall accuracy of the graffiti's absolute georeferencing by overlaying the obtained results with the so-called multi-purpose map (German: *Mehrzweckkarte*), an official and freely available map created by the City of Vienna (<https://data.wien.gv.at>, accessed on 29 September 2022). This map is derived from terrestrial surveying campaigns and depicts significant features along the Donaukanal, such as walls, bridge pillars, and staircases. The two detailed maps in Figure 4.12 show deviations ranging from 0 cm to a maximum of 22 cm between Vienna's multi-purpose map and the derived graffiti outlines. The majority of these deviations are likely due to the generalisation of Vienna's multi-purpose map, which exhibits a comparatively low sampling of terrestrial measurements. Most points in the multi-purpose map correspond to points on the ground, while the graffiti are often located several meters above the ground. A smaller portion of the deviations may also be attributed to residual drift effects of the existing camera network and georeferencing errors. Despite the potential for some residual errors on the order of a few centimeters, there is overall excellent agreement with the reference data.

**Table 4.2:** Classification result of the orthophoto experiment. Adopted from [53]

Class	%	Examples
0	5 (3/2)	
1a	5	
1b	10	
2	80	

#### 4.4.4 Feasibility of the workflow

Besides the quality of the results and the large-scale applicability of the approach, computational effort plays an essential role in the assessment of the developed orthorectification pipeline. Thus, a strong emphasis is laid on the processing efficiency of the program both during development and testing. This experiment was conducted on two different computer setups, also to examine the influence of different hardware components on the computation times. Apart from the PC's hardware components, the experimental setup and results were identical. The PC specifications can be found in Table 4.3.



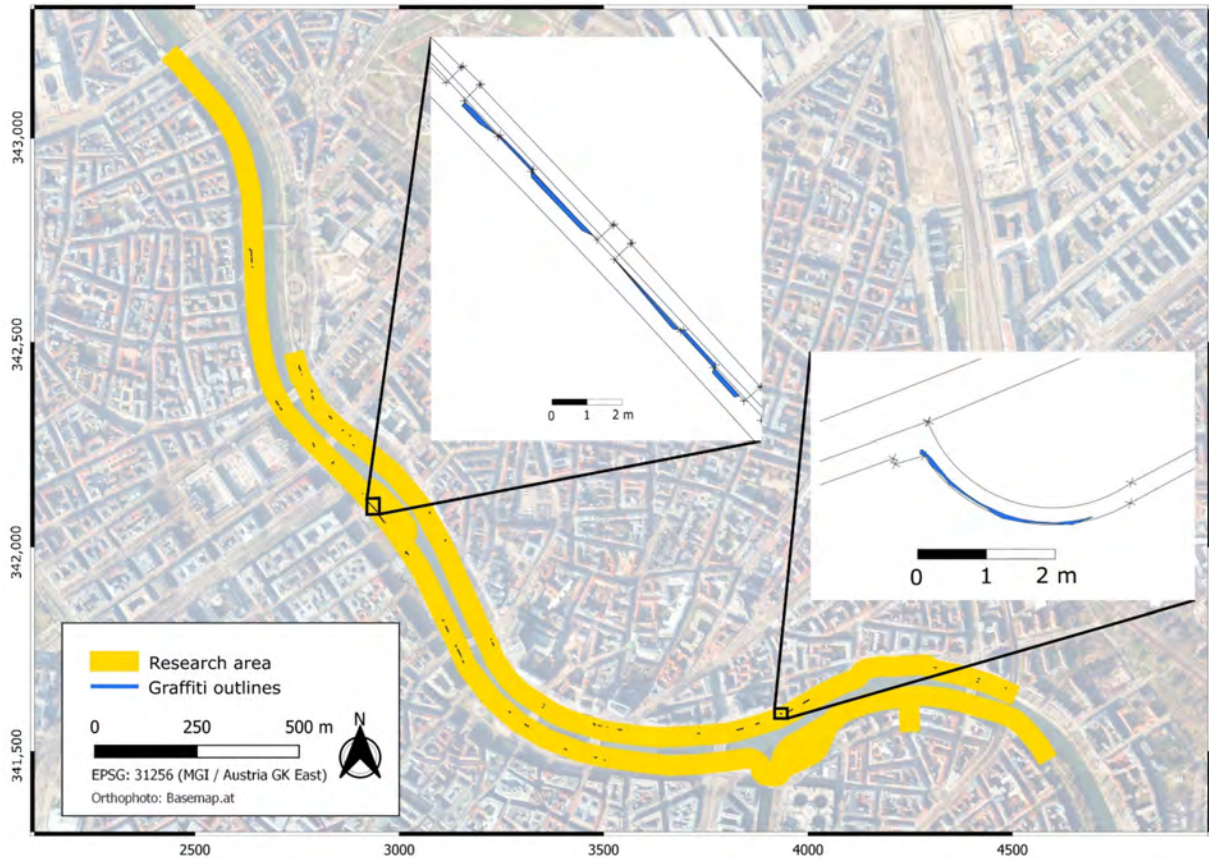


**Figure 4.12:** Overview map showing the orthophoto of the Donaukanal area and the outlines of all orthorectified graffiti projected in top view. The two detailed maps depict snippets of Vienna's multi-purpose map (Mehrzweckkarte), an infrastructural vector map provided by the city of Vienna (<https://data.wien.gv.at>, accessed on 29 September 2022). The multi-purpose map is overlaid with a detailed depiction of the derived outlines of five orthorectified graffiti. Adopted from [53]

**Table 4.3:** PC Specifications used in the experiment

Setup	Specifications
A	<b>CPU:</b> 2 × AMD EPYC 7302, 3.0 GHz, 16 core processor <b>GPU:</b> NVIDIA GeForce GTX 1650, 4 GB DDR5 VRAM, 896 CUDA cores <b>HDD:</b> Seagate Exos E 7E8 8TB, 6000 MB/s (read/write) <b>RAM:</b> 512 GB DDR4, 2667 MHz
B	<b>CPU:</b> Intel Core i9-12900KF, 3.2 GHz, 16 core processor <b>GPU:</b> NVIDIA GeForce RTX 3060, 12 GB DDR6 VRAM, 3584 CUDA cores <b>HDD:</b> Seagate FireCuda 530 2TB M.2 SSD, 7300 MB/s read, 6900 MB/s write <b>RAM:</b> 64 GB DDR4, 2200 MHz

In total, it took 22 hours and 50 minutes (Setup A) and 10 hours and 33 minutes (Setup B) to derive the 97 graffiti orthophotos from the 826 graffiti images (see Table 4.4). The manual preparatory tasks took approximately 1 hour and 20 minutes, which included splitting all photos into individual folders (50 minutes; the automated splitting based on the ColorChecker target was not yet implemented) and selecting the graffiti boundaries in the overview images (20 minutes) within the image space. On average, each graffiti required 42 seconds of manual intervention. This manual



preparation was done only once and used for both experiment runs.

**Table 4.4:** Processing times for the orthorectification experiments (100 graffiti and 826 images). Apart from the used processing hardware (Setup A/Setup B), the experiments were identical.

Task	Setup A		Setup B	
	Duration [h:m]	Average per Graffiti [m:s]	Duration [h:m]	Average per Graffiti [m:s]
Initial SfM	1:29	0:53	0:23	0:14
Initial quality checks	0:01	0:01	0:01	0:01
Incremental SfM	5:41	3:25	1:28	0:53
Data preparation	1:54	1:08	0:42	0:25
Orthophoto creation	12:35	7:33	6:49	4:05
<b>Time w.o. manual intervention</b>	21:40	13:00	9:23	5:38
Manual preparatory tasks	1:10	0:42	1:10	0:42
<b>Total</b>	<b>22:50</b>	<b>13:42</b>	<b>10:33</b>	<b>6:20</b>

Concerning the pure processing times (without manual interventions), an average graffiti image set was processed in 13 minutes (Setup A) and in 5 minutes 38 seconds (Setup B), highlighting the large dependency on the utilised hardware components. The most time-intensive computation step for both setups was the final creation of the orthophoto. This step includes demanding computational tasks such as creating the 3D surface model.

Extrapolation of these results shows that the current workflow in combination with PC setup B allows the orthorectification of approximately 6800 graffiti image sets, featuring around 56,000 images, per month. Although this number might not be fully reachable in the actual operational use of the software, it will still allow the sufficiently fast processing of the anticipated number of graffiti photographs. For comparison, the number of images acquired by the INDIGO team during their weekly photo tours between January 2022 and July 2022 was, on average, approximately 4000 per month, with a maximum of 6315 photos in May.

## 4.5 The potential of incorporating highly-accurate direct georeferencing

A critical and processing-intensive step in AUTOGRAF is the estimation of the exterior orientation of newly acquired images. The incremental SfM approach has demonstrated robust and efficient performance in the conducted experiments. However, as the photographs were captured shortly after the full photogrammetric coverage, there were only minor changes in the photographed scenes. Due to the frequent addition of graffiti and the ongoing renovations and infrastructure enhancements at Donaukanal, this methodology may become inadequate if the interval between acquisitions is significantly extended or if substantial alterations occur in the interim. This is particularly probable during the summer

months, when graffiti activity reaches its peak along Donaukanal. An additional issue pertains to the processing duration. Presently, the processing time for the incremental SfM approach is moderate, a result achieved by restricting the search space for image-matching utilising data from the GNSS receiver mounted on the camera. By employing this preliminary coarse georeferencing of the images, it is ensured that only images captured in proximity to the investigatory images are considered for matching. Under optimal circumstances, the GMAX Solmeta Geotagger utilised in this study can capture camera positions with an accuracy of approximately 2.5 meters. However, due to substantial shadowing effects between the numerous bridges along the Donaukanal, this level of accuracy is frequently unattainable, necessitating a relatively expansive search radius of 30 meters for potential images. In the absence of this step, the creation of a single orthophoto would extend to hours instead of minutes. This consideration raises the question whether the incremental SfM approach could be refined further, or even replaced, using more precise a priori knowledge of exterior camera orientations.

A recent study by [57] introduced a novel device (Figure 4.13) that significantly enhances the recording of exterior camera orientation parameters. This device incorporates a Real-Time-Kinematic (RTK) enabled GNSS receiver. The device obtains Real-Time Kinematic (RTK) GNSS corrections from the Austrian EPOSA service (Echtzeit-Positionierung-Austria, translated as Real-time Positioning Austria), with settings conveniently adjustable via a tablet or smartphone. Thanks to its precise time synchronisation with the camera shutter, the continuously recorded positional and rotational data can be aligned with the moment each photo is captured. An accuracy evaluation of the device was conducted at the designated INDIGO test site (Figure 3.4). For this purpose a dense image network was acquired and constrained using 41 coded targets establishing a highly accurate reference block. The camera positions expressed as X,Y,Z coordinates derived from the RTK/IMU device are compared with the exterior orientations of the reference block, where only the coded targets' 3D coordinates were utilised in the bundle block adjustment.



Figure 4.13: The RTK-enabled GNSS-IMU logging device. Adopted from [57].



Figure 4.14: Camera positions with colour-coded total positional error. The south-east portion of the map shows photos taken beneath the steel bridge. Camera symbols represent their orientations, while the border colours indicate the RTK solution status. The wall of interest with graffiti is marked by the orange line on the northern side. Adopted from [57].

This evaluation reveals that the 3D positions camera coordinates exhibit a root mean square error (RMSE) of 7.6 cm relative to the reference block. Notably, these errors can be significantly higher in areas beneath bridges,

where establishing a fixed RTK solution is not feasible (Figure 4.14). However, as demonstrated by Wieser et al. (2024) [57], quality flags that indicate the solution status (*Floating* or *Fix*) can be employed to filter out unreliable camera positions. This approach enables a dynamic adaptation of the search radius in the incremental bundle block adjustment (e.g. 10 m for images flagged as *Floating* and 30 m for images flagged as *Fix*). This would have a significant impact on the processing speed of AUTOGRAF. What is equally remarkable about the proposed solution is its ability to measure angular rotations (roll, pitch, and yaw) and to precisely time-synchronise these measurements with the moment the shutter button is pressed. The comparison with the reference block reveals very high accuracy for the direct measurements of roll and pitch ( $\text{RMSE}_{\text{Roll}} = 1.23^\circ$ ,  $\text{RMSE}_{\text{Pitch}} = 1.09^\circ$ ), while the errors for yaw are moderate ( $\text{RMSE}_{\text{Yaw}} = 15.6^\circ$ ). For comparison, Wieser et al. (2024) [57] demonstrate that Nikon's internal IMU is capable of delivering roll and pitch values with similar accuracy. However, the results for yaw ( $\text{RMSE}_{\text{Yaw}} = 124.5^\circ$ ) make the rotation information practically unusable.

The achieved accuracies of this direct georeferencing solution do not eliminate the need for the incremental SfM step. However, it enables a significant tightening of the search space for feature point matching.

## 4.6 Potential dissemination of the results

As outlined in Chapter 2.2 a major aim of the research project INDIGO is the development of an open-access online platform to visualise and analyse the documented graffiti. This aim has proven to be very ambitious considering the many challenges related to the enormous data volume. How such a platform could look like was researched in the form of a Master Thesis by the cartography student Oskar Baumann who was supervised as part of this dissertation. In the course of this work an interactive 2D and 3D platform was developed featuring graffiti orthophotomaps created with AUTOGRAF. The 2D mode (Figure 4.15) of the web map prototype uses adaptive symbols to represent graffiti effectively at different zoom levels. At close zoom, original polygon geometries are displayed, while at wider views, simplified representations like polylines and dynamic point clusters enhance visual clarity. The clusters are positioned at the centroid of the original polygons, and polylines are generated by connecting the two most distant vertices of each polygon [47].

The 3D map mode (Figure 4.16) enhances the visualisation of graffiti, particularly for vertical surfaces, by allowing full  $360^\circ$  interactive camera rotation. This enables users to view graffiti in relation to their surroundings, providing a more complete representation of graffiti-covered walls. Graffiti features are represented in 3D by extruding 2D polygons, with elevation determined based on the minimum and maximum height values of the original 3D polygon. While this method simplifies the representation and may not achieve perfect accuracy, it offers an efficient solution for web mapping, particularly for smaller geographic areas.

Additional 3D building features improve orientation, provide context for graffiti placement, and emphasise the Donaukanal area. They also con-

[47]: Baumann (2024), 'The Nuances of Mapping Street Art-Developing a Web Map for Interactive Graffiti Exploration (Master Thesis)'



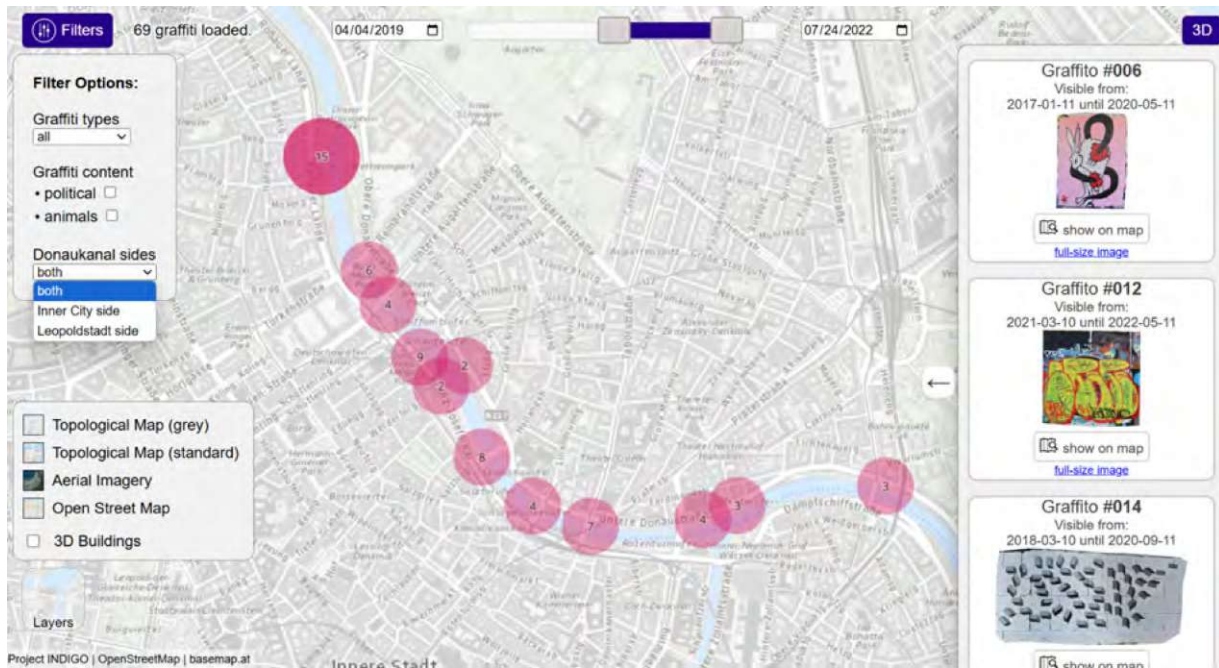


**Figure 4.15:** Screenshot of the developed interactive webmap in 2D view featuring various filtering options and density clustering. Screenshot taken on 27 February 2025 from [https://oacbaumann.github.io/graffiti\\_map\\_UserStudy/2D\\_version.html](https://oacbaumann.github.io/graffiti_map_UserStudy/2D_version.html)

tribute to a more structured representation of the environment, ensuring that graffiti appear within their spatial context rather than as isolated elements [47]. Both maps (2D and 3D) include various interactive features. To access information about map features, users can, for example, hover over graffiti, which triggers popup boxes and updates the sidebar with additional details. Left-clicking on 3D buildings opens their respective popup boxes. Filtering options, located in the top-left corner, allow users to apply spatial, semantic, and temporal filters, with a time range slider for further refinement. The map can be reprojected by switching between 2D and 3D modes, and in 3D mode, users can rotate the view by holding the right mouse button and dragging the cursor.

[47]: Baumann (2024), 'The Nuances of Mapping Street Art-Developing a Web Map for Interactive Graffiti Exploration (Master Thesis)'



**Figure 4.16:** Screenshot of the developed interactive webmap in 3D view featuring various filtering options and density clustering. Screenshot taken on April 15, 2025 from [https://oacbaumann.github.io/graffiti\\_map\\_UserStudy/3D\\_version.html](https://oacbaumann.github.io/graffiti_map_UserStudy/3D_version.html)



## 5 Documenting graffiti related to clandestine migration along the Turkish west coast

This chapter presents the findings from a research trip conducted as part of the archaeological pilot project *Flüchtige Spuren*. Portions of this chapter have been submitted under the title *Documenting migrant graffiti in the borderscapes of the Eastern Mediterranean* for peer review as an extended abstract to the ISPRS Archives, serving as the conference proceedings for the CIPA 2025 conference in Seoul, South Korea [56].

### 5.1 A brief overview on recent clandestine migration in the Eastern Mediterranean region

During the summer and autumn of 2015, undocumented migration from west and Central Asia towards Europe intensified to extraordinary levels. By the end of the year, over 850,000 people, most of them fleeing the war in Syria, crossed the land and maritime borders between Turkey to Greece. Many of these individuals sought to continue their journey northward, aspiring to reach countries in Central Europe. The island of Lesbos has since then seen the highest rate of refugee arrivals (Figure 5.2). The sudden rise in border crossers to Europe via Greece in the summer of 2015 triggered policy changes within the European Union tightening its migration prevention mechanisms, particularly as the conflict in Syria showed no signs of abating.

In 2016, the EU implemented the *EU-Turkey Statement* also referred to as the *EU-Turkey Deal*, aiming to sharply reduce numbers in arrival of asylum seekers by controlling who could enter and claim asylum [118]. This agreement specifically targeted Syrian nationals fleeing the Syrian conflict, with Turkey agreeing to take back Syrians who crossed into Greece. In return, the EU pledged to accept one Syrian refugee for every one returned to Turkey, prioritising those who had not previously attempted to cross, and offering Turkey financial aid and the possibility of visa-free travel talks. Although the visa discussions have stalled, the EU has renewed its financial support to Turkey, providing an additional €3 billion in 2018 and promising another €3 billion for 2021–2023. This deal had severe effects on refugee numbers but also on the lives of Syrian refugees in Turkey. The agreement aimed to keep refugees in Turkey by designating it as a *safe third country* while reducing their movement to Europe, but this has resulted in precarious living conditions for many refugees [119]. The deal has essentially shifted the burden of refugee care

5.1 A brief overview on recent clandestine migration in the Eastern Mediterranean region . . . . .	85
5.2 Status-quo in documentation of clandestine migration stations . . . . .	87
5.3 Research project <i>Flüchtige Spuren</i> . . . . .	89
5.4 The importance and challenges of documenting migrant graffiti . . . . .	90
5.5 Ethical considerations . . . . .	93
5.6 Photogrammetric data acquisition . . . . .	94
5.7 Photogrammetric processing . . . . .	95
5.8 Deriving other value-added products . . . . .	96
5.9 Conclusions and outlook . . . . .	99

[118]: European Council (2016), *Press Release: EU-Turkey Statement*, 18 March 2016

[119]: Demirbaş et al. (2024), 'Looking at the EU-Turkey Deal: The Implications for Migrants in Greece and Turkey'

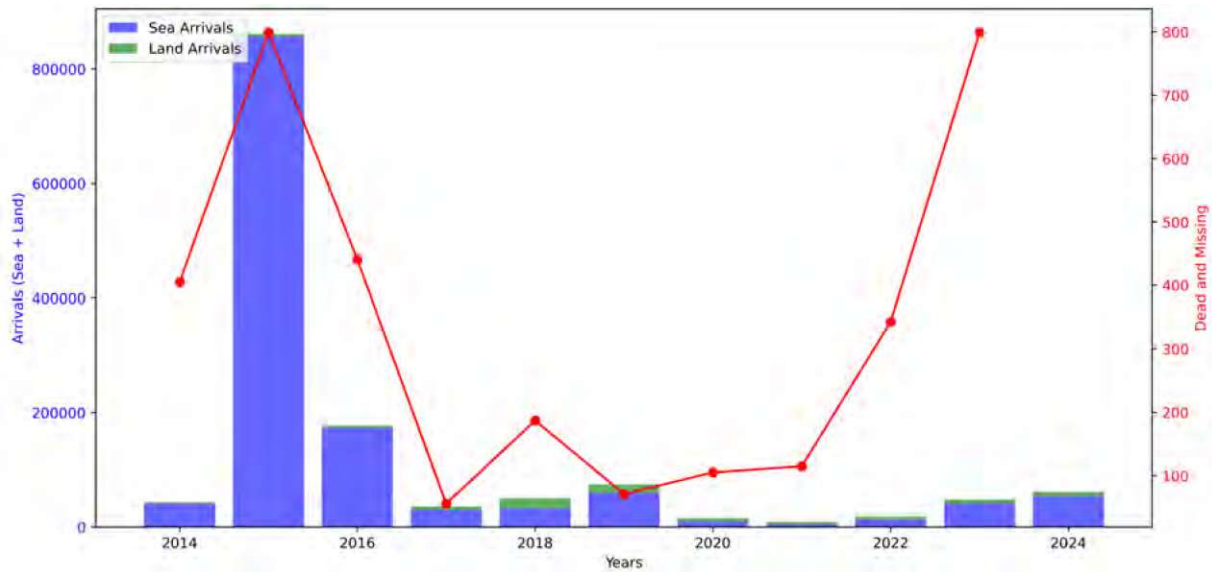


**Figure 5.1:** Evolution of clandestine sea and land arrivals from Turkey to Greece between 2014 and 2024 including the number of missing and dead people. The dead and missing figures correspond to the entire Eastern Mediterranean route for which no data was available for the year 2024 at the time of writing this thesis (Data source: <https://data.unhcr.org/en/situations/europe-sea-arrivals/location/24489>, last accessed: April 15, 2025)

to Turkey, enabling the EU to avoid its responsibilities under the 1951 Geneva Convention while creating a system where refugees' rights are restricted and their exploitation is normalized [120].

In early 2020, the Turkish president Recep Tayyip Erdoğan declared that Turkey would no longer block migrants from crossing the border into the EU, deviating from the commitments outlined in the 2016 EU-Turkey Statement [121, 122]. Following this announcement concerns and reports about violent and often deadly pushbacks conducted by the Hellenic Coast Guard surged with The European Border and Coast Guard Agency, Frontex, being accused of tolerating those practices [123]. Following reports of the Legal centre of Lesbos [124] survivors of expulsions reported that Greek authorities sabotaged their boats by damaging or removing the motor or fuel tank. Since 2020, there has been a notable decline in the number of (sea) arrivals in Greece, while the number of deaths and disappearances in the Eastern Mediterranean has significantly increased (Figure 5.1).

[120]: Rygiel et al. (2016), 'The Syrian refugee crisis: The EU-Turkey 'deal' and temporary protection'

[121]: Perisic et al. (2023), 'Pushbacks of Migrants in the Mediterranean: Reconciling Border Control Measures and the Obligation to Protect Human Rights'

[122]: France 24 (2020), *Erdogan warns Europe to expect 'millions' of migrants after Turkey opens borders*

[123]: Frontex (2020), *Frontex launches internal inquiry into incidents recently reported by media*

[124]: Legal Centre Lesbos (2020), *Collective Expulsions in the Aegean*

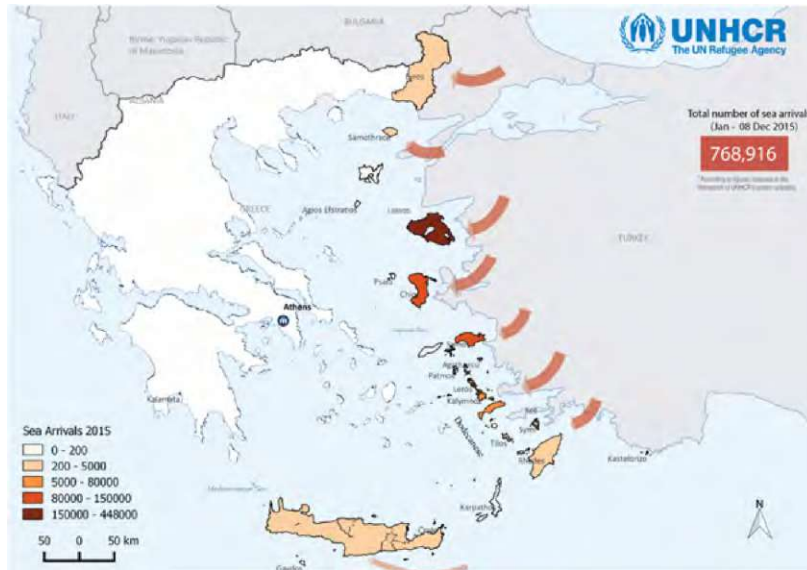


**Figure 5.2:** Sea arrivals in Greece: Breakdown by island for the period from January to December 8, 2015. (Source: <https://data.unhcr.org/es/documents/details/46550>, last accessed: April 15, 2025)

## 5.2 Status-quo in documentation of clandestine migration stations

Generally, clandestine migration events are well-documented by national government institutions, the United Nations High Commissioner for Refugees (UNHCR), various Non-Governmental Organizations, and journalists. For instance, the Turkish Coast Guard Command records and publishes data on pushback incidents conducted by Greek authorities. Table 5.1 provides a short excerpt of the information they collect and share. Each documented incident is accompanied by a written report, supplemented with photographs and video footage [125].

[125]: Republic of Turkey Ministry of Interior Directorate General of Migration Management (2024), *Push-Back Incidents in the Year of 2024*

Date	Location/Place and Time	Asset	Total
31 Dec 2024	AYDIN/Kuşadası 23.40	2 Life Boats	39
29 Dec 2024	AYDIN/Kuşadası 10.50	Inflatable Boat	38
25 Dec 2024	BALIKESİR/Ayvalık 16.50	2 Life Boats	22
25 Dec 2024	BALIKESİR/Ayvalık 05.30	2 Life Boats	40
20 Dec 2024	İZMİR/Seferihisar 11.55	Inflatable Boat	28
20 Dec 2024	İZMİR/Dikili 04.50	Inflatable Boat	27
19 Dec 2024	AYDIN/Didim 10.15	Inflatable Boat	26+1 (Organizer)

**Table 5.1:** Pushback incidents as documented by the Turkish Coast Guard Command. The *Total* column refers to the number of migrants involved in the incident [125]

Given the collected data and media coverage concerning this topic, knowledge about the various stages of the refugee journey — from the sea passage between the Turkish mainland and the Greek islands



to the process of applying for asylum in Central Europe — appears, at first glance, to be extensive. Nevertheless, the conditions migrants face while waiting along Turkey's western coast before crossing to the Aegean islands are hardly documented and understood compared to other stages of their journey [126]. If covered by the media, such events are often sensationalized—what Jason de León [127] starkly describes as *immigration pornography*.

In this context, contemporary archaeology, also through the use of photogrammetric methodologies, can make a significant contribution to the field. By providing tangible evidence of this “*backstage world of violence*” [128], such work plays a critical role in contextualising past, present, and future migration events and policies.

Establishing a comprehensive overview of the documentation of clandestine migration stations is challenging due to the diverse forms and interpretations within this field. A traditional literature review is complicated by the wide range of terminology used. For instance, terms like *migrant* and *refugee* are sometimes treated as synonyms and at other times as distinct categories. A comprehensive literature review on this topic is thus beyond the scope of this thesis and beyond my area of expertise. Nevertheless, this chapter seeks to offer an overview of projects and key publications (e.g., [126, 127]) that have engaged with this subject, while also providing a broader overview of other relevant studies referenced in these publications.

Various studies on the Mexico-US border have highlighted the importance of documenting migrant stations. These works emphasize material culture's role in survival, the growing dangers of migration due to stricter and more violent border controls, and the human experiences of migrants, offering crucial insights into the urgent social and humanitarian issues surrounding clandestine migration. [126, 129–132]. A notable initiative in this context is the *Undocumented Migration Project*, a long-term anthropological study combining archaeological surveys of migrant trails and stations in the Arizona desert [133].

In the European context, the events of 2015 and 2016, widely referred to in media as the *refugee crisis*, had profound effects on policies and politics. Various studies have correlated the number of refugees and related media coverage with variables such as rising euro-scepticism [134], declining trust in national political leaders and parties, and increasing support for populist movements like the Alternative für Deutschland (AfD, eng. *Alternative for Germany*) [135]. Given this historical significance of events, it seems crucial to document the very circumstances under which those migration events happen. Despite the importance of this topic, only a few researchers have so far focused on the material remnants directly linked to the clandestine crossing of sea or land borders within the European context.

A notable exception is the work of Seitsonen et al. [136] who documented and reflected on abandoned refugee vehicles left behind by multinational refugees at Finnish Lapland's border checkpoints in winter 2015–2016. In the Eastern Mediterranean, a recent anonymously conducted study investigated material traces of recent migration to Europe by examining the Turkish west coast, Lesvos, and Athens in 2017 [126].

[127]: De León et al. (2015), *The Land of Open Graves: Living and Dying on the Migrant Trail*

[126]: Anonymous (2023), ‘Materielle Spuren der rezenten Migration nach Europa: Ein archäologischer Blick auf die türkische Westküste, Lesbos und Athen im Jahr 2017’

[129]: De León (2012), ‘“Better to Be Hot than Caught”: Excavating the Conflicting Roles of Migrant Material Culture’

[130]: De León (2015), ‘“By the Time I Get to Arizona”: Citizenship, Materiality, and Contested Identities Along the US–Mexico Border’

[131]: De León (2013), ‘Undocumented migration, use wear, and the materiality of habitual suffering in the Sonoran Desert’

[132]: Gokee et al. (2014), ‘Sites of Contention: Archaeological Classification and Political Discourse in the US-Mexico Borderlands’

[133]: De León (2012), ‘Victor, archaeology of the contemporary, and the politics of researching unauthorized border crossing: a brief and personal history of the Undocumented Migration Project’

[134]: Hartevelde et al. (2018), ‘Blaming Brussels? The Impact of (News about) the Refugee Crisis on Attitudes towards the EU and National Politics’

[135]: Solodoch (2021), ‘Regaining Control? The Political Impact of Policy Responses to Refugee Crises’

[136]: Seitsonen et al. (2016), ‘Abandoned refugee vehicles “In the Middle of Nowhere”: Reflections on the global refugee crisis from the Northern Margins of Europe’



### 5.3 Research project *Flüchtige Spuren*

A recent research project named *Flüchtige Spuren* (eng. *Ephemeral traces*) set out to build upon this work by focusing on migration stations along the Turkish west coast close to the Greek island of Lesbos. This project involved a 12-day research trip in mid-October to Turkey, featuring an international team of four archaeologists and myself. I was invited to join as a photogrammetry specialist, primarily responsible for the photogrammetric documentation of various sites.

A key focus of this project was the documentation of various open-air migration stations along the coast, which were visited and, in some cases, archaeologically and photogrammetrically recorded. This aspect of the work included the systematic gathering, documentation and description of materials left behind by clandestine migrants while waiting for their passage across the Mediterranean. This part of the work is only briefly and very selectively illustrated here (Figure 5.3). It is anticipated to disseminate and discuss the extensive documentation results in a separate, more suitable format.



**Figure 5.3:** Collection of photos acquired during visits at different clandestine migration stations along the Turkish west coast. A: Overview of a typical migration station within an olive grove only meters away from the Mediterranean. B: A collection of socks found and assembled by the research team. C: A selection of packaging for rubber inner tubes, used as less visible alternative means of sea rescue. D: Empty tuna cans. E: Life jacket for infants.

Instead, this chapter will focus on the second key objective of the trip: the documentation of two abandoned buildings and the graffiti created therein (Figure 5.4). These structures were primarily used by clandestine migrants in 2015 and 2016, but the conducted research revealed that one

of them remained in use as recently as 2024. Of particular interest in these buildings are the extensive graffiti left behind by migrants during their periods of waiting inside. The majority of the graffiti can be found in Building 1 (Figure 5.4), while Building 2 contains only a few, though still notable, examples. Although the abandoned buildings were discovered during earlier field trips, they were only minimally documented at that time due to limited resources. Revisiting those sites offered the opportunity to comprehensively capture the sites using photogrammetry. Key info about the buildings can be found in Table 5.2.

**Table 5.2:** Details of the surveyed buildings

Building	Date	Number of Floors	Number of Rooms	Approx. Total Area
<b>Building 1</b>	9 October 2024	2	10	140 m <sup>2</sup>
<b>Building 2</b>	15 October 2024	3	16	325 m <sup>2</sup>

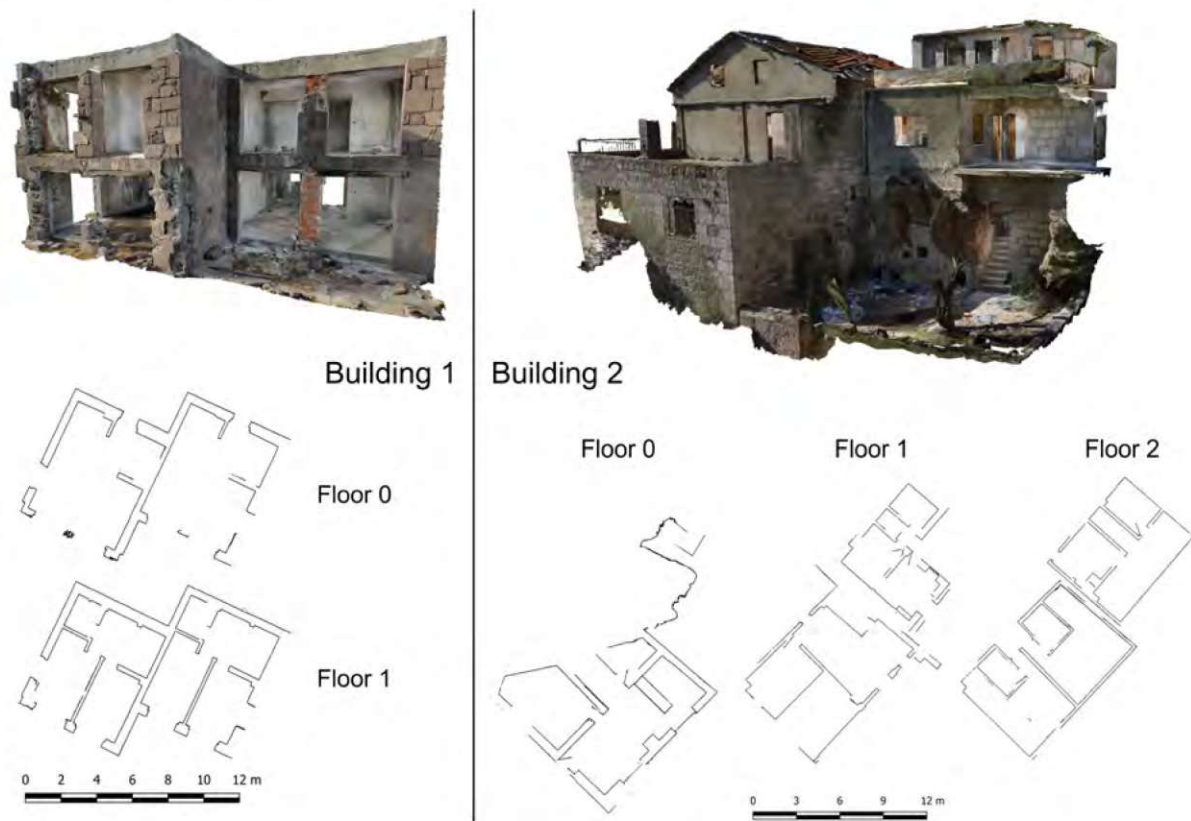


**Figure 5.4:** Textured 3D mesh of the two buildings and the extracted floor plans per building. The floorplans were extracted at ca. 1m room height and are based on the results from the dense image matching point cloud.

## 5.4 The importance and challenges of documenting migrant graffiti

As highlighted throughout this thesis, graffiti is an omnipresent yet understudied phenomenon, particularly in the context of clandestine



migration. This lack of scientific engagement is surprising, given that such graffiti serve as visual records of experiences that profoundly affect hundreds of thousands of lives, shaping political debates and public discourse. One notable contribution in this area is Soto's (2016) study [137], which examines migrant graffiti hidden beneath rural highways created by undocumented migrants crossing the border from Mexico into Arizona. The 85 inscriptions Soto documented at two sites in southern Arizona bear witness to migrants' encounters with border patrol and convey messages to future travellers. Alongside names, places, and greetings, the word "recuerdo"—Spanish for "remember"—appeared most frequently, underscoring the commemorative purpose of these markings. Other inscriptions reflected themes of sex, sadness, and religion, as well as the hardships of migration, such as warnings like *The Border Patrol was here* and records of sleeping in hiding under rural highways. These markings transform sterile transit routes into spaces of memory, reflecting both the migrants' agency and the profound precarity of their journeys [137].

At the same time, documentation of graffiti created during events of clandestine migration poses other, more fundamental challenges than the documentation of graffiti that are created in urban areas:

- **Ephemerality:** Graffiti are often created spontaneously, though the degree of spontaneity can vary. In urban contexts, the prevalence of tags and quick drawings often reflects a combination of long-term preparation—such as carrying a marker or spray can—and opportunistic action, seizing the moment when circumstances allow. As observed at graffiti sites linked to migration, the logistical and strategic planning required for clandestine border crossings rarely includes consideration or preparation for mark-making. The graffiti examined in this study are defined by the basic tools used for their production, including wooden pencils, soft limestone as chalk, sharp stones for scratching, burnt sticks as improvised charcoal and, as found in one instance, lipstick (Figure 5.5). Aside from scratched graffiti, these methods are inherently transient. Although these graffiti are often created—or at least found—in enclosed spaces like abandoned buildings, they are still susceptible to weathering from air moisture, heat, solar radiation, and wind exposure. Soto et al. [137] explicitly demonstrated this fragility by revisiting the two Arizona study sites three and six years later, where most of the chalked graffiti had faded and become illegible.

Additionally, the medium on which the graffiti are created is ephemeral. The buildings where these graffiti are typically found along the Turkish west coast are abandoned, making them proable subjects to removal or demolition—either through natural processes or human intervention—in the foreseeable future.

- **Accessibility:** Graffiti created in the context of clandestine migration is inherently difficult to access, as migration stations are typically located in hidden and hard-to-access areas. As a result, a substantial portion of the work involves identifying potential sites, which necessitates both prior analysis of the area using satellite imagery and, more importantly, extensive landscape exploration. Once potential locations, such as abandoned buildings in proximity

[137]: Soto (2016), 'Place making in Non-places: Migrant Graffiti in Rural Highway Box Culverts'

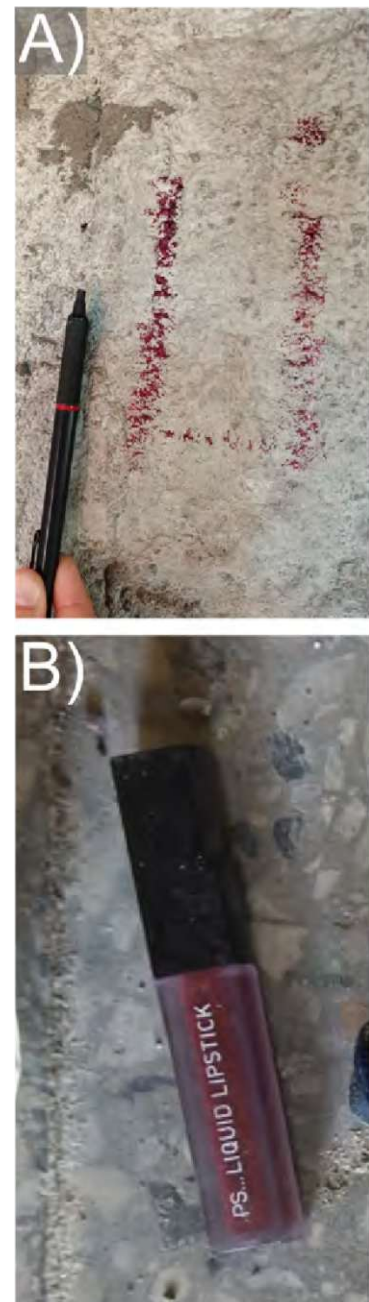


**Figure 5.5:** A) A (presumably) unfinished graffiti found in Building 2. A pen is placed for scale. B) A red lipstick, matching the tone of the graffiti, found just a few meters away from the mark.

to the coast, are identified, it is essential to assess their safety for entry and verify whether they were indeed used as migrant stations. The safety evaluation involves a rudimentary assessment of the structural integrity of the buildings, as well as the identification of other potential hazards, including sharp objects and venomous animals. For instance, a scorpion, whether venomous or not was not further analysed, was discovered concealed beneath blankets in one building.

- **Visibility:** Adequate photographing inside abandoned buildings is not trivial due to the challenging lighting conditions. Even though every room in the researched buildings receives some natural lightning through windows, it is for some rooms barely sufficient to adequately see the graffiti. Another challenge concerns the high contrast between brightly lit areas and dark areas, making it hard to capture details in both. To state the obvious, there is no pre-installed artificial lightning present in those abandoned building, thus the usage of artificial illumination in the form of a flash which was mounted on the camera's hot shoe was imperative, enabling the documentation of dark rooms, but also creating other challenges (see Chapter 5.12)
- **Stress:** A constant factor during on-site documentation was stress. There is always the risk of being noticed by the police or encountering human traffickers, both of whom could react unpredictably. Police may mistake researchers for migrants or traffickers, which can lead to uncertain outcomes. Similarly, human traffickers might see researchers as law enforcement, creating the potential for conflict. While the latter scenario has not occurred, the police often became aware of research activities and intervened with varying levels of involvement. Fortunately, with the help of a Turkish citizen and native Turkish speaker with a calmative approach, no situation escalated.

These situations, however, caused considerable mental strain, creating an environment of stress and discomfort during the documentation. The scenes being documented added to this, as they often carried heavy emotional weight. For instance, locations where large groups of migrants had clearly waited under precarious conditions just days earlier to the documentation left a particularly strong impact. The work in the group was beneficial to mitigate the stress but it still influenced the documentation process.

This photogrammetric survey aimed to document the graffiti in the two abandoned buildings (Figure 5.4) geometrically and texturally. Although not every room contained graffiti, documenting the entire buildings, from the outside as well as from the inside, was deemed essential for comprehensive and seamless visualisation and dissemination.

Eventually this survey shall set the basis for a thorough analysis and contextualisation of the present artefacts and graffiti. Essentially the output of this work shall be a virtual yet tangible reconstruction of events by providing comprehensive and accurate reconstruction of the scenes and artefacts.



## 5.5 Ethical considerations

Documenting objects and graffiti left behind by refugees crossing the Mediterranean involves navigating ethical challenges in a sensitive and evolving landscape [138]. Many of these objects, such as blankets, clothes, money or food, may appear abandoned but could still be needed by future migrants, local communities, or NGOs. Removing or disturbing them potentially risks disrupting survival strategies. Thus seemingly abandoned but potentially useful objects were left at the sites.

Another, ethical risk associated with this research concerns the potential disruption of this sensitive system possibly even redirecting migration routes, thereby further increasing dangers. Thus, efforts were made to avoid presence during active migration events by only being present at those sites during bright daylight when the probability of disruption is minimised. This risk mitigation, however, did not fully eliminate the ethical tension of working in such contexts. On the other hand, there is an urgency to document arising from the fact that these objects and their context can disappear quickly, making timely recording crucial to preserve evidence. Balancing the need to document with the responsibility to avoid harm is essential.

Lastly, in the following chapters specific geographical details are intentionally withheld. Although unlikely, state authorities could potentially use such information about events before and during border crossings, even long after they occurred, in their efforts to prevent migration. Consequently the following chapters do not mention exact geographical location. As geographical reference, this chapter focuses on the region along the Turkish coast, where the Greek island Lesbos is visible to the naked eye (Figure 5.6).

[138]: Soto (2018), 'Object Afterlives and the Burden of History: Between "Trash" and "Heritage" in the Steps of Migrants'



**Figure 5.6:** The island of Lesbos (Greece) as seen from the Turkish mainland. The photo was taken during a field trip to collect data supporting this use case.

## 5.6 Photogrammetric data acquisition

Full photographic coverage of the buildings was conducted using a Nikon D800 camera (Figure 5.7) with a Sigma 14mm f/2.8 lens. Following photogrammetric protocols, it was aimed at taking the photos with a fixed focus distance per building to maintain the camera's interior orientation. This was achieved by manually focusing at approximately 2 meters from the wall at the beginning of each building's photographic session. This focus distance was a compromise, balancing multiple factors: capturing sufficient textural detail, navigating the narrow interiors, ensuring proper illumination with the mounted flash, and keeping acquisition times manageable.

**Table 5.3:** Summary of photo acquisition and processing results for the two surveyed buildings. The duration of acquisition refer to the time difference between the first and last photo acquired.

Building	Number of Acquired/Oriented Photos	Number of Tie Points	Duration of acquisition	Length of Control Scale-bar + Residual
<b>Building 1</b>	414/399	407,282	47 min	100 cm + 6.7 mm
<b>Building 2</b>	1309/1247	1,031,355	59 min	28 cm + 6.1 mm

In tight staircases and smaller rooms, some images were inevitably out of focus. These areas were rephotographed using adapted auto-focus immediately after completing the main photographic session to ensure adequate coverage. Images of the buildings' exteriors were taken afterward, using an infinite focus distance, to capture the facade and surrounding environment. The different focusing were taken into account in the processing (Chapter 5.7). Not the entire exterior of the buildings could be captured due to some inaccessible parts around the houses. The entire image acquisition for each building was completed within an hour (Table 5.3).

Lighting conditions posed a major challenge, as anticipated based on prior site visits by parts of the research team. All indoor images were captured using a Nikon Speedlight SB-700 flash mounted on the camera's hot shoe (Figure 5.7A). This ensured generally sharp and well-lit images, even in dark environments. However, the flash sometimes failed to fully illuminate the wide field of view of the 14 mm wide-angle lens (Figure 5.8), and the combination of the flash and camera setup increased the overall weight, adding to the difficulty of non-stop image acquisition. Variations in lighting conditions, sensor-to-object distances, and inconsistent natural light further contributed to underexposed and overexposed areas in some images. Lastly, shadows cast during the photography on some of the walls were impossible to avoid creating some artefacts in the final texture. Despite the rapid pace and challenges, such as narrow spaces and poor lighting, most images were successfully acquired.

The Solmeta GMAX geotagger was mounted on the camera's hot shoe (Figure 5.7B) during outdoor photography to collect GNSS-derived absolute georeferencing data. Indoors, georeferencing data was not



**Figure 5.7:** The two camera setups used for the image acquisition of the two abandoned buildings. A) The Nikon D800 with the Nikon Speedlight SB-700 flash for the building's inside. B) The Nikon D800 with the Solmeta GMAX geotagger which was used for the photos taking on the outside of the buildings

captured due to limited device accuracy and the need to use the hot shoe for the flash. The geotagger provided positional accuracy of about 2.5 meters under ideal conditions, which was sufficient for the study's requirements. Accurate scaling of the photogrammetric models was ensured by placing and photographing folding rulers within the buildings (Figure 5.8A).



**Figure 5.8:** Two example photographs of the buildings' interior. A) Example from Building 1 showing the vastly varying sensor to object distances and the effects it has on the resulting image. B) A dark room within Building 2 showing the challenge of using a wide angle camera in combination with a flash.

## 5.7 Photogrammetric processing

The collected image sets were processed using Agisoft Metashape Professional 1.8.4 to determine the exterior orientations of the photos and to calculate camera calibration parameters. Calibration parameters were estimated separately for image sets based on their focus distances, resulting in three calibration groups per building: one for the 2-meter focus distance, one for the infinity focus distance, and one for images captured with short, varying focus distances. The orientation process successfully aligned 96% of the images for Building 1 and 95% for Building 2. It was possible to establish tie points also between the images taken from the façade and from the inside (Figure 5.9). A visual inspection of the calculated exterior orientations and the resulting tie point cloud revealed no significant errors.

Following orientation, a dense point cloud and a triangle-based polymesh was generated using depth-map-based multi-view stereo matching [116]. The texture of the polymesh was computed using all collected images (Figure 5.10). While it would have been tedious but possible to remove blurry or poorly exposed images manually or automatically, such removal was avoided, prioritising a complete texture over avoiding suboptimal areas. Rendered views of the resulting meshes are depicted in Figures 5.4 and 5.11.

The Solmeta GMAX geotagger provided coarse absolute georeferencing for outdoor images by embedding GNSS-derived coordinate triplets into the metadata. For scaling, the folding rulers photographed during image acquisition were used. Measurements between clearly identifiable



**Figure 5.9:** Example of tie points established between one outdoor photo of Building 1 and one photo taken from the inside.

[116]: Seitz et al. (2006), 'A comparison and evaluation of multi-view stereo reconstruction algorithms'



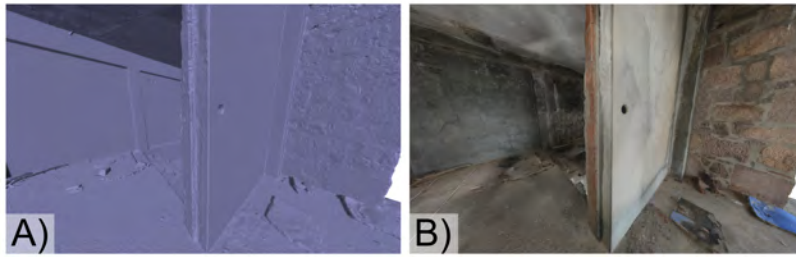


**Figure 5.10:** A) Generated polmyesh of one room in Building 1 without texture and B) the same polymesh rendered from the same perspective with texture



**Figure 5.11:** Diagonal cross section of the textured 3D mesh of Building 1

points on the rulers (Figure 5.8A) were taken. These measurements were introduced as additional observations to constrain the photogrammetric models. Residuals from the scaling process were used as accuracy estimates. For Building 1, three rulers were used for scaling and one for quality control, while Building 2 relied on two rulers, supplemented by comparisons with the dimensions of a rubber inner tube package for quality control (Table 5.3).

## 5.8 Deriving other value-added products

Despite challenges with lighting and geometry, the polymesh and texture processing produced satisfactory results. Issues such as underexposed and overexposed regions due to inconsistent lighting conditions, as well as flash-related shadows in wide-angle shots, created some suboptimal result. Nonetheless, detailed, accurate, and nearly complete 3D models of both buildings were created, providing a foundation for the generation of other value-added products. The derived dense point cloud and polymesh serve as basis for the derivation of floorplans (Figure 5.4) and



orthophotomosaics (Figure 5.12).

For the floor plans, horizontal cross-sections per floor at ca. 1m floor height were generated using the *Cross Section* tool implemented in CloudCompare. The resulting cross section were manually filtered for artefacts created by objects such as a sinks, toilet or staircase. These floorplans provide a quick and easy-to-understand overview of the building's geometry, allowing for room counting and area estimation (Table 5.2). Additionally, they may serve as a foundation for visualising graffiti occurrences, which are unevenly distributed across the rooms and tend to cluster within specific areas of the houses, thereby enabling a deeper understanding of the graffiti's geography.



**Figure 5.12:** A, B, C, and D: Examples of graffiti orthophotomosaics created based on data collected in Building 1.

Orthophotomosaics of most graffiti covered walls were derived using the oriented images, the derived 3D model and a projection plane manually defined in Agisoft's Metashape (Figure 5.12). The resulting orthophotomosaics are exported with a raster cell size of 1 mm, which closely matches the native ground sampling distance—typically slightly smaller in most cases. This approach simplifies retrieving the dimensions of the graffiti within the image by converting measurement in the image with

simple conversion factors, e.g. 1 pixel corresponds to 1 mm on the object. To date, orthophotomosaics of ca. half of the graffiti covered walls in the buildings have been generated. The remaining data will be processed in a similar fashion. The derived 2D floorplans and the orthophotomosaics are especially suitable for the dissemination in 2D formats such as this thesis and other written publications. The orthophotomosaics can serve as a foundation for translating the predominantly Farsi and Arabic graffiti content, a task intended to be performed by a professional translator. For this purposes, it might also be beneficial to apply some further image processing onto the orthophotomosaic to increase the legibility

In addition to geometric processing, digital image processing algorithms can be employed to enhance features such as the visibility of partially faded graffiti and low-contrast images. For example, Figure 5.13 showcases a noteworthy graffito from Building 2, likely inscribed with an ordinary pencil during the autumn of 2015. This graffito, initially difficult to read, was revealed through the application of Sobel Edge Detection followed by morphological opening, which significantly improves its readability. The inscription, written in Turkish, contains a striking economic calculation:

Original Text (Turkish)	English Translation
27/09/2015	27/09/2015
418 Bot Geçirildi	418 boats sent
× 50,000 \$ Dolar	× 50,000 \$ Dollar
= 20,900,000 \$ Dolar elde edildi	= 20,900,000 \$ Dollars earned

This discovery, first made during a previous visit to the building in 2023, aligns with evidence of the exploitative economic logic of traffickers. The creator of this graffito remains unknown, it nevertheless highlights the profit-seeking behaviour of those organising the sea crossings and serves as a self-incriminating testimony to the exploitative nature of these operations.

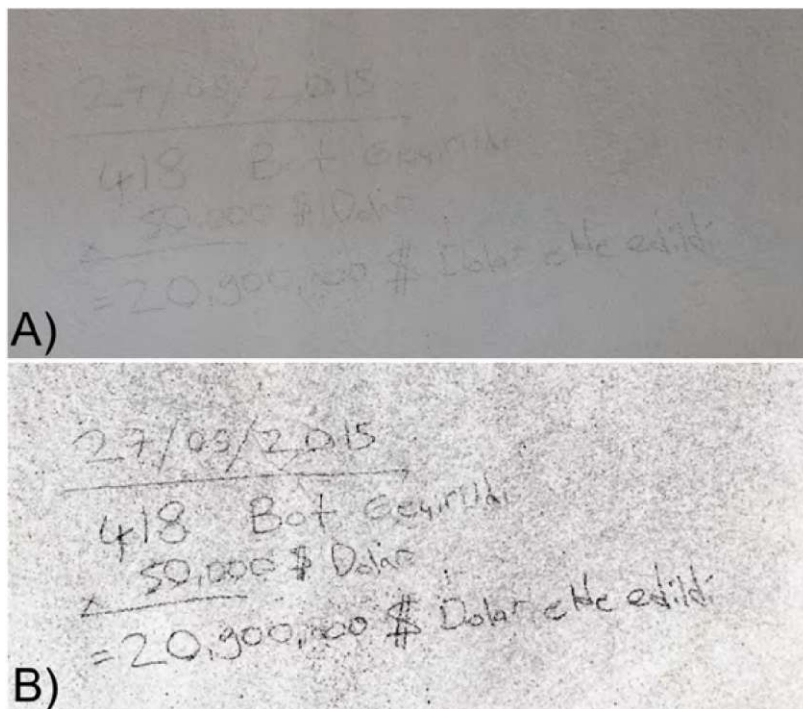


**Figure 5.13:** A) Original image of one graffito from Building 2. B) The same image after applying Sobel Edge Detection and morphological opening to enhance readability.

## 5.9 Conclusions and outlook

Much work remains to be done with the collected data. The graffiti shall and will be transcribed and professionally translated, enabling a deeper analysis of their messages and forms. This will hopefully provide valuable insights into the thoughts and experiences of those being in the process of risking their lives during migration.

This chapter highlighted graffiti created at so-called migration stations in the Eastern Aegean and its documentation, a field that has received little attention, whether scientific or otherwise. These silent witnesses reflect events that not only shape individual lives but, through policy changes, impact entire societies and generations. By providing a thorough documentation of these expressions, this study seeks to bring them to the forefront—not only for current researchers and the general public but also for future historians, who will have to rely on tangible evidence and concrete facts, which disappear unnoticed every day.

## 6 Summary, Outlook and Conclusions

### 6.1 Summary Chapter 3 and 4

Graffiti is a unique study object for various reasons. One key feature of graffiti is its ephemerality which makes it a hard-to-capture phenomenon. Photographs are key to documenting graffiti but only capture a single moment, whereas graffiti is dynamic, evolving over time accumulating non-recoverable physical layers and potential conversations among their creators. Current state-of-the-art graffiti documentation rarely addresses this temporal aspect, mostly because capturing new graffiti shortly after they appear is logistically challenging and because distinguishing between new and existing elements is inherently complex. This challenge applies both to the human visual system, where recognizing changes on a frequently graffitied wall requires careful observation, and to computer-aided vision, which relies on image analysis for automated graffiti detection. The latter is mainly complicated by factors such as illumination variability, weather effects, camera inconsistencies, co-registration errors, and image noise, all of which can obscure true changes.

To address these technical issues, and setting the foundation for improving the accounting of the temporal aspect in graffiti documentation an automated image based change detection was developed as part of this thesis. This framework is based on two main processing steps: the co-registration phase and a hybrid change detection framework which employs and merges two independent change detection algorithms to automatically identify graffiti-related changes between two epochs, while ignoring other irrelevant image differences. The image acquisition for this methodology primarily relied on a triple GoPro setup, enabling dynamic image capture while walking along the graffitied walls. This approach serves as a proof of concept for the image acquisition strategy, demonstrating its feasibility. In the future, this setup could be further optimized by mounting the cameras on a bicycle or helmet, allowing for faster and more convenient image acquisition while cycling along the research area.

The acquired images were processed using an incremental SfM pipeline, which sequentially orients new images relative to a georeferenced base network. By identifying tie points in static elements of the scene, such as unchanged graffiti or infrastructure that remained consistent over time, the incremental SfM approach established a foundation for co-registering the 29 newly acquired image epochs of the test dataset. This process facilitated the generation of 29 unique texture atlases for the base mesh. The co-registered images were exported using a synthetic camera approach. Here, exterior orientations of synthetically fixed cameras were introduced, enabling image rendering from these predefined viewpoints for each epoch. This method produced images that were nearly pixel-perfectly co-registered, ensuring nearly pixel-perfect alignment for direct integration into the subsequent hybrid change-detection pipeline.

This pipeline employs a two-fold approach: first, images are analysed at the pixel level for changes. Therefore, the co-registered images undergo several pre-processing steps, including edge-aware image smoothing and RGB normalisation. These steps mitigate noise, minor co-registration errors, and, most importantly, variations in illumination conditions during image acquisition. After pre-processing, colour differences between images are computed using the CIEDE2000 metric. A threshold is then applied to classify pixels as either changed or unchanged. The second component of the hybrid change detection pipeline utilises a descriptor-based methodology. The core idea is to extract feature points and compute the corresponding descriptors, using four established feature extraction algorithms SIFT, AKAZE, SURF, and BRISK. Similar descriptor vectors appearing at similar image locations serve as a proxy for invariant image content, enabling the detection of unchanged graffiti. This approach benefits from two key factors: the nearly pixel-perfect co-registration of images and the fact that small graffiti, which are most difficult to detect for humans, exhibit



substantial textural change, facilitating descriptor matching. The extracted information is then translated into a machine-readable format by computing a so-called tie-point density map, which is subsequently binarised into change/no-change classifications using a threshold. As both methodologies rely eventually on binarisation using thresholds, choosing a suitable threshold is crucial. For this, a large reference test dataset comprising 6902 image pairs and their corresponding manually annotated reference change maps was semi-automatically created, curated and publicly shared via the official TU Wien data repository. By systematically testing a variation of potential thresholds, an optimal solution was found for the present dataset. Whether this threshold can be transferred for other scenes remains subject to further research on this topic.

When compared to the reference data, the threshold-optimized hybrid approach achieved promising results, with a high CCR (95%) and specificity (98%), alongside good recall (77%), precision (87%), and F1-score (80%). In a comparison with the IR-MAD, an established change detection method, the hybrid approach demonstrated similar performance but with significantly reduced variability. One challenge for the hybrid method lies in achromatic image regions, which become largely indistinguishable in RGB-normalised images. Additionally, very small graffiti, such as tags, are sometimes filtered out during the creation of the tie-point density map, which could lead to a detection bias towards larger graffiti, a known issue also for the conventional, human-based in-situ changed detection. Future improvements may include dynamic gridding, which adjusts grid cell sizes based on the density of feature points. Furthermore, the test zone exhibited relatively simple surface geometry, consisting mostly of straight walls with only a few protruding elements. More complex surfaces, such as staircases and bridges, may pose challenges for generating accurate 3D surface models due to occlusions which are unavoidable for the anticipated mobile data acquisitions. Also, complex geometries would lead to more excessive parametrisation needed for texture mapping which could also introduce artefacts. To minimise the negative impact of highly complex geometries, exclusion masks could be applied to these areas, similar to those used in the reference dataset. As these regions are generally difficult to access, changes in such locations are less likely, but unmonitored areas may still lead to some undetected graffiti.

In summary, the proposed hybrid change detection method shows significant promise for efficiently monitoring extensive graffiti-scapes like those along Vienna's Donaukanal. Whether the thresholds identified will perform similarly well at other scenes remains an open question which will require further and extensive testing. However, the automated nature and scalability of the method suggest it could be valuable for broader applications, especially when paired with even more efficient photo acquisition techniques such as employing cameras mounted on a bike.

Beyond the challenge of detecting change, an until recently largely unresolved issue concerns the contextualization of graffiti records. As discussed in this thesis, graffiti is inherently tied to both space and time, necessitating rigorous documentation that captures its spatio-temporal context. However, photographs alone are insufficient for preserving these dimensions. Therefore, this research explored how photogrammetric techniques can be leveraged to more effectively maintain this spatio-temporal context of graffiti. The fundamental premise regarding this topic is that the temporal context can be inferred by accurately resolving the spatial dimension. This approach is based on the assumption that graffiti is a purely additive phenomenon. Anything visible must have been created after anything below. To reconstruct spatial context, various photogrammetric techniques exist that enable accurate georeferencing. In this thesis, planar rectification was initially considered as a potential strategy. However, it is limited by the assumption that graffiti is created on perfectly planar surfaces, an assumption that does not hold for a significant portion of graffiti along the Donaukanal, leading to significant rectification errors even for surfaces which appear planar visually but exhibit slight deviations from planarity. As alternative orthophotos have been identified which do not assume surface planarity. Generally, orthophotos can be considered a solution to many problems. First, they allow to account for the three main types of distortions occurring in photographs: lens distortions, topographic distortions, and perspective distortions. Second, they enable highly accurate georeferencing of the documented graffiti, allowing for accurate measurements of proportions and dimensions. Additionally, by integrating them into 2D or 3D web maps, the graffiti can be displayed within their native, albeit virtual, environment. Thereby they do largely solve the problem of decontextualisation as they make it possible to digitally excavate old graffiti at their correct position, presumed that those have been photographed and processed accordingly.

Lastly, while the orthophoto generation incorporates several processing steps, their generation can be fully automated. Only for some exceptional cases (i.e. graffiti created around corners or obstructed graffiti) manual intervention is needed, suddenly making it possible to account for the sheer amount of new graffiti that occur at Donaukanal every week. All these advantages and considerations culminated in the development of AUTOGRAF, a software enabling the fully automated generation of graffiti orthophotomosaics.

AUTOGRAF is designed as add-on to the photogrammetric processing software Agisoft Metashape, and integrates and streamlines basic functionality of it to achieve a bespoke automated workflow. This workflow inputs a set of images of new graffiti and outputs the corresponding orthophotos including other potentially useful products such as the 3D model of the scene or metadata concerning the achieved accuracy of the output. This workflow can essentially be split in three main steps. In an initial phase the input photos are checked for consistency and quality, increasing quality of the output and limiting the execution time to the necessary minimum. Next, the tie points between existing oriented images (i.e. the photogrammetric backbone) and the input images are established allowing for the derivation of exterior camera orientations and scene specific interior orientation parameters of the camera accounting for differences in focusing distances during the acquisition. From these oriented images a 3D polymesh is generated and a projection plane is derived by fitting a plane into the established 3D tie point cloud. This plane estimation is implemented using RANSAC to ensure robustness. Using the images, their known 3D orientation in space, the up-to-date 3D mesh of the scene and an adjusted projection plane orthophotos of new graffiti can be derived. This approach has been tested on a sample dataset comprising 826 photographs featuring 100 randomly selected graffiti.

With 95% of the graffiti orthorectified without any major flaws, the results from this experiment confirmed the high usability of AUTOGRAF also in real-world scenarios. While the overall quality of the derived graffiti orthophotos is generally high, the experimental results also highlighted potential limitations of the methodology, particularly its strong reliance on specific image acquisition. Captured photographs must adhere to various SfM-specific acquisition guidelines and include significant portions of the surrounding environment. In three cases, the images lacked sufficient overlap with invariant parts of the graffiti's neighbouring environment. Completely eliminating this issue is challenging due to spatial constraints in certain locations, especially given that the photographing process already demands considerable time, physical effort, and focus from the photographer. A future challenge for AUTOGRAF to address is occlusions caused by pillars, vegetation, or other structures in front of the graffiti, which cannot always be fully removed using the current mesh filtering approach. While isolated mesh component filtering effectively handles occlusions in most cases, obstructing elements sometimes remain when they are connected to the main model. A more robust filtering method could incorporate RANSAC-derived plane information to remove 3D model vertices exceeding a certain distance from the plane. Implementing this distance-based filtering could help eliminate residual occlusions in orthophotos and further enhance results.

A potential improvement regarding the processing speed of the software concerns the current incremental SfM method. Therefore, the applicability of direct georeferencing was briefly investigated within this thesis. This approach could substantially speed up the computationally intensive tie point extraction and incremental bundle block adjustment. Combining an IMU with an RTK GNSS setup would substantially constrain the image search space for the incremental SfM step. However, a rough estimate concerning the runtime of AUTOGRAF shows that it is already well possible to process the required volume of graffiti photos to capture all changes along Donaukanal in great detail sufficiently fast. For future applications this direct georeferencing approach nevertheless hold potential to improve the efficiency of the workflow.

Lastly, the total coverage network forms a crucial but resource-intensive foundation, requiring extensive data acquisition, management, and processing. However, since the incremental SfM approach continuously updates large parts of the network as new graffiti images are added, a full update is only necessary after significant structural changes or in less frequently photographed areas. As more images accumulate, tensions in the bundle block (i.e. errors propagating through the fixed camera network) may arise. These can be mitigated by periodically rerunning a full bundle block adjustment, another area for future exploration.

Despite these challenges, AUTOGRAF already enables the generation of thousands of high-quality orthophotos each month, largely keeping pace with the rapid graffiti creations along the Donaukanal. While further optimization is needed in image acquisition, management, and dissemination, AUTOGRAF represents a

significant step toward automated, high-quality digital graffiti preservation. Beyond the graffiti documentation of extensive graffiti-scapes, the workflow has potential applications in other cultural heritage or infrastructure documentation projects as well. Although currently optimized for planar or slightly curved surfaces, the georeferenced 3D mesh remains valuable for more complex structures. By making the source code of AUTOGRAF freely available, broader adoption and further research and development is enabled and encouraged.

## 6.2 Summary Chapter 5

The last part of this dissertation moved away from the documentation of a constantly reinvented graffiti-scape like the Donaukanal to a, today, comparatively largely static environment exhibiting other, more fundamental challenges in documentation. The documentation of graffiti created in the course of clandestine migration events is another example of the vast diversity of graffiti. In the course of the research project *Flüchtige Spuren* several so-called migration stations were found and photogrammetrically and archaeologically documented. Among those, also two abandoned buildings which were extensively used during the peak of the migration events from West and Central Asia to Europe in 2015 and early 2016. The aim was to document and contextualise the many found graffiti to provide primary evidence of the human conditions experienced during events which shape public discourse and political policies around the world.

Graffiti documentation in the context of clandestine migration is a complex and sensitive task. Many of these sites are difficult to reach, often hidden in remote or potentially unsafe locations, making access challenging, time-consuming and distressing. Poor lighting conditions inside buildings further complicate photogrammetric data acquisition, while the constant risk of encountering authorities or individuals involved in human trafficking adds an element of diffuse danger and stress. Additionally, ethical concerns play a role as documenting these spaces requires a careful approach to avoid disrupting migration routes or altering the environment, all while ensuring that primary evidence is digitally preserved before it disappears.

By following photogrammetric principles, both the buildings and the graffiti-covered walls within them were documented in under an hour per site. This process produced georeferenced and textured 3D polymeshes of the buildings, along with orthophotomosaics of graffiti-covered walls and detailed floorplans, allowing for a deeper analysis of the geography of these migration stations. While the full significance of this documentation will become evident once the graffiti are translated using photogrammetric outputs and analysed in more detail, the collected material already serves as a silent witness to otherwise overlooked and undocumented yet historically significant events. This last part of the dissertation has thus produced a highly tangible form of results, triggering audiences emotionally by simply displaying the likely most objective abstraction of the environment: photos. Adding value to these photographs by producing standard photogrammetric products like textured 3D polymeshes and undistorted orthophoto mosaics, a more in-depth analysis and objectified storytelling is enabled.

## 6.3 Outlook and Conclusions

Currently, change detection and automated orthorectification are implemented as separate steps in the documentation process, leading to large redundancies during data acquisition. At the moment the documentation workflows foresees first the (image-based) detection of new graffiti which are then photographed again in great detail. Only those secondarily acquired images are input into the AUTOGRAF software. In the future, integrating these steps into a unified workflow could make use of faster mobile image acquisition, enabling automated change detection, and directly producing georeferenced orthophotos of newly detected graffiti. By adopting a mobile image acquisition method, such as mounting GoPro cameras on a bike, the need for weekly photo tours (as described in Chapter 4.3.2) would be eliminated. Instead, the continuously collected images would feed directly into the hybrid change detection framework, which would identify relevant images or subregions for orthophotomosaic generation. This integration would significantly enhance automation and documentation speed. While the image quality may decline due to the dynamic acquisition

strategy using GoPros, this trade-off seems necessary given the rapid emergence of new graffiti and the need for a sustainable workflow. Given the fact that overall much more resources are spent on physically removing graffiti than on digitally safeguarding them it seems imperative for any operational application that the used tools enable a highly cost-effective output of results. Furthermore, such an integrated approach would allow for a temporally denser documentation, mitigating the risk of overlooking graffiti, thus largely maintaining the temporality of graffiti along the Donaukanal which is a key problem in state-of-the-art graffiti documentation projects.

In parallel to this work, a master thesis by Dachs (2024) [139] explored the applicability of deep learning for graffiti change detection. In the initial step, pre-trained models were evaluated, but these models proved unsuitable for detecting changes in graffiti images, achieving an average F1-score of only 13%. To address this limitation, a graffiti-specific model was trained using synthetic images and the graffiti change detection reference dataset generated as part of this thesis [89]. This approach significantly improved the performance of the deep learning model, with the average F1-score increasing to 61% for models trained on all available data. Synthetic data had a positive impact on most models, notably enhancing precision across the board. The highest F1-score of 69% was achieved by a custom-implemented model trained exclusively on real data. While this performance falls short of the hybrid approach's F1-score of 0.79 presented in this thesis, future research could investigate how incorporating larger datasets might enhance both deep learning models and the hybrid approach.

In the long run, it would also be worthwhile to include the general public in the data collection process. In a first indirect step one could think of scraping data from publicly available resources such as social media. An advantage of such a resource is that they are often enriched by verbal non-standardised descriptions of the photographer, possibly adding additional context to the documentation. Such descriptions could likely be formalised using machine learning techniques such as large language models. A clear disadvantage of such an approach would be, besides the expected bias again towards large and flashy graffiti, the downsizing applied by most social media provider. The maximum image width for images posted on Instagram, for example, is 1080 pixels [140]. Also the images are not taken to be used for photogrammetric processing which likely complicates the integration in the existing workflows. In addition to collecting images from public sources, a more direct way to engage the general public is through dedicated citizen-science campaigns. This could involve encouraging individuals to photograph newly discovered graffiti and upload their graffiti images to a designated platform. To facilitate participation, informational materials with QR codes could be strategically placed throughout the study area. Such an initiative would not only enhance the documentation process but also foster inclusivity and transparency in scientific research by providing citizens with tangible visual evidence of their contributions. Another key goal for future research is the integration of the collected data into an interactive online 3D web platform that enables virtual tours along the Donaukanal, exploring both space and time. The concept of such a platform was explored in a Master's thesis, supervised as part of this dissertation, and holds significant potential for future development. However, a major challenge lies in rendering the vast amount of 3D data collected. To address this, a follow-up project, INDIGO 2.0, is proposed, with the aim of overcoming this challenge and tackling other issues in documenting extensive graffiti-scapes.

The graffiti documentation of clandestine migration stations, through the survey and photogrammetric processing conducted, offers valuable and objective evidence of two abandoned buildings along a small section of the Turkish West coast. Despite the significant global relevance of this issue, it remains severely underexplored and under-documented, not just in the European context but worldwide. The methodologies and challenges presented in this research are not limited to the specific sites studied but can support the documentation of migration sites globally. Looking ahead, the main challenges will be identifying such sites, ensuring the safety of all individuals involved, and securing public funding to continue the research, which will also aid in addressing potential concerns regarding the academic legitimacy and objectivity of the work.

In summary, this dissertation has tackled key challenges in the digital safeguarding of graffiti. Photogrammetry has proven to provide adequate methodologies, addressing gaps in current graffiti documentation practices and providing concrete solutions. By presenting these approaches, this work aims to offer valuable guidance



to both graffiti enthusiasts and professionals in their efforts to document this unique form of human expression.

# Bibliography

- [1] S. Merrill, G. J. Verhoeven, B. Wild, M. Carloni, M. de la Iglesia, F. Fernández Merino, L. Radošević, C. Ricci, J. Schlegel, and S. Wogrin. 'Different Folks, Different Strokes': goINDIGO 2022's Creators vs Academics Discussion Round'. In: *document | archive | disseminate graffiti-scapes (2022)* (2023), pp. 203–219. doi: <https://doi.org/10.48619/indigo.v0i0.701>.
- [2] G. Vasari. *Le vite de' più eccellenti architetti, pittori, et scultori italiani, da Cimabue insino a' tempi nostri*. Lorenzo Torrentino, 1550.
- [3] J. Lamb. 'Scratching the Surface: An Introduction to Sgraffito and its Conservation in England'. In: *Journal of Architectural Conservation* 5.1 (1999), pp. 43–58. doi: [10.1080/13556207.1999.10785234](https://doi.org/10.1080/13556207.1999.10785234).
- [4] J. Schlegel, M. Carloni, S. Wogrin, A. Graf, and G. J. Verhoeven. 'Making a Mark—Towards a Graffiti Thesaurus'. In: *document | archive | disseminate graffiti-scapes (2022)*, pp. 203–219. doi: <https://doi.org/10.48619/indigo.v0i0.710>.
- [5] I. J. Ross. *Routledge Handbook of Graffiti and Street Art*. Routledge International Handbooks. Routledge, 2016.
- [6] U. Blanché. 'Street Art and related terms'. In: *SAUC-Street Art and Urban Creativity* 1.1 (2015), pp. 32–39. doi: <https://doi.org/10.25765/sauc.v1i1.14>.
- [7] D. Krause and C. Heinicke. *Street Art, Die Stadt als Spielplatz*. Berlin: Archiv der Jugendkulturen Verlag KG, 2006.
- [8] N. Siegl. 'Kulturphänomen Graffiti. Das Wiener Modell der Graffiti-Forschung'. In: *Der Graffiti Reader, Essays internationaler Experten zum Kulturphänomen Graffiti*. Ed. by N. Siegl and S. Schaefer-Wiery. Vienna, 2009.
- [9] P. Bengtsen. *Street Art World*. Lund: Alemendros de Granada Press, 2014.
- [10] G. J. Verhoeven, B. Wild, J. Schlegel, M. Wieser, N. Pfeifer, S. Wogrin, L. Eysn, M. Carloni, B. Koschiček-Krombholz, A. Molada-Tebar, et al. 'Project INDIGO: document, disseminate & analyse a graffiti-scape'. In: *9th International Workshop 3D-ARCH" 3D Virtual Reconstruction and Visualization of Complex Architectures"* (3D-ARCH 2022). Vol. 46. 2022, pp. 513–520.
- [11] M. Saenz Gordon. *Mural MAST-ER: From painting in the streets to the Graffiti Museum in Miami, how muralist MAST managed to translate a teenage hobby into a career*. 2021. URL: <https://www.redbull.com/us-en/theredbulletin/graffiti-artist-mast>.
- [12] P. Lohberger. 'Graffiti - ist das Kunst?' In: *Die Presse* (2019).
- [13] S. Peteranderl. 'Corona-Graffitis weltweit: Wie Street-Art-Künstler ihre Nachbarn aufklären'. In: *Der Spiegel* (2020).
- [14] J. I. Ross, P. Bengtsen, J. F. Lennon, S. Phillips, and J. Z. Wilson. 'In search of academic legitimacy: The current state of scholarship on graffiti and street art'. In: *The Social Science Journal* 54.4 (Dec. 2017), pp. 411–419. doi: [10.1016/J.SOSCIJ.2017.08.004](https://doi.org/10.1016/J.SOSCIJ.2017.08.004).
- [15] A. M. Forster, S. Vettese-Forster, and J. Borland. 'Evaluating the cultural significance of historic graffiti'. In: *Structural Survey* 30.1 (2012), pp. 43–64.
- [16] G. J. Verhoeven, M. Carloni, J. Schlegel, B. Wild, and S. Wogrin. 'Finding listeners for walls that speak'. In: ed. by G. J. Verhoeven, J. Schlegel, B. Wild, S. Wogrin, and M. Carloni. Lisbon: Urban Creativity / AP2, 2023, pp. 6–15. doi: [10.48619/indigo.v0i0.699](https://doi.org/10.48619/indigo.v0i0.699).
- [17] A. M. Ronchi. *eCulture: cultural content in the digital age*. Springer Science & Business Media, 2009.

- [18] J. Deacon. 'Heritage Resource Management in South Africa'. In: *Cultural Heritage Management: A Global Perspective*. Ed. by P. M. Messenger and G. S. Smith. Cultural Heritage Studies. Gainesville, FL: University Press of Florida, 2010, pp. 162–175.
- [19] F. Tombari, L. Di Stefano, S. Mattoccia, and A. Zanetti. 'Graffiti detection using a time-of-flight camera'. In: *Advanced Concepts for Intelligent Vision Systems: 10th International Conference, ACIVS 2008, Juan-les-Pins, France, October 20-24, 2008. Proceedings 10*. 2008, pp. 645–654.
- [20] V. Gomes, A. Dionísio, and J. S. Pozo-Antonio. 'Conservation strategies against graffiti vandalism on Cultural Heritage stones: Protective coatings and cleaning methods'. In: *Progress in Organic Coatings* 113 (Dec. 2017), pp. 90–109. doi: [10.1016/J.PORGCOAT.2017.08.010](https://doi.org/10.1016/J.PORGCOAT.2017.08.010).
- [21] R. Holler. 'GraffDok — A Graffiti Documentation Application'. In: *Communications in Computer and Information Science* 500 (2014), pp. 239–251. doi: [10.1007/978-3-662-45006-2\\_{\\\_}19](https://doi.org/10.1007/978-3-662-45006-2_{\_}19).
- [22] M. d. I. Iglesia. 'Towards the scholarly documentation of street art'. In: *SAUC - Street Art and Urban Creativity* 1.1 (Dec. 2015), pp. 40–49. doi: [10.25765/SAUC.V1I1.15](https://doi.org/10.25765/SAUC.V1I1.15).
- [23] D. Novak. 'Photography and Classification of Information'. In: *SAUC-Street Art and Urban Creativity* 1.1 (2015), pp. 13–25.
- [24] N. Careddu and O. Akkoyun. 'An investigation on the efficiency of water-jet technology for graffiti cleaning'. In: *Journal of Cultural* (2016). doi: [10.1016/j.culher.2015.11.009](https://doi.org/10.1016/j.culher.2015.11.009).
- [25] S. Chapman. 'Laser technology for graffiti removal'. In: *Journal of Cultural Heritage* 1 (Aug. 2000), S75–S78. doi: [10.1016/S1296-2074\(00\)00153-9](https://doi.org/10.1016/S1296-2074(00)00153-9).
- [26] J. S. Pozo-Antonio, T. Rivas, M. P. Fiorucci, A. J. López, and A. Ramil. 'Effectiveness and harmfulness evaluation of graffiti cleaning by mechanical, chemical and laser procedures on granite'. In: *Microchemical Journal* 125 (Mar. 2016), pp. 1–9. doi: [10.1016/J.MICROC.2015.10.040](https://doi.org/10.1016/J.MICROC.2015.10.040).
- [27] S. Samolik, M. Walczak, M. Plotek, A. Sarzynski, I. Pluska, and J. Marczak. 'Investigation into the removal of graffiti on mineral supports: Comparison of nanosecond Nd:YAG laser cleaning with traditional mechanical and chemical methods'. In: *Studies in Conservation* 60 (Aug. 2015), S58–S64. doi: [10.1179/0039363015Z.0000000000208](https://doi.org/10.1179/0039363015Z.0000000000208).
- [28] M. Carvalhão and I. 'Evaluation of mechanical soft-abrasive blasting and chemical cleaning methods on alkylid-paint graffiti made on calcareous stones'. In: *Elsevier* (2015).
- [29] A. Ramil, J. S. Pozo-Antonio, M. P. Fiorucci, A. J. López, and T. Rivas. 'Detection of the optimal laser fluence ranges to clean graffiti on silicates'. In: *Construction and Building Materials* 148 (Sept. 2017), pp. 122–130. doi: [10.1016/J.CONBUILDMAT.2017.05.035](https://doi.org/10.1016/J.CONBUILDMAT.2017.05.035).
- [30] M. P. Fiorucci, J. Lamas, A. J. López, T. Rivas, and A. Ramil. 'Laser cleaning of graffiti in Rosa Porriño granite'. In: <https://doi.org/10.1117/12.892158> 8001 (July 2011), pp. 1116–1123. doi: [10.1117/12.892158](https://doi.org/10.1117/12.892158).
- [31] M. P. Fiorucci, A. J. López, A. Ramil, S. Pozo, and T. Rivas. 'Optimization of graffiti removal on natural stone by means of high repetition rate UV laser'. In: *Applied Surface Science* 278 (Aug. 2013), pp. 268–272. doi: [10.1016/J.APSUSC.2012.10.092](https://doi.org/10.1016/J.APSUSC.2012.10.092).
- [32] T. Rivas, S. Pozo, M. P. Fiorucci, A. J. López, and A. Ramil. 'Nd:YVO4 laser removal of graffiti from granite. Influence of paint and rock properties on cleaning efficacy'. In: *Applied Surface Science* 263 (Dec. 2012), pp. 563–572. doi: [10.1016/J.APSUSC.2012.09.110](https://doi.org/10.1016/J.APSUSC.2012.09.110).
- [33] G. Daurelio. 'A Bronze Age Pre-Historic Dolmen: Laser Cleaning Techniques of Paintings and Graffiti (The Bisceglie Dolmen Case Study)'. In: (2005), pp. 199–205. doi: [10.1007/3-540-27176-7\\_{\\\_}25](https://doi.org/10.1007/3-540-27176-7_{\_}25).
- [34] P. Pouli, C. Fotakis, B. Hermosin, C. Saiz-Jimenez, C. Domingo, M. Oujja, and M. Castillejo. 'The laser-induced discoloration of stonework; a comparative study on its origins and remedies'. In: *Spectrochimica Acta Part A: Molecular and Biomolecular Spectroscopy* 71.3 (Dec. 2008), pp. 932–945. doi: [10.1016/J.SAA.2008.02.031](https://doi.org/10.1016/J.SAA.2008.02.031).
- [35] C. Gómez, A. Costela, I. García-Moreno, and R. Sastre. 'Comparative study between IR and UV laser radiation applied to the removal of graffiti on urban buildings'. In: *Applied Surface Science* 252.8 (Feb. 2006), pp. 2782–2793. doi: [10.1016/J.APSUSC.2005.04.051](https://doi.org/10.1016/J.APSUSC.2005.04.051).

- [36] A. Costela, I. García-Moreno, C. Gómez, O. Caballero, and R. Sastre. 'Cleaning graffitis on urban buildings by use of second and third harmonic wavelength of a Nd:YAG laser: a comparative study'. In: *Applied Surface Science* 207.1-4 (Feb. 2003), pp. 86–99. doi: [10.1016/S0169-4332\(02\)01241-2](https://doi.org/10.1016/S0169-4332(02)01241-2).
- [37] E. Urones-Garrote, A. J. López, A. Ramil, and L. C. Otero-Díaz. 'Microstructural study of the origin of color in Rosa Porriño granite and laser cleaning effects'. In: *Applied Physics A: Materials Science and Processing* 104.1 (July 2011), pp. 95–101. doi: [10.1007/S00339-011-6344-X/METRICS](https://doi.org/10.1007/S00339-011-6344-X/METRICS).
- [38] R. Valente and L. Barazzetti. 'Methods for Ancient Wall Graffiti Documentation: Overview and Applications'. In: *Journal of Archaeological Science: Reports* 34 (2020), p. 102616. doi: <https://doi.org/10.1016/j.jasrep.2020.102616>.
- [39] J. F. DiBiasie Sammons. 'Application of Reflectance Transformation Imaging (RTI) to the study of ancient graffiti from Herculaneum, Italy'. In: *Journal of Archaeological Science: Reports* 17 (2018), pp. 184–194. doi: <https://doi.org/10.1016/j.jasrep.2017.08.011>.
- [40] R. R. Benefiel and H. M. Sypniewski. 'Documenting Ancient Graffiti: Text, Image, Support and Access'. In: *Graffiti Scratched, Scrawled, Sprayed: Towards a Cross-Cultural Understanding* 35 (2023), p. 425.
- [41] D. Abate and M. Trentin. 'HIDDEN GRAFFITI IDENTIFICATION ON MARBLE SURFACES THROUGH PHOTOGRAMMETRY AND REMOTE SENSING TECHNIQUES'. In: *The International Archives of the Photogrammetry, Remote Sensing and Spatial Information Sciences* XLII-2-W15.2/W15 (Aug. 2019), pp. 1–8. doi: [10.5194/ISPRS-ARCHIVES-XLII-2-W15-1-2019](https://doi.org/10.5194/ISPRS-ARCHIVES-XLII-2-W15-1-2019).
- [42] R. Benefiel, H. Sypniewski, and E. Z. Damer. 'Wall Inscriptions in the Ancient City: The Ancient Graffiti Project'. In: Leiden, The Netherlands: Brill, 2019, pp. 179–196. doi: [10.1163/9789004382886\\\_\\\_013](https://doi.org/10.1163/9789004382886\_\_013).
- [43] S. Niemann. 'INGRID—Archiving Graffiti in Germany'. In: *document | archive | disseminate graffiti-scapes* (2022), pp. 231–238.
- [44] M. Papenbrock and D. Tophinke. 'Graffiti digital. Das Informationssystem Graffiti in Deutschland (INGRID)'. In: *Zeithistorische Forschungen* 15 (2018).
- [45] M. A. Sherif, A. A. M. da Silva, S. Pestryakova, A. F. Ahmed, S. Niemann, and A. C. N. Ngomo. 'IngridKG: A FAIR Knowledge Graph of Graffiti'. In: *Scientific Data* 2023 10:1 10.1 (May 2023), pp. 1–12. doi: [10.1038/s41597-023-02199-8](https://doi.org/10.1038/s41597-023-02199-8).
- [46] B. Webb. 'Building Art Crimes'. In: *goINDIGO* (Sept. 2024), pp. 12–21. doi: [10.48619/indigo.v0i0.972](https://doi.org/10.48619/indigo.v0i0.972).
- [47] O. Baumann. 'The Nuances of Mapping Street Art-Developing a Web Map for Interactive Graffiti Exploration (Master Thesis)'. In: (2024).
- [48] L. Radošević. 'Art in the Streets in the Virtual World'. In: *document | archive | disseminate graffiti-scapes* (2022), pp. 276–288. doi: [10.48619/INDIGO.V0I0.716](https://doi.org/10.48619/INDIGO.V0I0.716).
- [49] D. Brown. 'Decentering distortion of lenses'. In: *Photogrammetric engineering* 32.3 (1996), pp. 444–462.
- [50] C. Curtis and E. Rodenbeck. 'Graffiti archaeology'. In: *ACM SIGGRAPH 2004 Web Graphics*. SIGGRAPH '04. New York, NY, USA: Association for Computing Machinery, 2004, p. 1. doi: [10.1145/1186194.1186196](https://doi.org/10.1145/1186194.1186196).
- [51] B. Wild, G. J. Verhoeven, N. Pfeifer, E. Bonadio, D. HERO, F. ', J. ONE, M. SKIRL, M. Carloni, C. Ricci, C. Koblit, S. Niemann, L. Radošević, J. Schlegel, A. Watzinger, and S. Wogrin. 'Imagine Being a Racist': goINDIGO 2022's «Ethics & Legality in Graffiti (Research)» Discussion Round'. In: *document | archive | disseminate graffiti-scapes* (2022), pp. 45–62. doi: [10.48619/INDIGO.V0I0.702](https://doi.org/10.48619/INDIGO.V0I0.702).
- [52] G. Verhoeven, J. Schlegel, and B. Wild. 'Each Graffito Deserves Its Polygon'. In: *goINDIGO* 0.0 (Sept. 2024). doi: [10.48619/indigo.v0i0.981](https://doi.org/10.48619/indigo.v0i0.981).
- [53] B. Wild, G. J. Verhoeven, M. Wieser, C. Ressler, J. Schlegel, S. Wogrin, J. Otepka-Schremmer, and N. Pfeifer. 'AUTOGRAF—AUTomated Orthorectification of GRAffiti Photos'. In: *Heritage* 5.4 (2022), pp. 2987–3009. doi: <https://doi.org/10.3390/heritage5040155>.
- [54] B. Wild, G. J. Verhoeven, R. Muszyński, and N. Pfeifer. 'Detecting change in graffiti using a hybrid framework'. In: *The Photogrammetric Record* n/a.n/a (2024). doi: <https://doi.org/10.1111/phor.12496>.



- [55] B. Wild, G. J. Verhoeven, and N. Pfeifer. 'TRACKING THE URBAN CHAMELEON - TOWARDS A HYBRID CHANGE DETECTION OF GRAFFITI'. In: *ISPRS Annals of the Photogrammetry, Remote Sensing and Spatial Information Sciences* (2023), pp. 285–292.
- [56] B. Wild, J. Jungfleisch, and N. Pfeifer. 'Documenting Migrant Graffiti in the Borderscapes of the Eastern Mediterranean'. In: *Proceedings of the CIPA 2025 Symposium*. Seoul, South Korea: International Society for Photogrammetry and Remote Sensing (ISPRS), 2025.
- [57] M. Wieser, G. Verhoeven, B. Wild, and N. Pfeifer. 'Exterior Orientation in a Box: Cost-Effective RTK/IMU-Based Photo Geotagging'. In: *The International Archives of the Photogrammetry, Remote Sensing and Spatial Information Sciences XLVIII-2/W8-2024* (2024), pp. 463–470. doi: [10.5194/isprs-archives-XLVIII-2-W8-2024-463-2024](https://doi.org/10.5194/isprs-archives-XLVIII-2-W8-2024-463-2024).
- [58] B. Wild, G. J. Verhoeven, S. Wogrin, M. Wieser, C. Ressler, J. Otepka-Schremmer, and N. Pfeifer. 'Urban Creativity Meets Engineering. Automated Graffiti Mapping along Vienna's Donaukanal'. In: ed. by G. J. Verhoeven, J. Schlegel, B. Wild, S. Wogrin, and M. Carloni. Lisbon: Urban Creativity / AP2, 2023, pp. 131–145. doi: [10.48619/indigo.v0i0.705](https://doi.org/10.48619/indigo.v0i0.705).
- [59] G. J. Verhoeven, S. Wogrin, J. Schlegel, M. Wieser, and B. Wild. 'Facing a chameleon - how project INDIGO discovers and records new graffiti'. In: ed. by G. J. Verhoeven, J. Schlegel, B. Wild, S. Wogrin, and M. Carloni. Lisbon: Urban Creativity / AP2, 2023, pp. 63–85. doi: [10.48619/indigo.v0i0.703](https://doi.org/10.48619/indigo.v0i0.703).
- [60] B. Wild, G. J. Verhoeven, M. Wieser, C. Ressler, J. Otepka-Schremmer, and N. Pfeifer. 'Graffiti-Dokumentation: Projekt INDIGO'. In: Herbert Wichmann Verlag, 2023, pp. 322–325.
- [61] M. Rachbauer. *Analyse verschiedener Methoden zur Graffiti-Segmentierung (Bachelor Thesis)*. Vienna, Austria, 2022.
- [62] C. Neumayr. *Assessing forest parameters through the evaluation of smartphone-based measurement techniques (Master Thesis)*. Vienna, Austria, 2024.
- [63] K. Starzer. *Smartphone-basierte Bestimmung des Brusthöhendurchmessers von Bäumen (Bachelor Thesis)*. Vienna, Austria, 2024.
- [64] T. Leitner. *Segmentierung und Klassifizierung von Bäumen auf Basis von Smartphone-Aufnahmen (Bachelor Thesis)*. Vienna, Austria, 2024.
- [65] J. Lamprecht. *3D-Modellierung von Stadtbäumen mit RayCloudTools (Bachelor Thesis)*. Vienna, Austria, 2024.
- [66] A. Ringhofer and S. Wogrin. 'Die Kunst der Straße—Graffiti in Wien'. In: *Wiener* 428 (2018), pp. 46–53.
- [67] A. Molada-Tebar, G. J. Verhoeven, D. Hernández-López, and D. González-Aguilera. 'Practical RGB-to-XYZ Color Transformation Matrix Estimation under Different Lighting Conditions for Graffiti Documentation'. In: *Sensors* 24.6 (2024). doi: [10.3390/s24061743](https://doi.org/10.3390/s24061743).
- [68] E. Nocerino, F. Menna, and G. J. Verhoeven. 'GOOD VIBRATIONS? HOW IMAGE STABILISATION INFLUENCES PHOTOGRAMMETRY'. In: *The International Archives of the Photogrammetry, Remote Sensing and Spatial Information Sciences XLVI-2/W1-2022* (2022), pp. 395–400. doi: [10.5194/isprs-archives-XLVI-2-W1-2022-395-2022](https://doi.org/10.5194/isprs-archives-XLVI-2-W1-2022-395-2022).
- [69] C. Fraser. 'Automatic Camera Calibration in Close Range Photogrammetry'. In: *Photogrammetric Engineering & Remote Sensing* 79 (Dec. 2013), pp. 381–388. doi: [10.14358/PERS.79.4.381](https://doi.org/10.14358/PERS.79.4.381).
- [70] L. Barazzetti. 'NETWORK DESIGN IN CLOSE-RANGE PHOTOGRAMMETRY WITH SHORT BASELINE IMAGES'. In: *ISPRS Annals of the Photogrammetry, Remote Sensing and Spatial Information Sciences IV-2/W2* (2017), pp. 17–23. doi: [10.5194/isprs-annals-IV-2-W2-17-2017](https://doi.org/10.5194/isprs-annals-IV-2-W2-17-2017).
- [71] D. Angiati, G. Gera, S. Piva, and C. S. Regazzoni. 'A novel method for graffiti detection using change detection algorithm'. In: *IEEE Conference on Advanced Video and Signal Based Surveillance, 2005*. 2005, pp. 242–246.
- [72] L. Di Stefano, F. Tombari, A. Lanza, S. Mattoccia, and S. Monti. 'Graffiti detection using two views'. In: *The Eighth International Workshop on Visual Surveillance-VS2008*. 2008.
- [73] A. Asokan and J. Anitha. 'Change detection techniques for remote sensing applications: A survey'. In: *Earth Science Informatics* 12 (2019), pp. 143–160.

- [74] A. P. Tewkesbury, A. J. Comber, N. J. Tate, A. Lamb, and P. F. Fisher. 'A critical synthesis of remotely sensed optical image change detection techniques'. In: *Remote Sensing of Environment* 160 (2015), pp. 1–14.
- [75] D. Y. K. S. Y. C. W. L. Ting Bai Le Wang and D. Li. 'Deep learning for change detection in remote sensing: a review'. In: *Geo-spatial Information Science* 26.3 (2023), pp. 262–288. doi: [10.1080/10095020.2022.2085633](https://doi.org/10.1080/10095020.2022.2085633).
- [76] E. J. Parelius. 'A Review of Deep-Learning Methods for Change Detection in Multispectral Remote Sensing Images'. In: *Remote Sensing* 15.8 (2023). doi: [10.3390/rs15082092](https://doi.org/10.3390/rs15082092).
- [77] H. Jiang, M. Peng, Y. Zhong, H. Xie, Z. Hao, J. Lin, X. Ma, and X. Hu. 'A Survey on Deep Learning-Based Change Detection from High-Resolution Remote Sensing Images'. In: *Remote Sensing* 14.7 (2022). doi: [10.3390/rs14071552](https://doi.org/10.3390/rs14071552).
- [78] S. Dong, L. Wang, B. Du, and X. Meng. 'ChangeCLIP: Remote sensing change detection with multimodal vision-language representation learning'. In: *ISPRS Journal of Photogrammetry and Remote Sensing* 208 (2024), pp. 53–69. doi: <https://doi.org/10.1016/j.isprsjprs.2024.01.004>.
- [79] W. Shi, M. Zhang, R. Zhang, S. Chen, and Z. Zhan. 'Change detection based on artificial intelligence: State-of-the-art and challenges'. In: *Remote Sensing* 12.10 (2020), p. 1688.
- [80] A. Singh. 'Review Article Digital change detection techniques using remotely-sensed data'. In: *International Journal of Remote Sensing* 10.6 (1989), pp. 989–1003. doi: [10.1080/01431168908903939](https://doi.org/10.1080/01431168908903939).
- [81] R. J. Radke, S. Andra, O. Al-Kofahi, and B. Roysam. 'Image change detection algorithms: a systematic survey'. In: *IEEE transactions on image processing* 14.3 (2005), pp. 294–307.
- [82] L. Bruzzone and F. Bovolo. 'A novel framework for the design of change-detection systems for very-high-resolution remote sensing images'. In: *Proceedings of the IEEE* 101.3 (2013), pp. 609–630. doi: [10.1109/JPR0C.2012.2197169](https://doi.org/10.1109/JPR0C.2012.2197169).
- [83] R. Arnheim. *Art and visual perception: A psychology of the creative eye*. Univ of California Press, 1954.
- [84] G. Bitelli, R. Camassi, L. Gusella, A. Mognol, et al. 'Image change detection on urban area: the earthquake case'. In: *International Archives of the Photogrammetry, Remote Sensing and Spatial Information Sciences* 35 (2004), pp. 692–697.
- [85] T. Luhmann, C. Fraser, and H.-G. Maas. 'Sensor modelling and camera calibration for close-range photogrammetry'. In: *ISPRS Journal of Photogrammetry and Remote Sensing* 115 (2016), pp. 37–46.
- [86] E. Nocerino, F. Menna, and F. Remondino. 'Accuracy of typical photogrammetric networks in cultural heritage 3D modeling projects'. In: *ISPRS - International Archives of the Photogrammetry, Remote Sensing and Spatial Information Sciences* XL5 (June 2014), pp. 465–472. doi: [10.5194/isprsarchives-XL-5-465-2014](https://doi.org/10.5194/isprsarchives-XL-5-465-2014).
- [87] C. Stamatoopoulos and C. Fraser. 'Automated Target-Free Network Orientation and Camera Calibration'. In: *ISPRS Annals of Photogrammetry, Remote Sensing and Spatial Information Sciences* II-5 (Nov. 2014), pp. 339–346. doi: [10.5194/isprsannals-II-5-339-2014](https://doi.org/10.5194/isprsannals-II-5-339-2014).
- [88] G. J. Verhoeven. 'Computer graphics meets image fusion: the power of texture baking to simultaneously visualise 3D surface features and colour'. In: *ISPRS Annals of Photogrammetry, Remote Sensing and Spatial Information Sciences* IV-2/W2 (Nov. 2017), pp. 295–302. doi: [10.5194/isprs-annals-IV-2-W2-295-2017](https://doi.org/10.5194/isprs-annals-IV-2-W2-295-2017).
- [89] B. Wild, G. J. Verhoeven, R. Muszyński, and N. Pfeifer. *INDIGO Change Detection Reference Dataset*. 2023.
- [90] L. Xu, Q. Yan, Y. Xia, and J. Jia. 'Structure Extraction from Texture via Relative Total Variation'. In: *ACM Transactions on Graphics (TOG)* 31 (Nov. 2012). doi: [10.1145/2366145.2366158](https://doi.org/10.1145/2366145.2366158).
- [91] G. D. Finlayson, B. Schiele, and J. L. Crowley. 'Comprehensive colour image normalization'. In: *Computer Vision—ECCV'98: 5th European Conference on Computer Vision Freiburg, Germany, June, 2–6, 1998 Proceedings, Volume I* 5. 1998, pp. 475–490.

- [92] M. Kampel, H. Wildenauer, P. Blauensteiner, and A. Hanbury. 'Improved motion segmentation based on shadow detection'. In: *Progress in Computer Vision and Image Analysis*. World Scientific, 2010, pp. 519–533.
- [93] K. McLaren. 'XIII—The development of the CIE 1976 ( $L^* a^* b^*$ ) uniform colour space and colour-difference formula'. In: *Journal of the Society of Dyers and Colourists* 92.9 (1976), pp. 338–341.
- [94] G. Sharma. 'Color fundamentals for digital imaging'. In: *Digital color imaging handbook*. CRC press, 2003, pp. 1–114.
- [95] D. G. Lowe. 'Object recognition from local scale-invariant features'. In: *Proceedings of the seventh IEEE international conference on computer vision*. Vol. 2. 1999, pp. 1150–1157.
- [96] G. V. Pillai, N. Gupta, and S. Ari. 'Descriptors based unsupervised change detection in satellite images'. In: *2017 International Conference on Communication and Signal Processing (ICCSP)*. 2017, pp. 1629–1633.
- [97] J. Seo, W. Park, and T. Kim. 'Feature-based approach to change detection of small objects from high-resolution satellite images'. In: *Remote Sensing* 14.3 (2022), p. 462.
- [98] G. Liu, Y. Gousseau, and F. Tupin. 'A contrario comparison of local descriptors for change detection in very high spatial resolution satellite images of urban areas'. In: *IEEE Transactions on Geoscience and Remote Sensing* 57.6 (June 2019), pp. 3904–3918. doi: [10.1109/TGRS.2018.2888985](https://doi.org/10.1109/TGRS.2018.2888985).
- [99] Y. Wang, L. Du, and H. Dai. 'Unsupervised SAR Image Change Detection Based on SIFT Keypoints and Region Information'. In: *IEEE Geoscience and Remote Sensing Letters* 13.7 (July 2016), pp. 931–935. doi: [10.1109/LGRS.2016.2554606](https://doi.org/10.1109/LGRS.2016.2554606).
- [100] M. T. Pham, G. Mercier, and J. Michel. 'Change detection between SAR images using a pointwise approach and graph theory'. In: *IEEE Transactions on Geoscience and Remote Sensing* 54.4 (Apr. 2016), pp. 2020–2032. doi: [10.1109/TGRS.2015.2493730](https://doi.org/10.1109/TGRS.2015.2493730).
- [101] S. A. K. Tareen and Z. Saleem. 'A comparative analysis of SIFT, SURF, KAZE, AKAZE, ORB, and BRISK'. In: *2018 International Conference on Computing, Mathematics and Engineering Technologies: Invent, Innovate and Integrate for Socioeconomic Development, iCoMET 2018 - Proceedings 2018-January* (Apr. 2018), pp. 1–10. doi: [10.1109/ICOMET.2018.8346440](https://doi.org/10.1109/ICOMET.2018.8346440).
- [102] G. Bradski. *The OpenCV Library*. Vol. 25. Oct. 2000.
- [103] H. Bay, T. Tuytelaars, and L. Van Gool. 'Surf: Speeded up robust features'. In: *Computer Vision—ECCV 2006: 9th European Conference on Computer Vision, Graz, Austria, May 7–13, 2006. Proceedings, Part I* 9. 2006, pp. 404–417.
- [104] P. Fernández Alcantarilla. 'Fast Explicit Diffusion for Accelerated Features in Nonlinear Scale Spaces'. In: Nov. 2013. doi: [10.5244/C.27.13](https://doi.org/10.5244/C.27.13).
- [105] S. Leutenegger, M. Chli, and R. Y. Siegwart. 'BRISK: Binary robust invariant scalable keypoints'. In: *2011 International conference on computer vision*. 2011, pp. 2548–2555.
- [106] OpenCV. *Feature Matching with FLANN*. 2024. URL: [https://docs.opencv.org/3.4/d5/d6f/tutorial\\_feature\\_flann\\_matcher.html](https://docs.opencv.org/3.4/d5/d6f/tutorial_feature_flann_matcher.html).
- [107] D. G. Lowe. 'Distinctive image features from scale-invariant keypoints'. In: *International journal of computer vision* 60 (2004), pp. 91–110.
- [108] J. R. Kender. *Saturation, hue, and normalized color: Calculation, digitization effects, and use*. Department of Computer Science, Carnegie-Mellon University, 1976.
- [109] A. A. Nielsen. 'The regularized iteratively reweighted MAD method for change detection in multi-and hyperspectral data'. In: *IEEE Transactions on Image processing* 16.2 (2007), pp. 463–478.
- [110] A. A. Nielsen, K. Conradsen, and J. J. Simpson. 'Multivariate alteration detection (MAD) and MAF postprocessing in multispectral, bitemporal image data: New approaches to change detection studies'. In: *Remote Sensing of Environment* 64.1 (1998), pp. 1–19.
- [111] H. Hotelling. 'Relations between two sets of variates'. In: *Breakthroughs in statistics: methodology and distribution*. Springer, 1992, pp. 162–190.

- [112] ChenHongruixuan. *ChangeDetectionRepository*. 2024. URL: <https://github.com/ChenHongruixuan/ChangeDetectionRepository>.
- [113] K. Kraus. *Photogrammetrie: Geometrische Informationen aus Photographien und Laserscanneraufnahmen*. Walter de Gruyter, 2012.
- [114] F. Deng, J. Kang, P. Li, and F. Wan. 'Automatic true orthophoto generation based on three-dimensional building model using multiview urban aerial images'. In: <https://doi.org/10.1117/1.JRS.9.095087> 9.1 (Mar. 2015), p. 095087. DOI: [10.1117/1.JRS.9.095087](https://doi.org/10.1117/1.JRS.9.095087).
- [115] S. Ullman. 'The interpretation of structure from motion'. In: *Proceedings of the Royal Society of London. Series B. Biological Sciences* 203.1153 (Jan. 1979), pp. 405–426. DOI: [10.1098/RSPB.1979.0006](https://doi.org/10.1098/RSPB.1979.0006).
- [116] S. M. Seitz, B. Curless, J. Diebel, D. Scharstein, and R. Szeliski. 'A comparison and evaluation of multi-view stereo reconstruction algorithms'. In: *Proceedings of the IEEE Computer Society Conference on Computer Vision and Pattern Recognition* 1 (2006), pp. 519–526. DOI: [10.1109/CVPR.2006.19](https://doi.org/10.1109/CVPR.2006.19).
- [117] M. A. Fischler and R. C. Bolles. 'Random sample consensus'. In: *Communications of the ACM* 24.6 (June 1981), pp. 381–395. DOI: [10.1145/358669.358692](https://doi.org/10.1145/358669.358692).
- [118] European Council. *Press Release: EU-Turkey Statement, 18 March 2016*. 2016. URL: <https://www.consilium.europa.eu/en/press/press-releases/2016/03/18/eu-turkey-statement/>.
- [119] E. Demirbaş and C. Miliou. 'Looking at the EU-Turkey Deal: The Implications for Migrants in Greece and Turkey'. In: *Migrations in the Mediterranean: IMISCOE Regional Reader*. Ed. by R. Zapata-Barrero and I. Awad. Cham: Springer International Publishing, 2024, pp. 11–27. DOI: [10.1007/978-3-031-42264-5\\_{\\\_}2](https://doi.org/10.1007/978-3-031-42264-5_{\_}2).
- [120] K. Rygiel, F. Baban, and S. Ilcan. 'The Syrian refugee crisis: The EU-Turkey 'deal' and temporary protection'. In: *Global Social Policy* 16.3 (Nov. 2016), pp. 315–320. DOI: [10.1177/1468018116666153](https://doi.org/10.1177/1468018116666153).
- [121] P. Perisic and P. Ostojić Domika. 'Pushbacks of Migrants in the Mediterranean: Reconciling Border Control Measures and the Obligation to Protect Human Rights'. In: *Poredbeno Pomorsko Pravo* 61 (Jan. 2023), pp. 614–658. DOI: [10.21857/yvjrdcvpry](https://doi.org/10.21857/yvjrdcvpry).
- [122] France 24. *Erdogan warns Europe to expect 'millions' of migrants after Turkey opens borders*. Mar. 2020. URL: <https://www.france24.com/en/20200303-erdogan-warns-europe-to-expect-millions-of-migrants-after-turkey-opens-borders>.
- [123] Frontex. *Frontex launches internal inquiry into incidents recently reported by media*. Oct. 2020. URL: <https://www.frontex.europa.eu/media-centre/news/news-release/frontex-launches-internal-inquiry-into-incidents-recently-reported-by-media-ZtuEBP>.
- [124] Legal Centre Lesvos. *Collective Expulsions in the Aegean*. July 2020. URL: <https://legalcentrelesvos.org/wp-content/uploads/2020/07/Collective-Expulsions-in-the-Aegean-July-2020-LCL.pdf>.
- [125] Republic of Turkey Ministry of Interior Directorate General of Migration Management. *Push-Back Incidents in the Year of 2024*. 2024. URL: <https://en.sg.gov.tr/push-back-incidents-in-the-year-of-2024>.
- [126] Anonymous. 'Materielle Spuren der rezenten Migration nach Europa: Ein archäologischer Blick auf die türkische Westküste, Lesbos und Athen im Jahr 2017'. In: *Theorie | Archäologie | Reflexion 1: Kontroversen und Ansätze im deutschsprachigen Diskurs*. Ed. by M. Renger, S. Schreiber, and A. Veling. Theoriedenken in der Archäologie. 2023, pp. 453–490. DOI: [10.11588/propylaeum.1092.c15034](https://doi.org/10.11588/propylaeum.1092.c15034).
- [127] J. De León, M. Wells, and R. Borofsky. *The Land of Open Graves: Living and Dying on the Migrant Trail*. 1st ed. Vol. 36. University of California Press, 2015.
- [128] R. Andersson. *Illegality, Inc.: Clandestine migration and the business of bordering Europe*. Univ of California Press, 2014.
- [129] J. De León. "'Better to Be Hot than Caught': Excavating the Conflicting Roles of Migrant Material Culture". In: *American Anthropologist* 114.3 (Sept. 2012), pp. 477–495. DOI: <https://doi.org/10.1111/j.1548-1433.2012.01447.x>.



- [130] J. De León. “‘By the Time I Get to Arizona’: Citizenship, Materiality, and Contested Identities Along the US–Mexico Border”. In: *Anthropological Quarterly* (Jan. 2015).
- [131] J. De León. ‘Undocumented migration, use wear, and the materiality of habitual suffering in the Sonoran Desert’. In: *Journal of Material Culture* 18.4 (Dec. 2013), pp. 321–345. doi: [10.1177/1359183513496489/ASSET/IMAGES/LARGE/10.1177/1359183513496489-FIG12.JPEG](https://doi.org/10.1177/1359183513496489/ASSET/IMAGES/LARGE/10.1177/1359183513496489-FIG12.JPEG).
- [132] C. Gokee and J. De León. ‘Sites of Contention: Archaeological Classification and Political Discourse in the US–Mexico Borderlands’. In: *Journal of Contemporary Archaeology* 1.1 (Sept. 2014), pp. 133–163. doi: [10.1558/JCA.V1I1.133](https://doi.org/10.1558/JCA.V1I1.133).
- [133] J. De León. ‘Victor, archaeology of the contemporary, and the politics of researching unauthorized border crossing: a brief and personal history of the Undocumented Migration Project’. In: *Forum Kritische Archäologie*. Vol. 1. 2012, pp. 141–148.
- [134] E. Harteveld, J. Schaper, S. L. De Lange, and W. Van Der Brug. ‘Blaming Brussels? The Impact of (News about) the Refugee Crisis on Attitudes towards the EU and National Politics’. In: *JCMS: Journal of Common Market Studies* 56.1 (2018), pp. 157–177. doi: <https://doi.org/10.1111/jcms.12664>.
- [135] O. Solodoch. ‘Regaining Control? The Political Impact of Policy Responses to Refugee Crises’. In: *International Organization* 75.3 (2021), pp. 735–768. doi: [DOI:10.1017/S0020818321000060](https://doi.org/10.1017/S0020818321000060).
- [136] O. I. Seitsonen, V. P. Herva, and M. Kunnari. ‘Abandoned refugee vehicles “In the Middle of Nowhere”: Reflections on the global refugee crisis from the Northern Margins of Europe’. In: *Journal of Contemporary Archaeology* 3.2 (2016), pp. 244–260. doi: [10.1558/JCA.31697](https://doi.org/10.1558/JCA.31697).
- [137] G. Soto. ‘Place making in Non-places: Migrant Graffiti in Rural Highway Box Culverts’. In: *Journal of Contemporary Archaeology* 3 (Sept. 2016), p. 174. doi: [10.1558/jca.31830](https://doi.org/10.1558/jca.31830).
- [138] G. Soto. ‘Object Afterlives and the Burden of History: Between “Trash” and “Heritage” in the Steps of Migrants’. In: *American Anthropologist* 120.3 (Sept. 2018), pp. 460–473. doi: <https://doi.org/10.1111/aman.13055>.
- [139] F. Dachs. *Change Detection in Graffiti Images (Master Thesis)*. Wien, 2024. doi: [10.34726/hss.2024.106190](https://doi.org/10.34726/hss.2024.106190).
- [140] Instagram. *Image resolution of photos you share on Instagram*. 2025. URL: <https://help.instagram.com/1631821640426723>.

# Benjamin Wild

## Curriculum Vitae



### Zur Person

Name: **Dipl. Ing. Benjamin Wild, B.Sc.**  
Geburtstag **1996-10-01**  
Geboren in: **Lienz in Osttirol, Österreich**

### Ausbildung

2022–heute **Doktoratsstudium, TU Wien.**  
Dr.-Studium der techn. Wissenschaften Vermessung und Geoinformation  
2020–2021 **Masterstudium, TU Wien.**  
Masterstudium Geodäsie und Geoinformation (Dipl. Ing.)  
2020–2021 **(Erasmus+) Auslandssemester Master, Aalto University,**  
Aalto University, School of Engineering, Espoo, Finland  
2016–2020 **Bachelorstudium, TU Wien.**  
Bachelorstudium Geodäsie und Geoinformation (B.Sc)

### Beruflicher Werdegang

2021–heute **Projektassistent | Universitätsassistent (Prae-Doc), TU Wien.**  
Forschung im Bereich der Photogrammetrie  
Lehre und Betreuung von Bachelor- und Masterarbeiten  
Publizieren und Präsentieren der Forschungsergebnisse  
2019–2021 **Studienassistent, TU Wien.**  
Forschung im Bereich der Klima- und Umweltfernerkundung  
Publizieren und Präsentieren der Forschungsergebnisse  
2014–2019 **Diverse Praktika und Nebenjobs**